AFRL-RX-TY-TR-2013-0016

EVALUATION OF THE PERFORMANCE OF IODINE-TREATED BIOCIDAL FILTERS UNDER THE INFLUENCE OF ENVIRONMENTAL PARAMETERS

Myung-Heui Woo, Hsing-Wang Li, Chang-Yu Wu

Engineering School of Sustainable Infrastructure and Environment
Department of Environmental Engineering Sciences
University of Florida
406 Black hall, P.O. Box 116450
Gainesville, FL 32611-6450

Contract No. FA8650-06-C-5913

February 2013

AIR FORCE RESEARCH LABORATORY
MATERIALS AND MANUFACTURING DIRECTORATE

■ **Air Force Materiel Command** ■ **United States Air Force** ■ **Tyndall Air Force Base, FL 32403-5323**

DISCLAIMER

Reference herein to any specific commercial product, process, or service by trade name, trademark, manufacturer, or otherwise does not constitute or imply its endorsement, recommendation, or approval by the United States Air Force. The views and opinions of authors expressed herein do not necessarily state or reflect those of the United States Air Force.

This report was prepared as an account of work sponsored by the United States Air Force. Neither the United States Air Force, nor any of its employees, makes any warranty, expressed or implied, or assumes any legal liability or responsibility for the accuracy, completeness, or usefulness of any information, apparatus, product, or process disclosed, or represents that its use would not infringe privately owned rights.

NOTICE AND SIGNATURE PAGE

Using Government drawings, specifications, or other data included in this document for any purpose other than Government procurement does not in any way obligate the U.S. Government. The fact that the Government formulated or supplied the drawings, specifications, or other data does not license the holder or any other person or corporation; or convey any rights or permission to manufacture, use, or sell any patented invention that may relate to them.

This report was cleared for public release by the 88th Air Base Wing Public Affairs Office at Wright Patterson Air Force Base, Ohio available to the general public, including foreign nationals. Copies may be obtained from the Defense Technical Information Center (DTIC) (http://www.dtic.mil).

AFRL-RX-TY-TR-2013-0016 HAS BEEN REVIEWED AND IS APPROVED FOR PUBLICATION IN ACCORDANCE WITH ASSIGNED DISTRIBUTION STATEMENT.

WANDER.JOSEPH.D.1230231660 Digitally signed by WANDER.JOSEPH.D.1230231660 DN: c=US, o=U.S. Government, ou=DoD, ou=PKI, ou=USAF, cn=WANDER.JOSEPH.D.1230231660 Date: 2013.04.22 17:18:46 -05'00'

JOSEPH D. WANDER, PhD
Work Unit Manager

HENLEY.MICHAEL.V.1231823332 Digitally signed by HENLEY.MICHAEL.V.1231823332 DN: c=US, o=U.S. Government, ou=DoD, ou=PKI, ou=USAF, cn=HENLEY.MICHAEL.V.1231823332 Date: 2013.04.23 09:44:38 -05'00'

MICHAEL V. HENLEY, DR-III
Program Manager

RHODES.ALBERT.N.III.1175488622 Digitally signed by RHODES.ALBERT.N.III.1175488622 DN: c=US, o=U.S. Government, ou=DoD, ou=PKI, ou=USAF, cn=RHODES.ALBERT.N.III.1175488622 Date: 2013.04.30 12:03:37 -05'00'

ALBERT N. RHODES, PhD
Chief, Airbase Technologies Division

This report is published in the interest of scientific and technical information exchange, and its publication does not constitute the Government's approval or disapproval of its ideas or findings.

REPORT DOCUMENTATION PAGE

Form Approved
OMB No. 0704-0188

PLEASE DO NOT RETURN YOUR FORM TO THE ABOVE ADDRESS.

1. REPORT DATE *(DD-MM-YYYY)*	2. REPORT TYPE	3. DATES COVERED *(From - To)*
28-FEB-2013	Final Technical Report	08-FEB-2006 -- 30-SEP-2012

4. TITLE AND SUBTITLE

Evaluation of the Performance of Iodine-Treated Biocidal Filters Under the Influence of Environmental Parameters

5a. CONTRACT NUMBER

FA8650-06-C-5913

5b. GRANT NUMBER

5c. PROGRAM ELEMENT NUMBER

0909999F

6. AUTHOR(S)

Woo, Myung-Heui; Li, Hsing-Wang; Wu, Chang-Yu

5d. PROJECT NUMBER

GOVT

5e. TASK NUMBER

L0

5f. WORK UNIT NUMBER

X0CJ (QL102008)

7. PERFORMING ORGANIZATION NAME(S) AND ADDRESS(ES)

Engineering School of Sustainable Infrastructure and Environment
Department of Environmental Engineering Sciences, University of Florida
406 Black Hall, P.O. Box 116450
Gainesville, FL 32611-6450

8. PERFORMING ORGANIZATION REPORT NUMBER

9. SPONSORING/MONITORING AGENCY NAME(S) AND ADDRESS(ES)

Air Force Research Laboratory
Materials and Manufacturing Directorate
Airbase Technologies Division
139 Barnes Drive, Suite 2
Tyndall Air Force Base, FL 32403-5323

10. SPONSOR/MONITOR'S ACRONYM(S)

AFRL/RXQ

11. SPONSOR/MONITOR'S REPORT NUMBER(S)

AFRL-RX-TY-TR-2013-0016

12. DISTRIBUTION/AVAILABILITY STATEMENT

Distribution A. Approved for public release; distribution unlimited.

13. SUPPLEMENTARY NOTES

Ref Public Affairs Case # 88ABW-2013-2355, 15 May 2013. Document contains color images.

14. ABSTRACT

This project final report summarizes a collaborative effort to evaluate the ability of a patented product in which a contact-transfer disinfectant, poly(4-styrene[trimethylammonium]methyl triiodide) [PSTI] is incorporated into an air filter medium to disinfect penetrating bioaerosols. After several false starts a quenching experiment capturing MS2 phage particles filtered through PSTI and captured in thiosulfate solution in an impinger showed that the iodine--aerosol chemistry is slow, and that earlier work based on capture-and-culture methods are blinded by the efficiency of kill by iodine in any aqueous medium. Moderate dependencies of bioaerosol characteristics and stability on environmental conditions and delivery medium were measured and reported. A device and method to achieve reproducible, controlled deposition of viable viral and bacterial aerosol droplets was developed, which created a tool for "standardized contamination" of test articles that can be used to quantify and compare cleaning and decontamination methods. Alternative approaches to on-the-fly disinfection were developed and tested as possible alternatives to PSTI or another reactive air filtration medium as an enhancement to protectivity of next-generation individual and collective respiratory protective gear---particularly in potentially infective environments---and HVAC filters.

15. SUBJECT TERMS

antimicrobial, bioaerosol, contamination, disinfection, filter, iodine, MS2 coli phage, respiratory protection

16. SECURITY CLASSIFICATION OF:			17. LIMITATION OF ABSTRACT	18. NUMBER OF PAGES	19a. NAME OF RESPONSIBLE PERSON
a. REPORT	b. ABSTRACT	c. THIS PAGE			Joseph D. Wander
U	U	U	SAR	101	19b. TELEPHONE NUMBER *(Include area code)*

Reset

Standard Form 298 (Rev. 8/98)
Prescribed by ANSI Std. Z39.18

TABLE OF CONTENTS

LIST OF FIGURES iii
LIST OF TABLES v
PREFACE vi
1. SUMMARY 1
1.1. Objective 1
1.2. Background 1
1.3. Scope 1
1.4. Methodology 2
1.5. Test Description 2
1.6. Results 3
1.7. Conclusions 4
1.8. Recommendations 4
2. INTRODUCTION 6
2.1. Objective 6
2.2. Background 6
2.2.1. Biological threat 6
2.2.2. Viral Aerosols 6
2.2.3. Transmission Mode 7
2.2.4. Filtration 7
2.2.5. Decontamination Methods 8
2.2.6. Antimicrobial Chemicals 8
2.2.7. UV Decontamination 10
2.2.8. Microwave Decontamination 10
2.3. Scope 11
2.4. Approach 12
3. EXPERIMENTAL 14
3.1. Test Microorganisms 14
3.2. Effects of Relative Humidity and Spray Medium on Survivability of Viral Aerosols 14
3.3. Effects of Bioaerosol on the Release of Iodine from Iodine-Treated Filter 17
3.3.1. Experimental System 17
3.3.2. Iodine Analysis 17
3.4. Method for Contaminating Filtering Facepiece Respirators by Deposition of MS2 Viral Aerosols 18
3.4.1. Nebulization Fluid Preparation 18
3.4.2. Test Material 18
3.4.3. Droplet/Aerosol Loading System Design 18
3.4.4. Chamber Operation and Determination of Operating Conditions 20
3.4.5. Statistical Analysis 21
3.5. Effects of Relative Humidity and Spraying Medium on UV Decontamination of Viral Aerosols/Droplet Loaded Filter 21
3.5.1. Spraying Medium 21
3.5.2. Droplet and Aerosol Loading System 21
3.5.3. UV Exposure 22

3.6. Microwave-Irradiation-Assisted Filtration for Inactivation of Viral Aerosols 23
3.6.1. Experimental System 23
4. RESULTS 26
4.1. Effects of RH and Spray Medium on Survivability of Viral Aerosols 26
4.1.1. Collection Efficiency of BioSamplers 26
4.1.2. Particle Size Distribution of MS2 in Different Environmental Conditions 27
4.1.3. Particle size distribution of infectious MS2 28
4.2. Effects of Bioaerosol on the Release of Iodine from PSTI-treated Filter 31
4.3. Method for Contamination of Filtering Facepiece Respirators by Deposition of MS2 Viral Aerosols 33
4.3.1. Determination of Operating Conditions 33
4.3.2. Droplet Size Distribution 35
4.3.3. Loading onto NIOSH-certified FFRs 37
4.4. Effects of Relative Humidity and Spray Medium on UV Decontamination of Filter Loaded with Viral Aerosols 38
4.4.1. Effect of Transmission Mode with Different Media 38
4.4.2. Effect of RH during both Loading and Inactivation 42
4.4.3. Virus Susceptibility 43
4.5. Inactivation of Viral Aerosols by Microwave-Irradiation-Assisted HVAC Filtration 44
4.5.1. Temperature Measurement of Test Filters 45
4.5.2. Inactivation Efficiency and Survival Fraction 46
4.5.3. Effective Temperature 48
4.5.4. Effect of relative humidity on inactivation performance 51
4.5.5. Degradation of Filters after Microwave Irradiation 52
4.5.6. Comparison to other Disinfection Technologies 52
5. CONCLUSIONS AND RECOMMENDATIONS 53
5.1. Conclusions 53
5.2. Recommendations 54
6. REFERENCES 55
Appendix A: Preliminary Test for Droplet Loading Chamber 65
Appendix B: Microwave-Assisted PAN Nanofiber Filtration System for Viral Aerosol 70
LIST OF ABBREVIATIONS, SYMBOLS AND ACRONYMS 72

LIST OF FIGURES

Figure 1. Schematic Diagram of the Experimental Setup for Evaluating the Effect of Relative Humidity and Spray Medium on the Survivability of Viral Aerosols: A) the System Used to Determine the Collection Efficiency of BioSampler as a Function of Particle Size (Task 1) and B) the System Used to Measure Particle Size Distribution (Task 2) and to Enumerate Viable (Task 3) and Total (Task 4) Viruses 14
Figure 2. Schematic of Experimental System for Evaluating Iodine Release Induced by Bioaerosol 17
Figure 3. Schematic diagram of the droplet loading system: A) entire system, B) distributor on top, C) turntable, D) air outlet at bottom. (a) and (b) are needed only in certain conditions. 19
Figure 4. Schematic Diagrams: A) Droplet Loading System and B) Aerosol Loading System 22
Figure 5. Experimental Setup for Microwave-Irradiation-Assisted Filtration 23
Figure 6. Collection Efficiency of BioSampler as a Function of Particle Diameter with Sampling Flow Rates of 4.5 and 12.5 LPM 26
Figure 8. Particle Size Distribution of Number- (Solid) and Mass-based (Empty) MS2 Aerosols Obtained from Monitoring the SMPS and Infectious Viruses (Cross) through Plaque Assay. Error Bar Indicates the Standard Deviation of Triplicate Test 28
Figure 9. Infectious MS2 per Particle Generated in DI Water as a Function of Particle Size at Three Relative Humidities. Dashed Line Represents the Theoretical PFU per Particle. Error Bar Indicates the Standard Deviation of Triplicate Tests 29
Figure 10. Stability factors of MS2 as a function of diameter at three relative humidities: A) DI water, B) beef extract, and C) artificial saliva 30
Figure 11. Calibration Curve for the DR/4000 V Spectrometer 32
Figure 13. CVs for Q-T-Q and S-T-S as a Function of Turntable Speed 34
Figure 14. Scanning Electron Microscopic Images: A) Untreated FFR and B) Treated FFR at 250× 35
Figure 15. Size Distribution of Droplets Generated by Ultrasonic Nebulizer at Five Flow Rates: A) Number- and B) Mass-based 35
Figure 16. The Number- and Mass-based Particle Size Distributions of Generated Droplets and Loaded Droplets at 2 Lpm through the Aerosol Generator Plus 3 Lpm Dry Air at 2-rpm Turntable Speed 36
Figure 17. Recovery of Viable MS2 as a Function of Extraction Time for Three FFRs 38
Figure 18 Log Inactivation Efficiency (IE) by UV Exposure at HRH for Droplet and Aerosol Transmission Modes as a Function of UV Irradiation Time in Different Nebulizer Media at HRH during Virus Loading 39
Figure 19. SEM images of a Filter Contaminated with Viruses Aerosolized in A) and B) DI Water, C) and D) 0.3% Beef Extract, E) and F) Artificial Saliva, and G) and H) Artificial Saliva without Mucus under HRH. Magnification of A), C), E), and G) 3,000× and B), D), F), and H) 30, 000× 40
Figure 20. Log IE Virus Loading and UV Exposure at HRH for Aerosol Transmission Mode from 0.3% and 0.6% Mucin-free Artificial Saliva and 0.3% Salt-free Artificial Saliva as a Function of UV Irradiation Time 41

Figure 21. Log Natural Decay and Inactivation Efficiency as a Function of Relative Humidity during Both Loading and UV Inactivation: A) DI Water, B) 0.3% Beef Extract, and C) Artificial Saliva 42
Figure 23. Temperature of the Filters as a Function of Microwave Application Time at Three Different Microwave Power Levels 46
Figure 24. Log Inactivation Efficiency and Log Survival Fraction: A) and B) Filter 1, C) and D) Filter 2, and E) and F) Filter 3 47
Figure 25. Microwave Inactivation Performance: A) Log Inactivation Efficiency and B) Log Survival Fraction As a Function of the Temperature Reached during Microwave Irradiation of Filter 1 for 125, 250 and 375 W and Filter 3 for 500 and 750 W 48
Figure 26. Temperature of Microwave and Conventional Ovens As a Function af Application Time. The Error Bar Represents One Standard Deviation. 50
Figure 27. SEM Images: A) Untreated,Virus-contaminated Filter, B) Conventional-heat-treated, Virus-contaminated Filter, and C) Microwave-treated, Virus-contaminated Filter at 50,000× Magnification 50
Figure 28. Log Inactivation Efficiency by Microwave-irradiation-assisted Filtration System and Log Survival Fraction on Filter Surface As a Function of Microwave Power Level: A) and B) for 5 min/cycle and C) and D) for 10 min/cycle 51

LIST OF TABLES

Table 1. Composition of Artificial Saliva (Based on 979 mL of DI Water)
Table 2. Slope of least squares regression for NPFU as a function of particle size for different spray medium at three relative humidities 29
Table 3. Slope of least squares regression for NRNA as a function of particle size for different spray medium at three relative humidities 30
Table 4. Iodine concentration and its experimental conditions of each test 32
Table 6. Statistics in General Factor Analysis of Variances 42
Table 7. Virus susceptibility factor K (m2/J) for aerosol transmission under different conditions 44
Table 8. Virus susceptibility factors (m2/J) from other studies 44
Table 9. Linear relationship of the IE and SF of MS2 with temperature (T) 49
Table 10. Pressure drop of the filter at face velocity of 5.3 cm/s before and after microwave treatment at 375 W for 10 mins/cycle 52

PREFACE

This report was prepared by the Aerosol and Particulate Research Laboratory, Department of Environmental Engineering Sciences, Engineering School of Sustainable Infrastructure and Environment, University of Florida, Gainesville, FL 32611-6450, under Contract Number FA8650-06-C-5913 for the Air Force Research Laboratory (AFRL/RXQ), 139 Barnes Drive, Tyndall AFB, FL 32403-5323.

This is a final report being submitted to AFRL/RXQ. It describes work that was performed from August 2006 to December 2012. The Air Force technical program monitor was Dr. Joseph D. Wander. We greatly appreciate the assistance and valuable advices of Triosyn Corp., Dr. Dale Lundgren at the University of Florida, Dr. Chang-Yul Cha of Cha Corporation and Dr. Yu-Mei Hsu of Wood Buffalo Environmental Association. We also thank Diandra Anwar and Adam Grippin from the Department of Chemical Engineering and Tamara Smith from the Department of Environmental Engineering Sciences at the University of Florida for their assistance in the laboratory.

1. SUMMARY

1.1. Objective

The overall objective of this project was to evaluate the effectiveness of a triiodide resin filter as a disinfectant for viral aerosols under the influence of environmental parameters. The research findings also led to additional objectives to assess the effects of relative humidity and spraying media on the survivability of viral aerosols, and to examine the effects of viral aerosols on the release of iodine from the triiodide resin filter. For comparison, the performance of different decontamination techniques, including ultraviolet (UV) light and microwave irradiation, was also investigated. Ultimately, the goal was to advance our knowledge in the behavior of viral aerosols and to develop technologies that can better protect the general public as well as healthcare workers against respiratory infection by viral aerosols.

1.2. Background

The increasing threat of biological warfare and the spread of airborne pathogens among populations have spurred the public's attention on bioaerosols and the call for developing protection methods. The triiodide resin filter has been proposed as an effective means for protection of the public and healthcare workers against airborne viral agents. Results from previous studies of its capability to disinfect airborne viral agents appeared strongly positive. However, the effects of environmental parameters including relative humidity and spraying medium on such a biocidal filter had not been examined. We saw a clear opportunity to evaluate such effects by studying the behavior of viral agents under the influence of these environmental parameters. The effect of viral aerosol on the release of iodine from the triiodide filter was also a question to be clarified; it was suggested that the negative charge on the bioaerosol could induce the release of iodine from the filter.

Various techniques have been developed to capture and inactivate airborne biological agents. UV irradiation is a conventional approach that has long been considered effective for disinfecting viral aerosols. Microwave irradiation is a technique recently proposed for disinfecting airborne microbial agents. However, fair comparisons of their performance had been challenging because standard test conditions with reproducible loading of the agents had not been developed. A standard protocol that would allow such a comparison was needed. Examination of the effects of the environmental parameters on these technologies was also warranted. A comprehensive study of the development and evaluation of inactivation technologies based on the characteristics of the viral aerosol could lead to effective mitigation of the respirator stockpile shortage problem. It would also provide novel means for alleviating the threat of disease transmission by viral aerosols.

1.3. Scope

This project consisted of five tasks: 1) investigating the stability of MS2 virus under different relative humidities (RHs) and spraying media; 2) examining the effects of bioaerosol on the release of iodine from the triiodide resin filter; 3) developing a method for consistent, controlled delivery of droplets containing viral agents onto surface to allow for fair comparison of different

contamination technologies; 4) assessing the effects of RH and spraying medium on UV decontamination of respirators loaded with viral aerosols and viral droplets; 5) Evaluating microwave-irradiation-assisted filtration for capture and inactivation of viral aerosols.

1.4. Methodology

MS2 bacteriophage (MS2; ATCC®, 15597-B1™) was used as the challenging agent. Artificial saliva (AS) was used as a nebulization fluid to emulate droplets generated by coughing and sneezing. A droplet/aerosol loading system was custom-built for this study. Six samples were placed onto the supports on the turntable using sterile forceps. Theoretically, a titer of around 10^7 plaque-forming units (PFU)/mL in the ultrasonic nebulizer with 5-min loading time should provide sufficient loading density ($>10^3$ PFU/cm^2). Three types of spraying media were tested: deionized (DI) water, beef extract (BE) and AS. DI water was included to explore properties of the naked virus.

In assessing the effects of RH and spray medium on the stability of aerosolized virus, four types of characterization were performed: collection efficiency of BioSamplers, virus particle size distribution (PSD) by scanning mobility particle sizer (SMPS), plaque assay for virus infectivity, and polymerase chain reaction (PCR) analysis for total virus count. To examine the effects of bioaerosol on the release of iodine from the triiodide resin medium, MS2 aerosol was treated with or without charge neutralization. The treated viral aerosol was then passed through an iodine-treated filter medium. In addition, DI water was nebulized as the baseline condition.

To evaluate respirator decontamination by UV irradiation, droplets and aerosols containing viruses were loaded in differing spray media onto filtering facepiece respirators (FFRs). They were then exposed to UV light under different RHs. Two commercial heating, ventilation and air conditioning (HVAC) filters made of polyethylene–polypropylene and of a synthetic polymer were compared with a glass microfiber filter in an investigation of disinfection by microwave irradiation. A 2.45-GHz microwave oven with holes in the backside was used in this study.

1.5. Test Description

Droplets of three spray media produced by an ultrasonic nebulizer or a Collison nebulizer entered the chamber and loaded onto the surface of FFR coupons for 5 min. The frequency of the ultrasonic generator was 2.4 MHz and the environmental conditions were 20 ± 2 °C and 35 ± 5% RH. Various operating parameters were evaluated to identify conditions that provide desired droplet characteristics, including loading time (1–30 mins), virus titer (10^7–10^8 PFU/mL), turntable speed (0–3 rpm), airflow rate (1–5 Lpm), and mucin concentration (0.3–0.9%).

PSL particles of different sizes from 30 nm to 300 nm were used to determine the collection efficiency of BioSamplers at specific sizes and flow rates. MS2 in three spraying media (DI water, 0.3 % BE, and AS) was used instead of PSL particles in DI water. To elucidate the effect of RH on the stability of viruses, three RHs ((i.e., low RH (LRH, 30 ± 5%), medium RH (MRH, 60 ± 5%), and high RH (HRH, 90 ± 5%)) were applied. The liquid sample assayed was also used for PCR to determine the concentration of total viruses including infectious and non-infectious viruses, based on an assumption of no RNA distortion during the test.

The concentration of I_2 collected in the BioSampler medium was analyzed by the *N*, *N*-diethyl-*p*-phenylenediamine (DPD) colorimetric method. I_2 collected in the solution reacts with DPD to form a pink color, the intensity of which is proportional to the total I_2 concentration. A 10-mL sample of the collection medium was analyzed at 530 nm wavelength. Each filter was then cut into four equal quadrants for UV exposure at 1.0 mW/cm^2 from a UV-C (254 nm) lamp 10 cm above the samples.

In-flight microwave decontamination of two commercial HVAC filters and a glass microfiber filter was tested. Microwave irradiation was applied for three 10-min cycles that included selected periods of irradiation—1, 2.5, 5 and 10 min/10-min cycle—at three microwave power levels, 125, 250 and 375 W. To select the microwave application conditions, the thermal stability of three test filters was analyzed by thermogravimetric analysis (TGA) with simultaneous differential thermal analysis (TGA–SDTA), and the temperature (*T*) of filters on an SiC disk under different applied conditions was measured with an infrared (IR) pyrometer.

1.6. Results

PSDs of both infectious and total viruses in solute-free water followed a volumetric size distribution, whereas those aerosolized in a spray medium followed a lower size dimension, e.g., surface or number. Aggregation of MS2 and encasement by inert salts enhanced stability because of shielding effects and reduction of the air–water interface. MS2 aerosols generated in a gel-forming medium (AS) showed the protective effect but no discernible effect of RH.

In a study of iodine release induced by bioaerosol, the baseline experiment (DI water) measured iodine concentrations of 0.014 and 0.024 mg/L, respectively, before and after penetrating the test filter. Adding bioaerosol raised the corresponding concentrations to 0.017 and 0.0285 mg/L. The presence of bioaerosol showed no statistically observable influence on the release of iodine from the filter, although the data were close to the method detection limit.

Respective CVs (coefficients of variation) for S-T-S (sample-to-sample) and Q-T-Q (quarter-to-quarter) for six National Institute for Occupational Safety and Health (NIOSH)-certified FFRs tested were lower than 20% and 40%. Droplet size could be altered by tuning the frequency of the ultrasonic nebulizer, by changing the composition of the dispersion aerosolized and by adjusting *T* and RH inside the chamber. Droplets emulating bioaerosols released by coughing and sneezing could be produced using specific conditions and any loading density could be achieved by controlling the loading time and the virus titer in the nebulization medium.
For MS2 exposed to UV disinfection, the IE (inactivation efficiency) was lower following droplet transmission than that following aerosol transmission, largely owing to the higher water content of the larger droplets, which shielded viruses from UV exposure. The virus susceptibility factor *K* was lower for viruses in BE and AS than in DI water, which was attributed to protective effects exerted by solids present in the respective media. The protective effect of solids followed the order water-insoluble solid (BE powder) > water-insoluble viscous solid (mucin) > water-soluble solid (salts). When these solids were present, RH was not a significant variable in decontamination by UV exposure. The susceptibility factor obtained for the target microbial species can be used to determine the appropriate UV dose for surface decontamination.

Microwave power and application time were key operating parameters for controlling the effectiveness of disinfecting viral agents. Both factors combined to yield a threshold temperature near 90 °C. Both survival fraction (SF) and IE changed sharply above the 90 °C threshold temperature, and they reached 2 log at 109 and 116 °C, respectively. RH was another pivotal parameter for viability of viruses at medium temperature, but it became insignificant at high temperatures above 90 °C. The temperature can be selected using two simple equations below, if the target IE and survival fraction (SF) are known:

$$\log IE - \log IE_{\text{inherent filtration}} = \log IE_{\text{microwave}} = -7.57 + 0.08\,T$$

$$\log SF = 5.01 - 0.06\,T$$

If thermally stable filter material was applied, a high IE of around 5 logs through the system could be reached at lower temperatures compared to other dry heat treatments.

1.7. Conclusions

Both PSDs of infectious and total viruses in pure media without solute follow volumetric size distribution, whereas those in spray medium with solute follow a lower dimension size. Aggregation by MS2 itself and encasement by inert salts contribute to a higher stability factor because of shielding effect and reduced air/water interface. In addition, for MS2 aerosols generated in gel-forming media (e.g., AS), the protective effect is present but less than inert salts would provide.

The experiments using a charge neutralizer exhibit no observable difference in the results of induced release of iodine from the iodinated resin filter. However, the data are too close to the detection limit (0.024 mg/L) to allow any meaningful conclusion to be drawn whether MS2 bioaerosol has any significant effect on the release of iodine from iodine treated filter.

A droplet/aerosol loading system has been successfully developed for proper evaluation and comparison of different techniques for decontamination. This system can produce representative human respiratory secretions and can be applied for consistent and controlled delivery of aerosolized droplets containing viral agents. Because this system can be applied for inactivation of air or objects contaminated by all transmission modes, i.e., aerosol, droplet, and contact transmissions, it can be used to design proper protocol for decontamination test.

RH and the solid component in spraying medium are important parameters for UV disinfection of filters. High water content that absorbs UV and shielding of viruses near the center of the aggregate are responsible for low inactivation. When a protective medium is present, RH is not a significant parameter. For inactivation through microwave-irradiation assisted HVAC filtration system, the distortion due to thermal effect is one major mechanism. RH is a significant parameter from 50~80 °C, but it ceases to be significant above 90 °C.

1.8. Recommendations

Further studies are needed to apply the novel decontamination methods against viral aerosols:

1) Development of an analytical model for disposition of viruses in aerosol in different spray media. The model can be a very useful tool in designing an effective strategy to improve filtration and IE and for assessing the risk by respiratory deposition of viral aerosol.
2) Characterization of virus from 20–230 nm was not enough to complete the model. To further expand the applicability of the model, the stability factor of a wider size range should be included.
3) Further studies to elucidate the aggregation and encasement by transmission electron microscopy (TEM) will be helpful. TEM can be taken after staining the lipid with selective concentration of dye (uranyl acetate). Although higher dye concentration allows easy observation of the morphology of MS2, it can also alter the isoelectric point, resulting in different aggregation modes. Hence, after determining the optimal dye concentration for MS2, the morphology by TEM should be observed.
4) Microwave-incorporated HVAC ventilation system for practical applications should be tested because energy cost is another important factor in evaluating its performance.

2. INTRODUCTION

2.1. Objective

The ultimate goal of the project was to advance our knowledge of the behavior of viral aerosols and to develop technologies that can better protect both the general public and healthcare workers against respiratory infections by viral aerosols. The overall objective of this project was to evaluate the effectiveness of the triiodide resin filter as a device for disinfection of viral aerosols as a function of environmental parameters. The effects of RH and spray media on the survivability of viral aerosol were assessed, and the effects of viral aerosol on the release of iodine from the triiodide resin filter were examined. A method was devised that effects consistent and controlled delivery of droplets containing viral agents onto surfaces, which allows fair comparison of effectiveness of different decontamination technologies. For comparison to the triiodide chemistry, different decontamination techniques, including UV light and microwave irradiation, were developed, and their performance was investigated.

2.2. Background

2.2.1. Biological threat

The public's level of concern about bioterrorism and airborne pathogens has significantly increased in recent years (Lee 2011; Xu et al. 2011). During the 20th century, three major influenza pandemics occurred, each from a major genetic change in the influenza strain: the Spanish flu in 1918 (20–100 million deaths), the Asian flu in 1956 (2 million deaths), and the Hong Kong flu in 1968 (1 million deaths). The 2002 and 2003 Severe Acute Respiratory Syndrome (SARS) epidemic caused more than 8000 reported cases and 700 deaths. The recent swine flu outbreak, due to a new strain of H1N1 influenza A, had caused illness in over 70 countries and resulted in at least 14,000 deaths worldwide by October 2009 (ECDC 2009). On June 11, 2009, the World Health Organization (WHO) raised the pandemic alert level to Phase 6, indicating the onset of a global pandemic (CDC 2009). Reporting of these incidents raised the public's awareness of and concern about respiratory viruses of low infectious dose and the spread of airborne pathogens.

2.2.2. Viral Aerosols

Bioaerosols are airborne particles with biological origins, such as nonviable pollen, and viable fungi, bacteria, and viruses (Hinds 1999). The adverse health effect of bioaerosols depends on several factors, such as microorganism type and dose. Among them, a virus is the smallest in size (Prescott et al. 2006). Although the size of a single virion is small (20–300 nm), viruses in Nature exist in a wide range of sizes because they aggregate with other virions, attach onto other material, and can be encased inside droplets of respiratory secretions. One important concern of the aggregates is the adverse health effect imposed by the deposition in the respiratory system. Inhaled particles can deposit in various respiratory regions. After deposition, the aggregates may disperse into individual virions. More than 400 different viruses with different infective doses (IDs) cause human diseases—e.g., rubella, influenza, measles, mumps, smallpox and pneumonia—which involve the respiratory system either directly or indirectly. Aggregation, attachment and encasement of viruses also facilitate resistance to environmental stresses, such as heat, dryness, toxic gases, and UV light because of a shielding effect (Kowalski 2007). Although

the aggregation state of viruses with other materials and infectivity of viruses in aggregates under different environmental stresses are key parameters to assess their health risk, very limited research has been carried out with respect to this aspect.

2.2.3. Transmission Mode

An understanding of the transmission modes of viral aerosols is critical to protecting the public against major airborne pathogen pandemics. Effective prevention and treatment of infectious viral aerosols (i.e., vaccination and respiratory protection) also require specific information on the transmission mode. For the spread of infectious viruses, there are three recognized transmission modes (IOM 2006):

1) Droplet transmission mode—Droplet transmission results from infected individuals generating droplets containing microorganisms by coughing, sneezing, singing and talking,
2) Contact transmission mode—Contact transmission includes both direct body-to-body contact and indirect contact through a contaminated object (fomite—e.g., needle or towel). This mode frequently occurs in a healthcare facility, and
3) Aerosol transmission mode—Aerosol transmission includes the dispersion of droplet nuclei, which remain airborne after evaporation of a droplet, and dust particles to which the microorganism adheres.

2.2.4. Filtration

Filtration is one of the most commonly used methods for collecting aerosols because of its low cost and simple technology, and aerosol filtration has been widely applied in various applications such as respiratory protection, air purification and clean rooms (Hinds 1999). Several mechanisms, including interception, impaction, diffusion, gravity and electrostatic force determine filtration efficiency (FE). At the most-penetrating particle size (MPPS), FE is mainly determined by three mechanisms (Hinds 1999): (1) *interception*, by which particles following an airstream flow line come within one radius of a fiber and adhere to it; (2) *impaction*, whereby larger particles fail to follow the curving contours of airstreams around the fiber and strike the fiber; and (3) *diffusion*, a result of the collision of small particles with gas molecules, which deflects their path through the filter. To improve filtration performance, electret and nanofiber (NF) media have also been introduced (Barrett and Rousseau 1998; Lehtimaki and Heinonen 1994; Li et al. 2009; Wang 2001; Wang et al. 2008; Yang et al. 2007; Yang and Lee 2005; Yun et al. 2007). Electret filters utilize electrostatic attraction to improve aerosol collection, and NF filters lower the flow resistance through gas slip over the smaller-diameter fibers.

A high-efficiency particulate air (HEPA) filter is defined as one having at least 99.97% FE for 0.3-μm diameter particles, which is the nominal MPPS. HVAC systems with HEPA filters can effectively control and reduce airborne contaminants—including bioaerosols—based on the above mechanisms; however, reaerosolization of viruses collected inside an HVAC system in hospitals and residential buildings is a potential problem with this control strategy.

Surgical masks and respirators belong to another type of filters for individual protection. Surgical masks approved by the Food and Drug Administration (FDA) and FFRs certified by NIOSH are intended to be worn by healthcare persons and the general public during a pandemic event (CDC

2012; FDA 2007; Rengasamy et al. 2004). Viral aerosols may be filtered by the fibers of a regular surgical mask through diffusion. Also, aggregated viruses may be captured by impaction and interception. However, using surgical masks and N95 FFRs as countermeasures for bioaerosols has not been demonstrated to provide a complete response:

1) Although using surgical masks and N95 FFRs for tuberculosis has been shown to meet Centers for Disease Control (CDC) guidelines, the same has not yet been done for viral agents such as the swine flu virus.
2) There is no experimental basis upon which the FFR's life span in an H1N1 scenario can be estimated.
3) The stockpile of FFRs will be exhausted in the event of a severe pandemic. CDC estimates that more than 90 million FFRs will be required for healthcare workers in the US if a pandemic influenza event persists for 42 days (IOM 2006).

2.2.5. Decontamination Methods

One possible approach to augment insufficient supplies of FFRs is to decontaminate the FFRs by using disinfection agents or processes, such as heating, microwave irradiation, UV irradiation, bleach solution or peroxides and then for the original wearer to reuse the decontaminated respirator. Thermal treatment of microorganisms is the conventional approach, and the effectiveness of a high-*T*, short-exposure process toward bioaerosols has been demonstrated (Grinshpun et al. 2010; Jung et al. 2009; Lee and Lee 2006). High-*T* exposure can cause the denaturation of proteins by breaking the structures of polypeptides (Madigan and Martinko 2006). One concern about FFRs decontaminated by application of thermal treatment is the possibility of changing the FFR's characteristics. The second important criterion for a good decontamination method is that residues of any chemicals used in the process impose no adverse health effect on the wearer.

At the start of this project no realistic protocol existed for testing the efficacy of a decontamination method. First, there was no standard method for applying bioaerosol contamination to FFRs. Second, the unique properties of bioaerosols generated by respiratory secretions may affect the effectiveness of the decontamination process, and operating conditions to deposit bioaerosols with controlled and consistent properties were not available. Thus, an opportunity was present to develop methods that can consistently produce representative human respiratory secretions and a device that consistently aerosolizes, for an hour or longer, droplets of controlled size containing viral agents that, taken together, provide a tool to properly evaluate and compare decontamination techniques.

At the outset of this project, several inactivation methods existed that can be applied to decontaminate filters loaded with viral aerosol (Brion and Silverstein 1999; Fisher et al. 2009; Lee et al. 2009; Zhang et al. 2010), including antimicrobial chemicals, UV irradiation and microwave irradiation.

2.2.6. Antimicrobial Chemicals

Enhanced protection against infection by airborne bioparticles can be achieved by integrating topical antimicrobials such as silver and copper into filtration media (Borkow and Gabbay 2004; Cecchini et al. 2004; Lee 2011; Pollini et al. 2009; Sharma et al. 2009). Silver—one of the most

commonly used antimicrobials—has been used in the form of colloidal silver for more than 100 years and has been registered as a biocidal material in the United States since 1954 (Nowack et al. 2011). Yoon et al. (2008) evaluated antimicrobial activity of silver nanoparticles (NPs) coated on an activated carbon fiber (ACF) filter and reported complete inhibition of captured *Escherichia coli* and *Bacillus subtilis* within 10 and 60 min, respectively. Jung et al. (2011) reported that a hybrid carbon nanotube (CNT)/silver NP medium outperformed silver NPs alone or CNT alone for inactivating airborne *E. coli* and *Staphylococcus epidermidis*. Rengasamy et al. (2010) reported that four different biocidal filters (silver–copper-, envizO3-, iodine-, and TiO_2-treated filters) showed relative SFs of 0.25–0.79 and 0.001–0.08 at LRH and HRH, respectively. These additives are effective against microorganisms captured on the filtration medium. However, they exert no effect on microorganisms that penetrate the filter so, to decrease the risk of respiratory infection, a filtration medium would need to exhibit downstream antimicrobial capability for penetrating pathogens.

The exquisite efficiency of the polystyrene-4-(trimethylammonium)methyl triiodide ion-exchange resin (PSTI) as a broad-spectrum disinfectant in water was documented nearly half a century ago (Fina et al. 1982; Hatch et al. 1980; Lambert et al. 1980; Marchin et al. 1983; Taylor et al. 1970). The material was later patented as a reactive component of air filtration media for enhanced respiratory protection against pathogenic aerosols (Di Ionno and Messier 2004; Messier 1999; Messier 2000). The antimicrobial capability of PSTI can be ascribed to the reaction of iodine with select amino acids. The interaction results in disruption of microbial proteins, and it has been proposed to occur through near-contact transfer of iodine to microbial particles when they penetrate the filter (Ratnesar-Shumate et al. 2008). Its capability for inactivating airborne bacteria and viruses has been reported in several studies (Foarde et al. 2000; Heimbuch et al. 2004; Heimbuch and Wander 2006; Ratnesar–Shumate and Wu 2004; Ratnesar–Shumate et al. 2008). Other studies that also lacked appropriate controls reported no difference in the performance between conventional and iodine-treated FFRs for penetrating bioaerosols (Eninger et al. 2008; Lore et al. 2012). The capacity of various proteins (such as gelatin or bovine serum albumin, BSA) to take up iodine (Eninger et al. 2008), the reversibility of iodine attachment (Lee et al. 2009) and the use of water-based collection and analytical media, which are known to create an efficient kill mechanism (Taylor et al. 1970) combine to form challenges to attaining a definitive measurement to verify the antimicrobial mechanism of PSTI as well as its practical significance. Investigation using impingers containing sodium thiosulfate for collecting iodine exposed bioaerosol samples has proven useful at quenching available iodine, thereby eliminating further effects of iodine during culture (Berg et al. 1964; Lee et al. 2009).

Filters using NFs have also been demonstrated to be effective in inactivating microorganisms, in addition to the advantage of lowering pressure drop for filtration. CNTs exhibit strong toxicity toward *E. coli* (Brady–Estevez et al. 2010; Kang et al. 2009), and Xu and Yao (2011) reported the collection and inactivation of airborne microbial species using a CNT filter. Ceramic NF filters, on the other hand, can strongly adsorb and retain viruses on their high surface area, preventing any reaerosolization (Li et al. 2009).

The general limitation of an antimicrobial-treated filter is occlusion by abiological dust deposited on the filter surface during use. Therefore, how to avoid the deposition of dust on a biocidal filter becomes an important design consideration. Alternative approaches include development of hybrid methods that combine filtration with other control methods (Lee 2011).

2.2.7. UV Decontamination

UV light has sufficient energy to be a practical antimicrobial method. UV irradiation is now a common method for inactivating a wide variety of biological agents and in particular airborne microorganisms (Prescott et al. 2006). Recent increases in the incidence of airborne diseases such as tuberculosis have focused attention upon the use of UV. UV light at a wavelength of 254 nm strikes biological cells and the energy is specifically absorbed by adjacent thymine nucleotide bases in deoxyribonucleic acid (DNA), causing them to form covalent bonds with each other rather than with adenine bases in the complementary DNA strain (Perier et al. 2012). Pyrimidine dimers from thymine distort the shape of DNA and change the double-helical structure, making it impossible for the cell to accurately transcribe or replicate its genetic material, which ultimately leads to the death of the cell (Kowalski 2009; Prescott et al. 2006).

UV intensity, exposure time, lamp placement, air movement patterns and RH of the air affect the effectiveness of UV. Most studies focused on UV intensity and exposure time to increase disinfection efficacy (Beggs et al. 2006; Chang et al. 1985; Chuaybamroong et al. 2011; Duleba–Majek 2009; Kujundzic et al. 2007; Kujundzic et al. 2006; Kujundzic et al. 2005; Memarzadeh et al. 2010; Menzies et al. 2003; Rastogi et al. 2007; Ryan et al. 2010; Tseng and Li 2005; Viscusi et al. 2009; Xu et al. 2003). Peccia et al. (2001) pointed out the importance of RH to the performance of UV inactivation. Lin and Li (2002) observed lower susceptibility of *E. coli*, *B. subtilis* spores, cells of *Candida famata* var. flareri, and spores of *Penicillium citrinum* at 80% RH compared to 50% RH. Peccia and Hernandez (2001) observed higher photoreactivation of *Mycobacterium parafortuitum* by a factor of 4 at 95% RH than at 40%. Peccia and Hernandez (2004) also examined the effect of RH on the performance of UV irradiation to inactivate airborne *M. bovis* and *Bacillus* Calmette–Guerin (BCG) and reported a two-log higher rate at 50% RH than at 95% RH. Xu et al. (2005) reported significant degradation in UV inactivation of airborne *M. parafortuitum* when RH increased from 50% to 75–90% RH. However, no studies have considered the important aerosol parameters (e.g., nebulized medium and transmission mode) in determining susceptibility of viral agents. Therefore, investigating the effects of these parameters on decontamination efficiency is important in determining the optimal conditions.

The main concern of UV application is the production of ozone, exposure to which is detrimental to human health and to materials (Hwang et al. 2010). Keratoconjunctivitis and skin erythema caused by exposure of skin and eyes to UV irradiation are recognized safety concerns regarding the use of UV irradiation (Nardell 2008; Yen et al. 2004). Another concern related to decontamination is the potential for photolysis of the material when exposed to short-wavelength UV.

2.2.8. Microwave Decontamination

Microwaves are electromagnetic waves with wavelengths between 1 m and 1 mm, and frequencies between 300 MHz and 300 GHz (Jones et al. 2002). Microwave ovens generally

operate at a frequency of 2.45 GHz, corresponding to a wavelength of 12 cm and energy of 1.02×10^{-5} eV. Microwave radiation is non-ionizing but is sufficient to cause polar molecules such as water to vibrate, thereby resulting in friction, which produces heat.

The use of microwave irradiation to kill microorganisms through thermal and nonthermal effects has long been demonstrated in various studies in liquid media (Awuah et al. 2005; Campanha et al. 2007; Kiel et al. 2002; Pellerin 1994). Only in recent years has microwave inactivation of airborne microorganisms gained more interest, because of increasing concerns about health-related concerns regarding outbreaks of pathogenic airborne viruses (e.g., SARS, H1N1 and swine flu). For example, Hamid et al. (2001) measured 90% IE by applying microwave irradiation to heterogeneous airborne bacteria and fungi at 600 W for four periods of 2.5 min, each separated by 5 min from the next. Elhafi et al. (2004) demonstrated that infectious bronchitis virus, avian pneumovirus, Newcastle disease virus, and avian influenza virus were inactivated on dried swabs in less than 20 s at 1250 W. Another study, Wu and Yao (2010) reported IEs of 65% and 6% against airborne *B. subtilis* var niger spore and *Pseudomonas fluorescens*, respectively, in an air stream after exposure to microwaves at 700 W for 2 min, and Wu and Yao (2011) showed gene 82 mutation through PCR-denaturing gradient gel electrophoresis after microwave application.

More-recent studies have started to investigate microwave decontamination of contaminated filters. Heimbuch et al. (2011) reported that microwave-generated steam at 1250 W for 2 min induced a 5-log IE for H1N1 virus collected on FFRs. Zhang et al. (2010) demonstrated that microwave irradiation could provide an adequate method for inactivating *E. coli* and *B. subtilis* endospores in a microwave-assisted NF air filtration system.

Although HVAC systems can potentially mitigate transmission of infectious biological agents, no research has been conducted to evaluate the use of microwave irradiation of commercial HVAC filters, even though these filters are commonly used in hospitals and residential buildings for collective protection. For practical applications, the inactivation performance of microwave-irradiation assistance to HVAC filtration systems during filtration is important, but has not been studied yet. Key parameters, including RH and microwave power level and application time, should be investigated. Furthermore, thermal stability of the filter media under microwave irradiation needs to be examined.

2.3. Scope

To address the issues discussed above, this project was conducted as five tasks: 1) investigate the stability of MS2 virus in different RHs and spraying media; 2) examine the effects of bioaerosol on the release of iodine from the triiodide resin filter; 3) develop a method for consistent and controlled delivery of droplets containing viral agents onto surface that will allow for a standard comparison of different contamination technologies; 4) assess the effects of RH and spraying medium on UV decontamination of respirators loaded with viral aerosols and viral droplets; 5) evaluate microwave-irradiation-assisted filtration for capture and inactivation of viral aerosols.

Comprehensive development and evaluation of inactivation technologies based on the characteristics of viral aerosols will lead to mitigation of the problem of shortages in the

respirator stockpile and provide novel means for inactivating airborne biological agents. These efforts can subsequently mitigate the threat of disease transmission by viral aerosol. Successful implementation of the knowledge learned and technologies developed in this study can better protect the general public as well as healthcare facilities against viral agents.

2.4. Approach

In assessing the effects of RH and spray medium on the stability for virus, four types of characterization were performed: collection efficiency of BioSampler, virus PSD by SMPS, plaque assay for virus infectivity, and PCR analysis for total virus count. PSL particles (Duke Scientific) in different sizes from 30 nm to 300 nm were used to determine the collection efficiency of the BioSampler at each specific size and flow rate. MS2 (ATCC®, 15597-B1™) in three spraying media (i.e., DI water, 0.3 % BE, and AS) was used as the challenging agent instead of PSL particles in DI water. AS was used as the nebulization fluid to emulate droplets generated by coughing and sneezing. To elucidate the effect of RH on the stability of viruses, three RHs ((i.e., low RH (LRH, 30 ± 5%), medium RH (MRH, 60 ± 5%), and high RH (HRH, 90 ± 5%)) were applied. The liquid sample assayed was also tested by PCR to determine the concentration of total (infectious and noninfectious) viruses, under the assumption that no RNA distortion occurred during the test.

To examine the effects of bioaerosol on the release of iodine from the triiodide resin filter, MS2 aerosol was treated with or without charge neutralization. The treated viral aerosol was then passed through an iodine-treated filter medium. DI water was nebulized as the baseline condition. The concentration of I_2 collected in the BioSampler medium was analyzed by the DPD colorimetric method, in which I_2 in the solution reacts with DPD to form a pink color, proportional in intensity to the total I_2 concentration. A 10-mL portion of the collection medium was analyzed at 530 nm using a DR/4000 V spectrophotometer (HACH, Loveland, CO, USA).

A droplet/aerosol loading system was custom-built to enable fair comparison of the performance of different decontamination techniques. Sterile forceps were used to place six samples onto the supports on the turntable. A 5-min loading time from a titer of around 10^7 PFU/mL in the ultrasonic nebulizer was predicted to provide sufficient loading density (>10^3 PFU/cm^2). Three types of spraying media were tested: DI water, BE and AS. DI water was included to explore properties of the naked virus. Droplets of three spray media were produced by an ultrasonic nebulizer or a Collison nebulizer. They entered the chamber and deposited onto the surface of FFR coupons for 5 min. The frequency of the ultrasonic generator was 2.4 MHz and the environmental conditions were 20 ± 2 °C and 35 ± 5% RH. Various operating parameters, including loading time (1–30 min), virus titer (10^7–10^8 PFU/mL), turntable speed (0–3 rpm), air flow rate (1–5 Lpm) and mucin concentration (0.3–0.9%), were evaluated to identify conditions that provide desired droplet characteristics.

To evaluate respirator decontamination by UV irradiation, each test filter was cut into four equal quadrants. Droplets and aerosols containing viruses were loaded in various spray media onto FFRs and then exposed to UV light at one of three RHs. During UV exposure, the UV-C (254 nm) lamp (UVG-11, Ultraviolet Products, Cambridge, UK) was set at a height of 10 cm. UV intensity of 1.0 mW/cm^2 was measured using a radiometer (PS-300, Apogee, Logan, UT, USA).

A commercial HVAC filter made of polyethylene and polypropylene (Filter 1; 3M) and another fabricated from an unidentified synthetic polymer (Filter 2; True Blue) were selected as test filters for an investigation of on-the-fly disinfection by microwave irradiation. A glass microfiber LydAir MG filter (Filter 3; Lydall) was used for comparison. A microwave oven (Panasonic, NN-T945SF, 2.45-GHz, continuous irradiation) with two 1-in holes in the backside was used in this study. For the microwave-assisted filtration system, *T* was identified to be a key factor. RH was another pivotal parameter affecting viability of viruses at warm-to-hot-water temperatures. Microwave irradiation was applied for three 10-min cycles that included selected periods of irradiation—1, 2.5, 5 and 10 min/10-min cycle—at three different microwave power levels, 125, 250 and 375 W. To select the microwave application conditions, the thermal stability of three test filters was analyzed with TGA–SDTA (851E, Mettler–Toledo Inc., OH), and *T* of filters on the supporting SiC disk under different applied conditions was measured with an IR pyrometer (OS533E, Omega Engineering Inc., CT).

3. EXPERIMENTAL

3.1. Test Microorganisms

MS2 (ATCC®, 15597-B1™) was applied as the challenging bioaerosol. MS2 has a nonenveloped, icosahedral capsid of 27.5-nm nominal diameter, and it infects only male *E. coli* (Prescott et al. 2006; Valegard et al. 1990). It is commonly used as a nonpathogenic surrogate for human pathogenic viruses (e.g., poliovirus, influenza A, and rhinovirus) because of its similarity in resistance to antimicrobial agents, ease of preparation and assay (Aranha–Creado and Brandwein 1999; Brion and Silverstein 1999), and requirement of only a BSL-1 facility. Freeze-dried MS2 was suspended in DI water to a titer of approximately $10^{10} – 10^{11}$ PFU/mL and stored at 4 °C until experiments.

3.2. Effects of Relative Humidity and Spray Medium on Survivability of Viral Aerosols

The schematic of the experimental set-up is shown in Figure 1. Four tasks (i.e., collection efficiency of BioSampler (Task 1), PSD (Task 2), plaque assay (Task 3), and PCR analysis

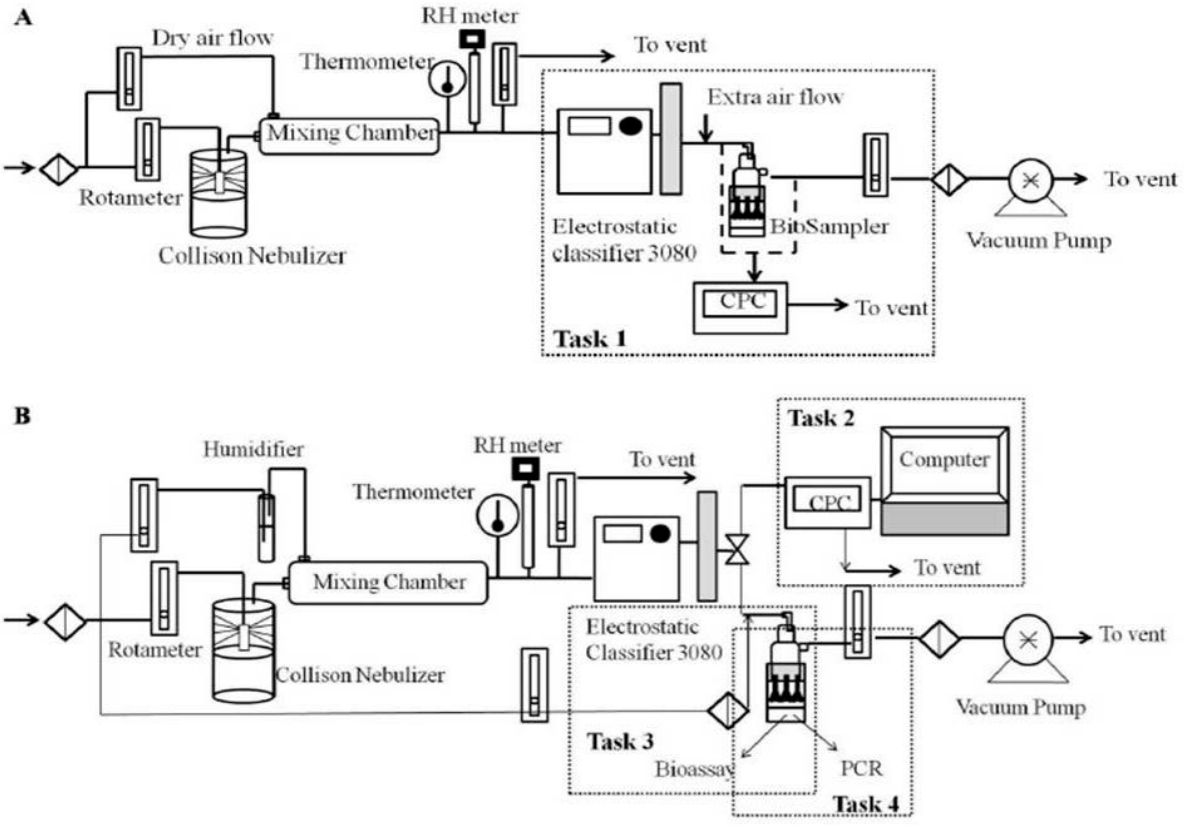

Figure 1. Schematic Diagram of the Experimental Setup for Evaluating the Effect of Relative Humidity and Spray Medium on the Survivability of Viral Aerosols: A) the System Used to Determine the Collection Efficiency of BioSampler as a Function of Particle Size (Task 1) and B) the System Used to Measure Particle Size Distribution (Task 2) and to Enumerate Viable (Task 3) and Total (Task 4) Viruses

(Task 4)) were performed. In Task 1, PSL particles (Duke Scientific) in different sizes from 30 nm to 300 nm were used to determine the collection efficiency of the BioSampler at select particle sizes and flow rates. As displayed in Figure 1, a six-jet Collison nebulizer (BGI Inc., CN25, Waltham, MA, USA) operated with a flow rate of 6 Lpm was used to generate aerosols containing viruses. A second, dry air stream was added to the mixing chamber with the aerosol flow to achieve LRH in the system. The aerosols in the combined flow were classified by the electrostatic classifier (EC; Model 3085, TSI Inc.) and collected in a BioSampler (SKC Inc., Eighty Four, PA) containing 15 mL of DI water. The BioSampler's collection efficiency is defined as:

$$E_{d_\mathrm{p}}(\%) = \left(\frac{N_{d_\mathrm{p,down}}}{N_{d_\mathrm{p,up}}}\right) \times 100 \quad (1)$$

where $N_{d_\mathrm{p,down}}$ and $N_{d_\mathrm{p,up}}$ are the number concentrations of particles collected by the condensation particle counter (CPC) at a specific particles size (d_p) downstream and upstream of the BioSampler, respectively.

Figure 1B illustrates experimental setups for Tasks 2–4, in which MS2 was delivered in three different spraying media (DI water, 0.3 % BE, and AS) instead of PSL particles. To elucidate the effect of RH on the stability of viruses, three RHs (LRH, 30 ± 5%; MRH, 60 ± 5%; and HRH, 90 ± 5%) were applied. Task 2 experiments measured number, surface and mass-based PSDs of the viral aerosols by using the SMPS. Task 3 experiments obtained distributions of infectious viruses at specific sizes by adjusting the applied voltage on the EC and plating individual fractions. Seven sizes from 30 nm—the bare MS2 virion—to 230 nm—effectively the upper limit of particle size that can be measured by the SMPS at a flow rate of 1.5 Lpm—and five intermediate sizes (60, 90, 120, 150, and 180 nm) were studied. The size-classified particles were collected in the BioSampler. To minimize any loss in collected viruses to long sampling times and to reaerosolization, a flow rate of 4.5 Lpm and sampling time of 5 min were applied (Riemenschneider et al. 2010). The number of viable viruses collected in BioSamplers was enumerated by a single-layer bioassay. The size distribution function of infectious viruses based on the results of the plaque assay was calculated following Equation 2.

$$\mathrm{PFU/cm^3} = \frac{C_\mathrm{PFU} \cdot V}{C_\mathrm{eff} \cdot Q_\mathrm{inlet} \cdot \Delta \log d_\mathrm{p} \cdot t} \quad (2)$$

where C_PFU is the concentration of virus in the collection medium, V is the volume of collection medium in the BioSampler, C_eff is a correction factor for its collection efficiency for the specific particle size (from Task 1), Q_inlet is the inlet flow rate of the EC, t is the collection time of the BioSampler, and $\Delta\log d_\mathrm{p}$ is the logarithm of the bin size of the EC.

The number of MS2 PFUs per particle (N_PFU) was determined by dividing C_PFU by the total number of aerosol particles and the theoretical value of N_PFU ($N_\mathrm{Theo\ PFU}$) was calculated from the volume fraction of MS2 in the solid content in the spray medium for the given particle size, according to Equation 3.

$$N_\mathrm{Theo\ PFU} = \frac{V_{d_\mathrm{p}} \times F_\mathrm{MS2}}{\frac{\pi}{6} d_\mathrm{MS2}^3} \quad (3)$$

where V_{d_p} is the volume of the droplet nuclei, F_{MS2} is the volume fraction of infectious viruses obtained from the plaque assay for MS2 stock suspension, and d_{MS2} is the particle diameter of an MS2 virion (~27 nm). Based on the composition of the medium, the volume fractions of solids in DI water, BE and AS were 1×10^{-4}, 3.1×10^{-3} and 6.0×10^{-3}, respectively. The corresponding particle size of MS2 aerosols generated were 0.046 d_d , 0.145 d_d, and 0.179 d_d, respectively, where d_d is the initial diameter of the droplet.

The liquid sample assayed in Task 3 was also examined by PCR to determine the total concentration of viruses—infectious and non-infectious. This approach included the assumption that no RNA distortion occurred during the test (Task 4). To prepare for the PCR procedure, nucleic acid extraction was conducted on 4-mL samples from the BioSampler. Because the concentration was insufficient to allow comparisons, this sample was concentrated to 280 μL by using an Amicon ultracentrifugal device (UFC 810096, Millipore, Bedford, MA, USA). The concentrated sample was processed using RNA extraction with a QIAamp Viral RNA mini kit (QIAGEN Inc., Valencia, CA, USA) and aliquots were stored at -80 °C.

Real-time PCR assays followed the design by O'Connell et al. (2006), and the sequence data for MS2 were obtained as a target of RNA replicase β from National Center for Biotechnology Information (NCBI), accession number NC-001417. The target sequences were as follows:

- MS2-F and MS2-R: Forward and reverse primers binding to target sequences on the internal MS2 control, 80 pmol/μL each.
- MS2-F: 5'-TGG CAC TAG CCC CTC TCC GTA TTC ACG-3'
- MS2-R: 5'-GTA CGG GCG ACC CCA CGA TGAC-3'
- MS2 ROX/Probe: Taqman probe that hybridizes to a target sequence on the MS2 internal control, 80 pmol/μL.
- 5'-ROX-CAC ATC GAT AGA TCA AGG TGC CTA CAA GC-BHQ2-3'

In this study, primers and the probe used were obtained from Applied Biosystems (ABI). The enzyme and buffers used were from the Invitrogen SuperScript™ Platinum kit.

One-step quantitative PCR (qPCR) was carried out on an ABI 7500 real-time PCR system under the following conditions: incubation at 50 °C for 15 min and then at 95 °C for 2 min, followed by 40 cycles of amplification with denaturation at 95 °C for 15 s and annealing and extension at 60 °C for 30 s, acquiring on the ROX and FAM channels. MS2 RNA (165948, Roche Diagnostics, Indianapolis, IN, USA) in five serial dilutions, and DNase–RNase-free sterilized water were substituted for MS2 RNA samples as the respective positive and negative controls.

By comparing the threshold cycle (CT) for positive controls to that for RNA samples, the total number of viruses (both infectious and non-infectious) was calculated. The number of MS2 RNA per particle (N_{RNA}) was then determined by dividing it by the total aerosol particles measured by the CPC following Equation 4, and the stability factor of virus can be obtained from N_{RNA}/N_{PFU}.

$$N_{RNA} = \frac{\text{RNA (ng) in the sample} \times 10^{-9}\ \text{g/ng}}{\left(\frac{1.0\times10^{6}\ \text{g}}{\text{mol}}\right)\times\left(\frac{1\ \text{mol}}{6.02\times10^{23}\ \text{molecules}}\right)} \Big/ N_{\text{aerosol particles}} \times C_{\text{eff}} \qquad (4)$$

3.3. Effects of Bioaerosol on the Release of Iodine from Iodine-Treated Filter

3.3.1. Experimental System

Figure 2 shows a schematic of the experimental system. Bioaerosol was generated by a six-jet Collison nebulizer at 7 Lpm. The Collison nebulizer was charged with 10^5–10^6 PFU/mL virus, prepared by diluting 0.10 or 0.20 mL of virus stock suspension in 50 mL sterile DI water. The bioaerosol flow was joined by a dry dilution flow (8 Lpm) at a dilution dryer. The combined flow then passed through a charge neutralizer (TSI, 3012A). *T* and RH of the air stream were measured by a thermometer and an RH meter, respectively. *T* was maintained at 23–24 °C, and the RH was 44–46%. Pressure drop across the test filter was measured using a Magnehelic pressure gauge. The penetrating bioaerosol was collected in a BioSampler containing 15 mL of phosphate-buffered saline (PBS). Sampling was conducted for 60 min. Eight sets of experiment were conducted. To ensure no residual from previous runs, the system was flushed with DI water for 30 min after each experiment. In addition, each piece of iodine-treated filter was used for only one set of experimental conditions.

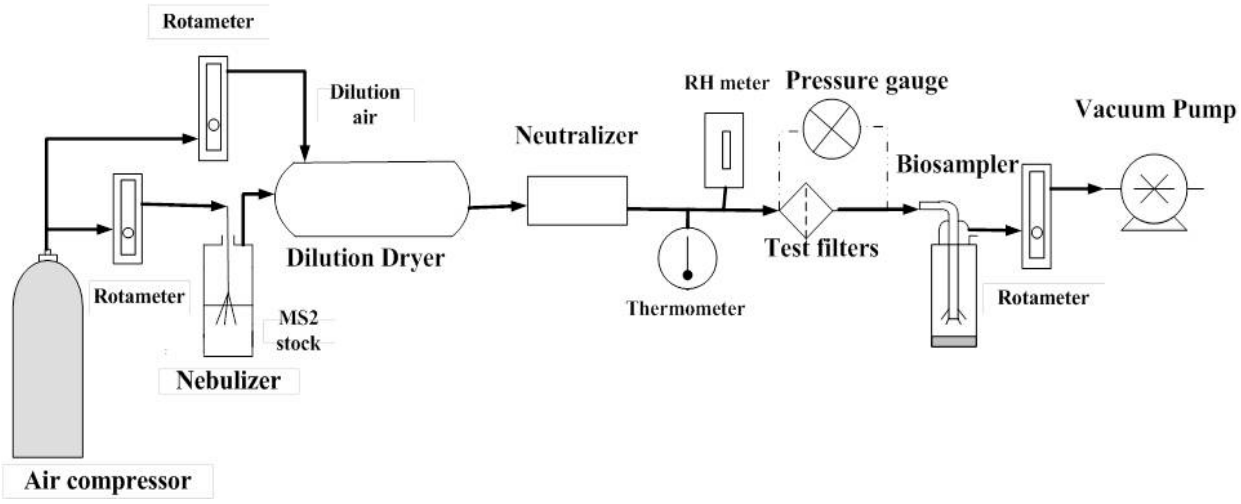

Figure 2. Schematic of Experimental System for Evaluating Iodine Release Induced by Bioaerosol

3.3.2. Iodine Analysis

The concentration of I_2 collected in the BioSampler medium was analyzed by the DPD colorimetric method adopted from *Standard Methods for the Examination of Water and Wastewater 4500-CI G* (APHA 1995). I_2 in the solution reacts with DPD to form a pink color, the intensity of which is proportional to the total I_2 concentration (Hach 2012; Lee et al. 2009). A 10-mL sample of the collection medium was analyzed at 530 nm using a DR/4000 V spectrophotometer (HACH, Loveland, CO, USA). The detection limit of this spectrophotometer following HACH Program Number 2100 Iodine with the DPD method is reported by the manufacturer to be 0.024 mg/L I_2.

3.4. Method for Contaminating Filtering Facepiece Respirators by Deposition of MS2 Viral Aerosols

3.4.1. Nebulization Fluid Preparation

AS was used as the nebulization fluid to emulate droplets generated by coughing and sneezing. Saliva is a very dilute fluid composed of more than 97% water, plus electrolytes, proteins, and enzymes (Diaz–Arnold and Marek 2002). Varieties of inorganic ions maintain osmotic balance and offer buffering (Diaz–Arnold and Marek 2002; Dodds et al. 2005; Humphrey and Williamson 2001). The compounds and their corresponding amounts in AS are listed in Table 1 (Aps and Martens 2005; Edwards et al. 2004; Veerman et al. 1996; Wong and Sissions 2001). Mucin from porcine stomach (Sigma–Aldrich, M1778) was chosen as the representative mucus simulant (Vingerhoeds et al. 2005).

Table 1. Composition of Artificial Saliva (Based on 979 mL of DI Water)

Chemical Species	Amount	Chemical Species	Amount
$MgCl_2 \cdot 7\ H_2O$	0.04 g	KSCN	0.19 g
$CaCl_2 \cdot H_2O$	0.13 g	$(NH_2)_2CO$	0.12 g
$NaHCO_3$	0.42 g	NaCl	0.88 g
0.2 M KH_2PO_4	7.70 mL	KCl	10.4 g
0.2 M K_2HPO_4	12.30 mL	Mucin	3.00 g
NH_4Cl	0.11 g	DMEM*	1.0 mL

DMEM*: Dulbecco's modified Eagle's medium

3.4.2. Test Material

Six different models of FFRs approved by NIOSH were employed in this study. Three of those models were also approved by the Food and Drug Administration (FDA) as surgical devices. Each FFR type has different characteristics, e.g., number of layers, hydrophilicity, and physical shape. Prior to FFR testing, 110-mm diameter discs of flat glass-fiber filter (Gelman Science, 61630) were used to determine workable operating conditions of virus concentration, flow rate and loading time.

3.4.3. Droplet/Aerosol Loading System Design

A droplet/aerosol loading system was custom-built for this study according to the following requirements: (1) width and height are less than 120 cm so that it can be placed in a biosafety cabinet; (2) parts can be easily disassembled for sterilization; (3) droplets/aerosols can be distributed uniformly onto substrates; (4) the droplet PSD is consistent; (5) environmental conditions that can affect the droplet size, such as RH and *T*, can be controlled. Figure 3 shows the schematic design of the loading system. The system consists of a chamber body, an ultrasonic generator (241T, Sonaer®, Farmingdale, NY) for producing droplets, a bubbler for generating moisture, compressed cylinder air to control RH and dilute virus concentrations, an RH meter to measure humidity, a six-port manifold for distributing the aerosols, a thermometer for measuring *T*, and six supports to hold flexible-form FFRs during loading (Baron et al. 2008; Feather and Chen 2003). This system can also include a charge neutralizer (Model 3012, TSI Inc., Shoreview, MN). The chamber body was fabricated from stainless steel sheet with welded

seams to withstand high temperatures for sterilization. The turntable and six perforated sample plates were employed to achieve uniformity of deposition. PSDs were measured by an aerodynamic particle sizer (APS; Model 3321, TSI Inc., Shoreview, MN) through a port on the side of the chamber. Before the droplet loading chamber was built, an experiment was conducted to verify the uniform deposition of aerosols using a small chamber, presented in Appendix A.

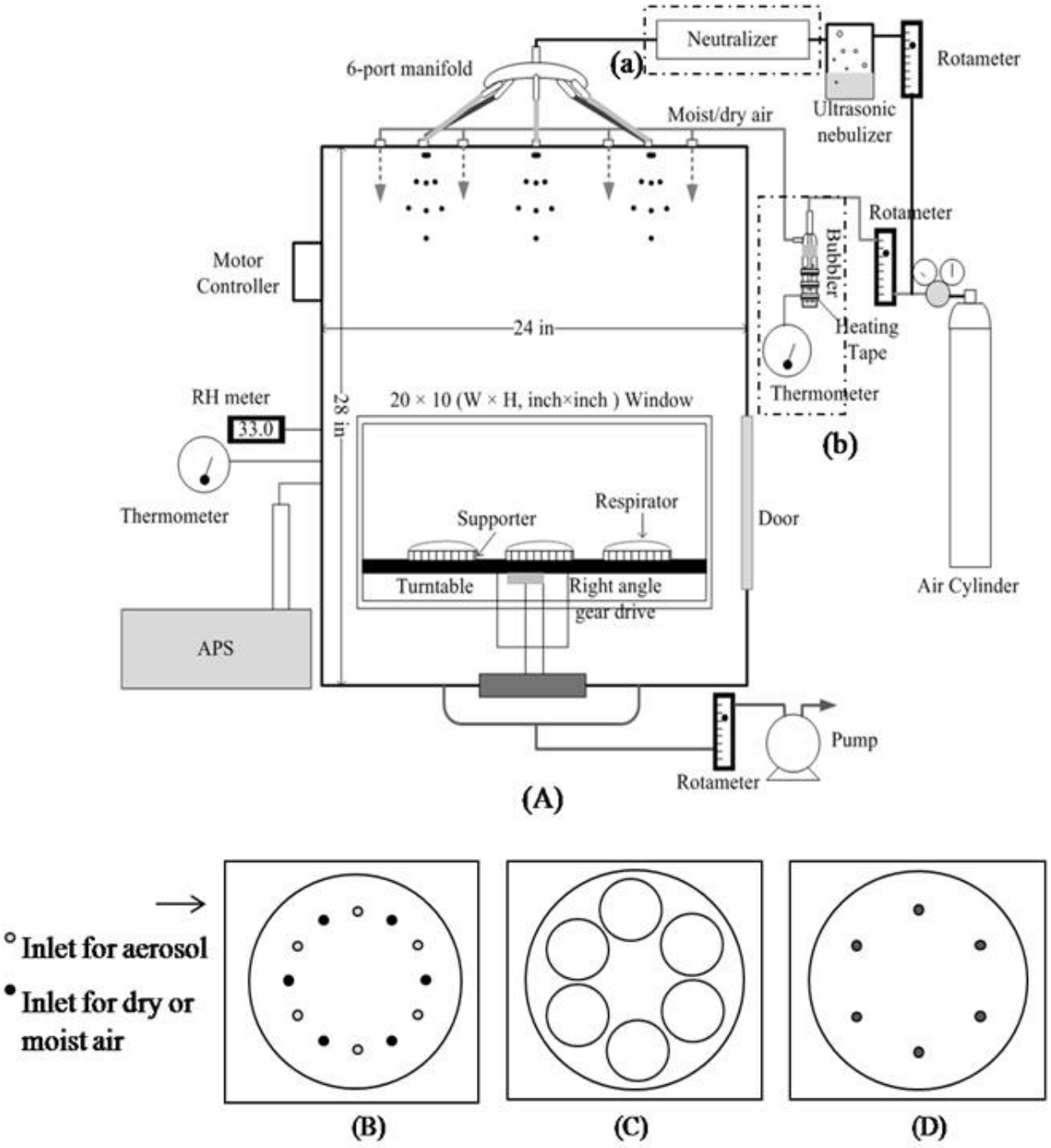

Figure 3. Schematic diagram of the droplet loading system: A) entire system, B) distributor on top, C) turntable, D) air outlet at bottom; (a) and (b) are used only in certain conditions

3.4.4. Chamber Operation and Determination of Operating Conditions

Before and after experiments, the chamber was decontaminated by wiping the interior with isopropyl alcohol and closing the chamber up for 30 min. Six samples were placed onto the supports on the turntable using sterile forceps. A titer of ~ 10^7 PFU/mL in the ultrasonic nebulizer and loading for 5 min time was calculated to provide sufficient loading density (>10^3 PFU/cm^2) for testing. The titer was prepared by adding 0.3 mL virus stock suspension into 30 mL AS. Droplets from the ultrasonic nebulizer passed the distributor and entered the chamber through six inlets. The size of droplets generated and loaded can be affected by the frequency of the ultrasonic generator and by environmental conditions such as RH and *T*. For this study, environmental conditions were 20 ± 2 °C and 35 ± 5% RH and the frequency of the generator was 2.4 MHz. LRH was chosen because the survivability of MS2 is high under this condition. After loading, the residual droplets were allowed to clear for 5 min, and the FFR samples were taken out for extraction and assay.

Various operating parameters were evaluated to identify conditions that deliver desired droplet characteristics: loading time (1–30 min), virus titer (10^7–10^8 PFU/mL), turntable rotation (0–3 rpm), airflow rate (1–5 Lpm), and mucin concentration (0.3–0.9%). Loading density was controlled by adjusting the loading time and the titer of the virus suspension. To evaluate how viability of the virus is influenced by the ultrasonic process, bioaerosols produced at different times were collected by a BioSampler and their viability was compared. The turntable speed was varied to determine its relationship with uniformity. Flow rate and mucin loading were also varied to investigate their effects on the consistency of delivered droplets. Three runs were carried out for each set of conditions.

After loading with virus, each filter sample was cut into four equal quarters. Each quarter was immersed in 25 mL of 0.25 M glycine extraction medium in a 50-mL conical tube. Agitation by a wrist-action shaker (Model 75, Burrell Scientific, Pittsburgh, Pa.) was applied at a 10° angle for 15 min to extract the MS2 from the quarter sample for analysis of the loading density (these conditions gave the best extraction efficiency in preliminary testing, see Appendix A). The extracted solution was assayed by using the single-layer method (USEPA 1984) to determine the loading density according to Equation 5 with the assumption of 100% extraction efficiency:

$$LD = \frac{PFU}{10^{-n}} \times \frac{V_1}{V_2} \times \frac{4}{\pi d^2} \tag{5}$$

where *LD* is the loading density, V_1 is the volume of extraction solution, V_2 is the volume of sample, *d* is the diameter of the filter, and *n* is the number of dilutions (Lee et al. 2009).

The single-layer bioassay method enumerates infectious viruses using *E. coli* (ATCC, 15597) as the host. Freeze-dried *E. coli* from the American Type Culture Collection (ATCC) was suspended in 1X PBS, inoculated into a solidified hard agar plate (1.5% agar) with a sterilized loop, and then incubated at 37 °C overnight. The single colony from the plate was transferred into tryptone soy broth (TSB) 271 to grow *E. coli* at 37 °C overnight. The 271medium (100 mL) was inoculated with 0.3 mL of the *E. coli* culture from TSB 271 and then incubated at 37 °C for

3 h. The TSB 271 and culture medium 271 were prepared following the ATCC procedure for MS2 assay. After incubating 3 h, the *E. coli* host was combined with 1.0 mL of MS2 sample and added to a sterile, conical, blue tube containing 9 mL of soft agar (0.5% agar) in a water bath at 40–50 °C. Serially diluted MS2 samples were used to ensure a measurement in the countable range of 30–300 PFU/mL. Each mixture was shaken thoroughly and then poured into a separate petri dish. After the agar hardened, the plate was inverted and placed in an incubator at 37 °C overnight. Plaques on each plate were counted and the titer of the sample was determined by multiplying the dilution factor times the plaque count. To visualize the particle loading, scanning electron microscopic (SEM; JEOL JSM-6330F, JEOL Inc.) images of the filter were taken before and after loading particles.

3.4.5. Statistical Analysis

The Q-T-Q and S-T-S CVs of loading density were obtained to evaluate the uniformity. R2 8.1 software (CRAN) and Microsoft Excel® were used to calculate one-way analysis of variance (ANOVA) and CV, respectively.

3.5. Effects of Relative Humidity and Spraying Medium on UV Decontamination of Viral Aerosols/Droplet Loaded Filter

3.5.1. Spraying Medium

Three types of spraying media were tested: DI water, BE and AS. DI water was included to explore properties of the naked virus. BE (0.3 vol %), which was used to provide nutrients, can contribute encasement. BE is a mixture of peptides, amino acids, nucleotide fractions, organic acids, minerals and some vitamins, derived from infusion of beef (Cote 1999). AS (0.6 vol %), 0.3% mucin from porcine stomach (Sigma–Aldrich, M1778) plus salts in DI water as a mucus simulant, was used to mimic human respiratory fluid. Mucin—viscous glycoproteins comprising approximately 75% carbohydrate and 25% amino acids linked via glycosidic bonds between *N*-acetylgalactosamine and serine or threonine residues—readily forms a gel in water. Details of AS composition were reported by Woo et al. (2010).

3.5.2. Droplet and Aerosol Loading System

The experimental setup for loading droplets and aerosols containing viruses onto the substrate is displayed in Figures 4 A and B, respectively. A 2.4-MHz ultrasonic nebulizer (241T, Sonear, Farmingdale, NY, USA) was used to generate droplets containing viruses at a flow rate of 2 Lpm. The MS2 suspension in the reservoir was prepared by dispersing 1 mL of stock solution in 25 mL of spraying medium (DI water, BE or AS). Circular coupons (Φ = 2.54 cm) were cut from a 3M 1870 (NIOSH-certified N95) FFR. The produced droplets entered the chamber and loaded onto the surface of FFR coupons for 5 min. Droplet size is affected by environmental conditions such as RH and *T*. Loading of droplets onto filter coupons was conducted at room temperature (20 ± 3 °C) and HRH. Each filter was then cut into four equal quadrants for UV exposure.

A Collison nebulizer was used to generate the virus-containing aerosols, at a flow rate of 6 Lpm. The MS2 suspension in the nebulizer was prepared by dispersing 2 mL of viral stock suspension in 50 mL of nebulizer medium. Aerosol from the nebulizer entered the mixing chamber and was mixed with dry or wet air as appropriate to adjust RH. Loadings were applied at each of the three RHs (LRH, MRH and HRH). The flow was split into three streams toward the filters (Φ = 47 cm,

3M 1870) to deliver 4 Lpm, corresponding to a face velocity of 5.3 cm/s, a standard face velocity for air filter system testing (ASME 2009). After loading with aerosol for 30 min at the selected RH, the filter was removed and cut into equal quadrants to prepare for UV exposure.

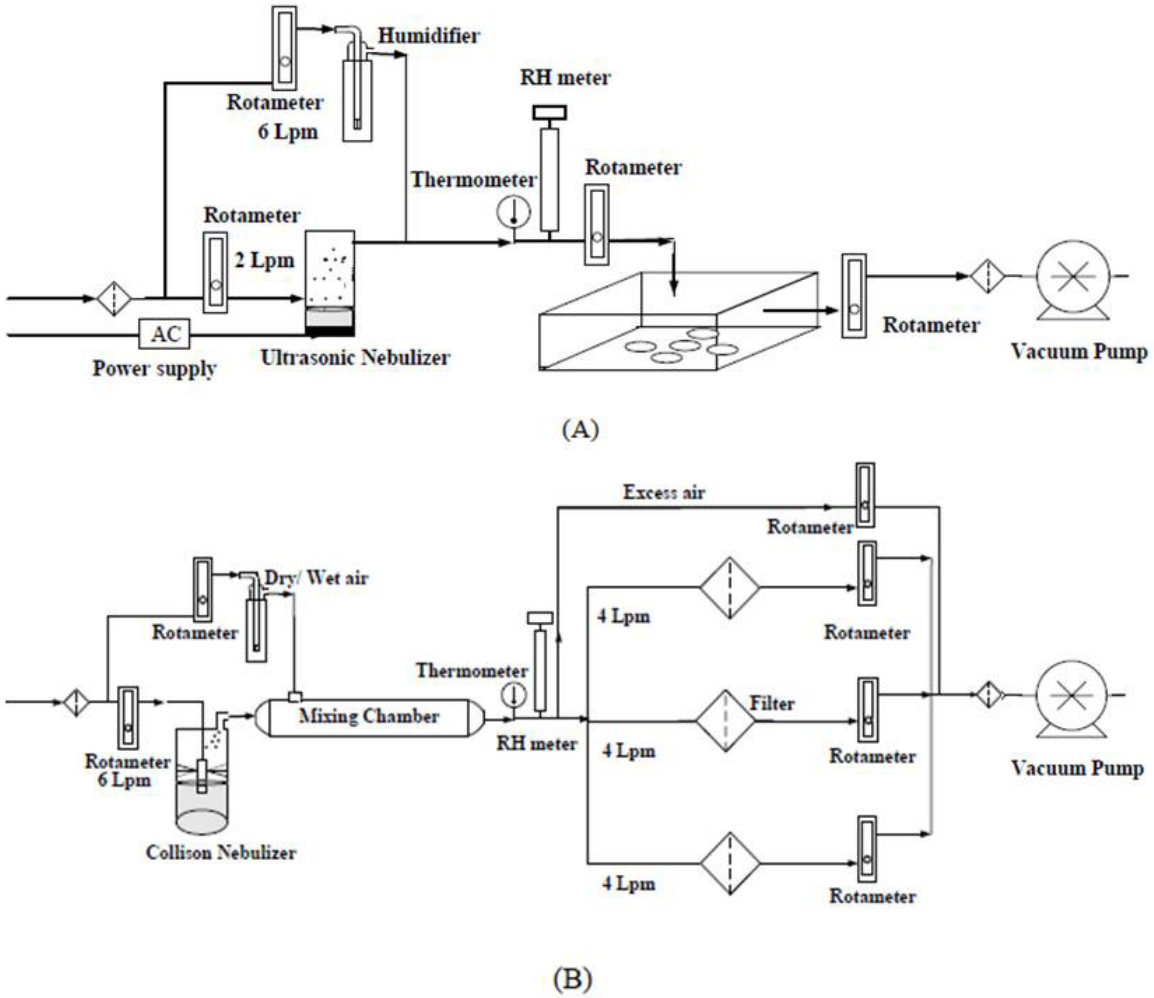

Figure 4. Schematic Diagrams: A) Droplet Loading System and B) Aerosol Loading System

3.5.3. UV Exposure

For UV exposure, the UV-C (254 nm) lamp (UVG-11, Ultraviolet Products, Cambridge, UK) was set to a height of 10 cm. UV intensity of 1.0 mW/cm^2 was measured using a radiometer (PS-300, Apogee, Logan, UT, USA). Filter quadrants were placed on a petri dish in a chamber and irradiated by UV at the selected RH. One quadrant used as a control was not exposed to UV, while the other three were exposed to UV for different times (0–2 h).

Dry or wet air was fed into the chamber to adjust the RH in the system. After exposure, each quadrant was placed in a 50-mL conical tube containing sterilized DI water and agitated with the Model 75 wrist action shaker inclined 20° for 15 min to extract MS2. The MS2 extracted was assayed with the single-layer method. The IE was determined by comparing the count (PFU_{exp}) from the irradiated coupon with that from the paired control (PFU_{ctl}):

$$\mathrm{IE} = \frac{PFU_{\mathrm{ctl}}}{PFU_{\mathrm{exp}}} \tag{6}$$

Triplicate tests for each condition and duplicate assay were conducted. Two-way ANOVA and three-factor ANOVA were used for statistical analysis (Design-Expert® 8.0). CVs of amounts loaded on the quadrants were less than 20%. SEM (JEOL JSM-6330F, JEOL Inc.) images of filters contaminated with viruses generated in different media were taken and compared to investigate the protective effect of solid components.

3.6. Microwave-Irradiation-Assisted Filtration for Inactivation of Viral Aerosols

3.6.1. Experimental System

Commercial HVAC filters made of polyethylene and polypropylene (Filter 1; 3M) and of an unspecified synthetic polymer (Filter 2; True Blue) were selected as test filters. A LydAir MG glass microfiber filter (Filter 3; Lydall) was used for comparison.

A microwave oven (Panasonic, NN-T945SF, 2.45 GHz, continuous irradiation) with two 1-in holes in the backside was used in this study. Because common filter holders won't survive microwaving, a custom-made quartz filter holder was placed inside the microwave. A SiC disk was employed inside the quartz reactor to support the filter material and to enhance heat transfer.

The experimental set-up for testing the inactivation of the virus is shown in Figure 5. Six Lpm of dry air was passed through a six-jet Collison nebulizer to aerosolize the viruses. A second air stream passed through the humidifier and then joined the flow. After the combined flow passed through the mixing chamber, it was split three equal ways, and each stream proceeded toward the filtration unit at 4 Lpm, corresponding to a face velocity of 5.3 cm/s, a standard face velocity for ventilation system testing (ASME 2009). Of the three flows, two were directed to filter holders outside the microwave, one with and one without an HVAC filter, as controls. The third passed

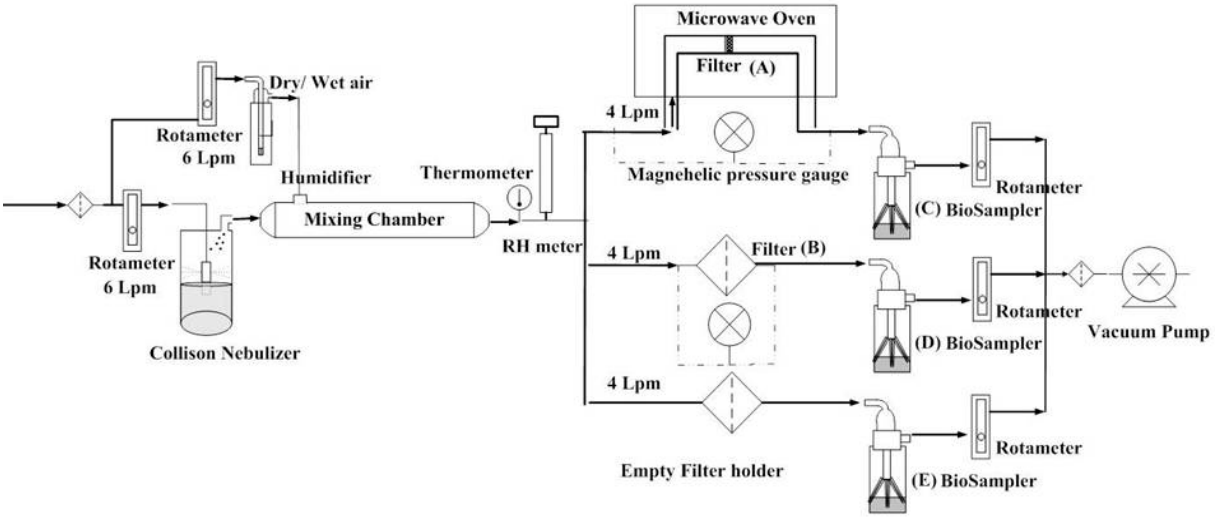

Figure 5. Experimental Setup for Microwave-Irradiation-Assisted Filtration

through an HVAC filter 47 mm in diameter (effective diameter 40 mm for the quartz reactor used) inside the microwave oven. The filters inside and outside the microwave oven were labeled A and B, respectively. The BioSamplers downstream of the microwave/filtration system and non-irradiated filter were labeled C and D, respectively. The BioSampler downstream of the empty filter holder (control) was labeled E. Tests were also conducted using polyacrylonitrile (PAN) and cross-linked PAN NF filters, for which the results are displayed in Appendix B.

For on-the-fly decontamination, microwave irradiation was applied during three 10-min cycles that included selected periods of irradiation—1, 2.5, 5 and 10 min/10-min cycle—at three microwave power levels, 125, 250 and 375 W. To select the microwave application conditions, the thermal stability of three test filters was examined using a TGA/SDTA (851E, Mettler–Toledo Inc., OH), and *T* of filters on the SiC disk under different applied conditions was measured with an infrared (IR) pyrometer (OS533E, Omega Engineering Inc., CT). After irradiation, the test filter was taken off the filter holder in the experimental system, immersed in 25 mL of glycine extraction medium in a 50-mL tube and subjected to wrist-action shaking at a shaking angle of 20° for 15 min to extract the viruses. Extracted MS2 was assayed with *E. coli* as a host by the single-layer method (USEPA 1984). To ensure enumeration of MS2 viruses within an adequate count range of 30–300 PFU/mL, serial dilutions of 1 mL of the extract were mixed with 9 mL of 271 agar and 1 mL of 271 medium with log-phase *E. coli* and poured into individual Petri dishes. The mixtures were solidified and the plates were stored in the incubator at 37 °C overnight before counting.

The effectiveness of this process was evaluated by using two parameters: SF and IE. The SF under microwave irradiation was calculated by comparing the viable MS2 in the two filters:

$$\mathrm{SF} = \frac{C_{\mathrm{A}}}{C_{\mathrm{B}}} \tag{7}$$

where C_A and C_B are the viral concentrations collected by filters A and B, respectively. Viral aerosols penetrating the test filters under microwave irradiation were collected in BioSamplers containing 15 mL of DI water. The IE through the microwave/filtration system was obtained by comparing the viable MS2 concentration in the two BioSamplers:

$$\mathrm{IE} = \frac{C_{\mathrm{E}}}{C_{\mathrm{C}}} \tag{8}$$

where C_C and C_E are the concentrations of viruses collected in the BioSamplers C and E, respectively.

The FE of the filter itself ($1\text{-}C_D/C_E$) was used to confirm the stability of this system after each test. The pressure drop of the filter was measured by a Magnehelic gauge to evaluate the degradation or change of filters after decontamination test. Triplicate experiments and duplicate assays were carried out, and one-way ANOVA was used for statistical analysis after confirming over 90% of normality (Design-Expert® 8.0).

The SEM images of virus-contaminated filters were taken after conventional oven heating and after microwave irradiation heating to investigate non-thermal effects of microwave irradiation. A conventional oven (ISOTEMP® oven 230G, Fisher Scientific, PA) was used to provide purely thermal effects. Filters contaminated with a virus suspension of 10^{10} PFU/mL of DI water were either microwaved or inserted into the conventional oven for 30 min.

4. RESULTS

4.1. Effects of RH and Spray Medium on Survivability of Viral Aerosols

This study was undertaken to investigate the effect of spray medium and RH on the stability of sprayed virions. By comparing the count of infectious viruses obtained by plaque assay with the count of total viruses measured by PCR, the stability factor was determined for different environmental conditions. Such information can provide a very useful tool in designing an effective strategy to improve filtration and IE and for assessing the risk imposed by respiratory deposition of viral aerosols.

4.1.1. Collection Efficiency of BioSamplers

Figure 6 shows the collection efficiency of the BioSampler as a function of particle size. At a flow rate of 12.5 Lpm, the collection efficiency increased as particle size increased except at ultrafine sizes (~30 nm), which is explained by the major collection mechanisms of impaction and centrifugation for large particles and diffusion for small particles (Hinds 1999). At 4.5 Lpm, the collection efficiency for all particle size tested was below 15%, which is presumably caused by the reduced collection by inertial impaction and centrifugation at the low flow rate. Lin et al. (2000) investigated the effect of flow rate on collection efficiency of the BioSampler and observed increases in collection efficiency with increasing flow rate. They used three flow rates of 8.5, 10.5, and 12.5 Lpm and large particles (0.8 and 1.0 μm); their results support higher collection efficiency at 12.5 Lpm for large particles. Hogan et al. (2005) also noted collection efficiencies below 20% for 25-nm particle at flow rates of 3.5–12.5 Lpm. In addition, because liquid behavior in BioSamplers was turbulent above 8.7 Lpm, the collection efficiency of 300-nm particles dramatically increased at flow rates above 8.7 Lpm. The data reported by Hogan et al. (2005) agree well for smaller (30 nm) and larger particles (300 nm) tested. Because a 4.5-Lpm flow rate was employed for further tests to avoid reaerosolization (Riemenschneider et al. 2010), collection efficiencies of 12%, 8%, 6%, 4%, 4%, 6% and 7% for 30-, 60-, 90-, 120-, 150-, 180- and 230-nm particles, respectively, were applied as a correction factor for other tasks.

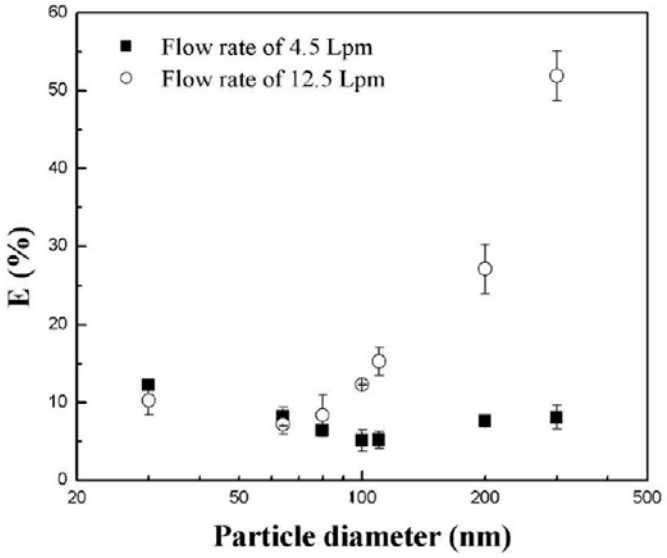

Figure 6. Collection Efficiency of BioSampler as a Function of Particle Diameter with Sampling Flow Rates of 4.5 and 12.5 LPM

4.1.2. Particle Size Distribution of MS2 in Different Environmental Conditions

Figure 7 displays number-based PSDs for aerosols generated from MS2 suspensions in DI water, BE and AS under three RHs. As shown, the PSD of MS2 aerosols had a mode near 27 nm, the

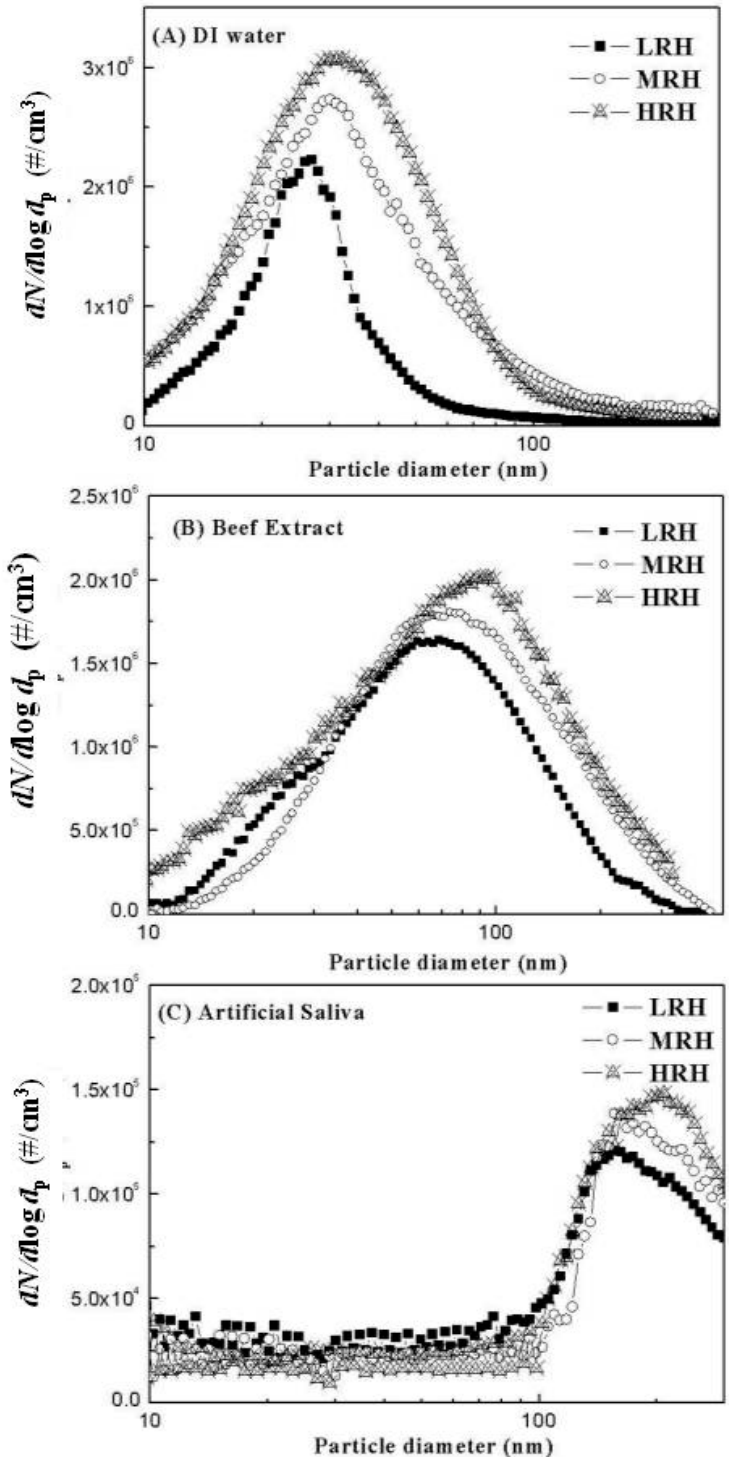

Figure 7. Particle Size Distributions of MS2 Aerosols Generated with DI Water, Beef Extract, and Artificial Saliva at Three Relative Humidities

size of an MS2 virion, at LRH/RT. The number-based PSDs for aerosols generated from MS2 suspensions in DI water slightly increased as RH increased, as did the geometric standard deviation (GSD). This is explained by incomplete evaporation of water at higher RH conditions, although in theory the residence time was sufficient for complete evaporation at all three RHs.

The PSDs of MS2 aerosol generated in BE and AS shifted to larger particle sizes than those generated from DI water. The modes of MS2 aerosol generated in DI, BE, and AS were 28 nm, 68 nm, and 151 nm, respectively, at LRH. The mode shifted to the larger size according to the increased volume fraction of spray medium, as explained in Hinds (1999) and Hogan et al. (2005). Values for BE and AS shifted to smaller and larger size, respectively, compared to the expectation of 84 nm and 106 nm. The larger size of AS is presumably caused by the intrinsic properties of the mucin component in AS. Mucin is a viscous glycoprotein, comprising 75% carbohydrate and 25% amino acids linked via glycosidic bonds between *N*-acetylgalactosamine and serine or threonine residues (Bansil et al. 1995). Hence, formation of mucin gels can readily retain water and retard the evaporation of water even at the LRH condition.

4.1.3. Particle size distribution of infectious MS2

The PSD of infectious MS2 in DI water is displayed in Figure 8. To investigate the dimension of the PSD of MS2, it was compared to number- and mass-based PSDs. The results showed that the PSD followed the volumetric distribution. To verify this trend, the infectious PFUs/particle was calculated and then regression analysis was conducted. The results are shown in Figure 9.

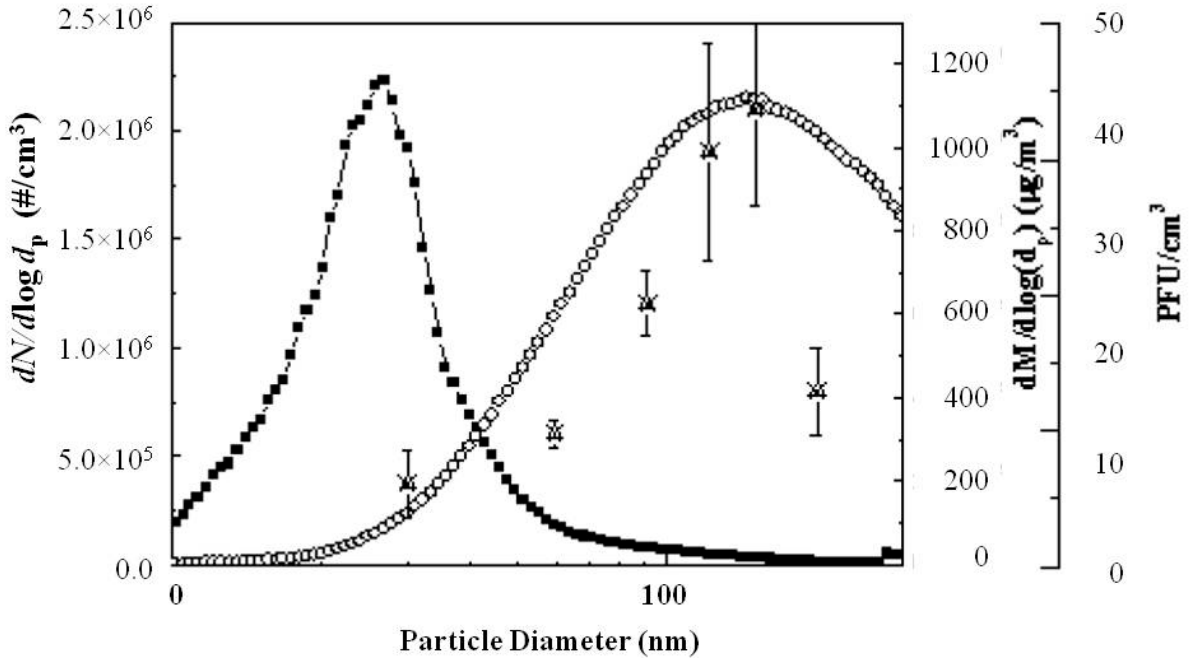

Figure 8. Particle Size Distribution of Number- (Solid) and Mass-based (Empty) MS2 Aerosols Obtained from Monitoring the SMPS and Infectious Viruses (Cross) through Plaque Assay. Error Bar Indicates the Standard Deviation of Triplicate Test

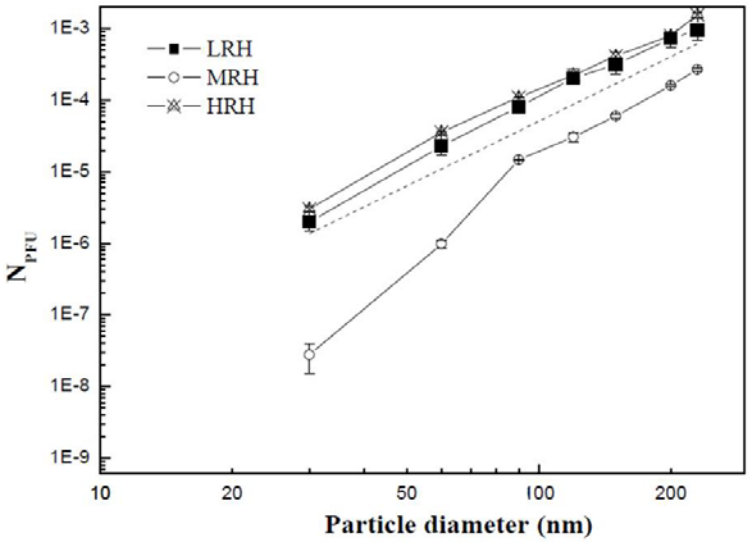

Figure 9. Infectious MS2 per Particle Generated in DI Water as a Function of Particle Size at Three Relative Humidities. Dashed Line Represents the Theoretical PFU per Particle. Error Bar Indicates the Standard Deviation of Triplicate Tests

When the same process was carried out for MRH and HRH, the slope of least square regression obtained for all three RHs was observed to be around 3, as seen in Table 2. However, at MRH the number of infectious virus was smaller than at LRH, although the total particle concentration was higher. This can be explained by the lower stability of MS2 at MRH (Prescott et al. 2006). Different from the other two RHs, the number of infectious MS2 at 30 nm was much lower than expected, indicating lower stability of virions at the MRH condition. The slopes of N_{PFU} for BE and AS for three RHs were also obtained and are listed in Table 2. The values were lower (2~3 in BE and ~2 in AS) than those in DI water.

Table 2. Slope of Least Squares Regression for N_{PFU} as a Function of Particle Size for Different Spray Media at Three Relative Humidities

Spray medium	Slope of N_{PFU} (R^2)		
	LRH	MRH	HRH
DI Water	2.98 (0.98)	3.22 (0.95)	2.83 (0.99)
Beef Extract	2.43 (0.98)	2.38 (0.98)	2.37 (0.98)
Artificial Saliva	2.11 (0.98)	1.98 (0.91)	2.10 (0.92)

Figure 10 shows the MS2 RNA content of particles generated in DI water as a function of diameter at three RHs, and $N_{theo,RNA}$ (assuming negligible impurities). As for N_{PFU}, the regression analysis of N_{RNA} was conducted for DI water, BE and AS, and the results are listed in Table 3. The slopes of N_{RNA} values in BE and AS were significantly lower than that in DI water. It can be explained by the larger volume fraction resulting from the presence of solid contents. BE consists of insoluble, hydrophobic solids, which cause a hydrophobic interaction with MS2 that attaches MS2 to the surface of insoluble salts. The slope of N_{RNA} in AS was less than in BE. This

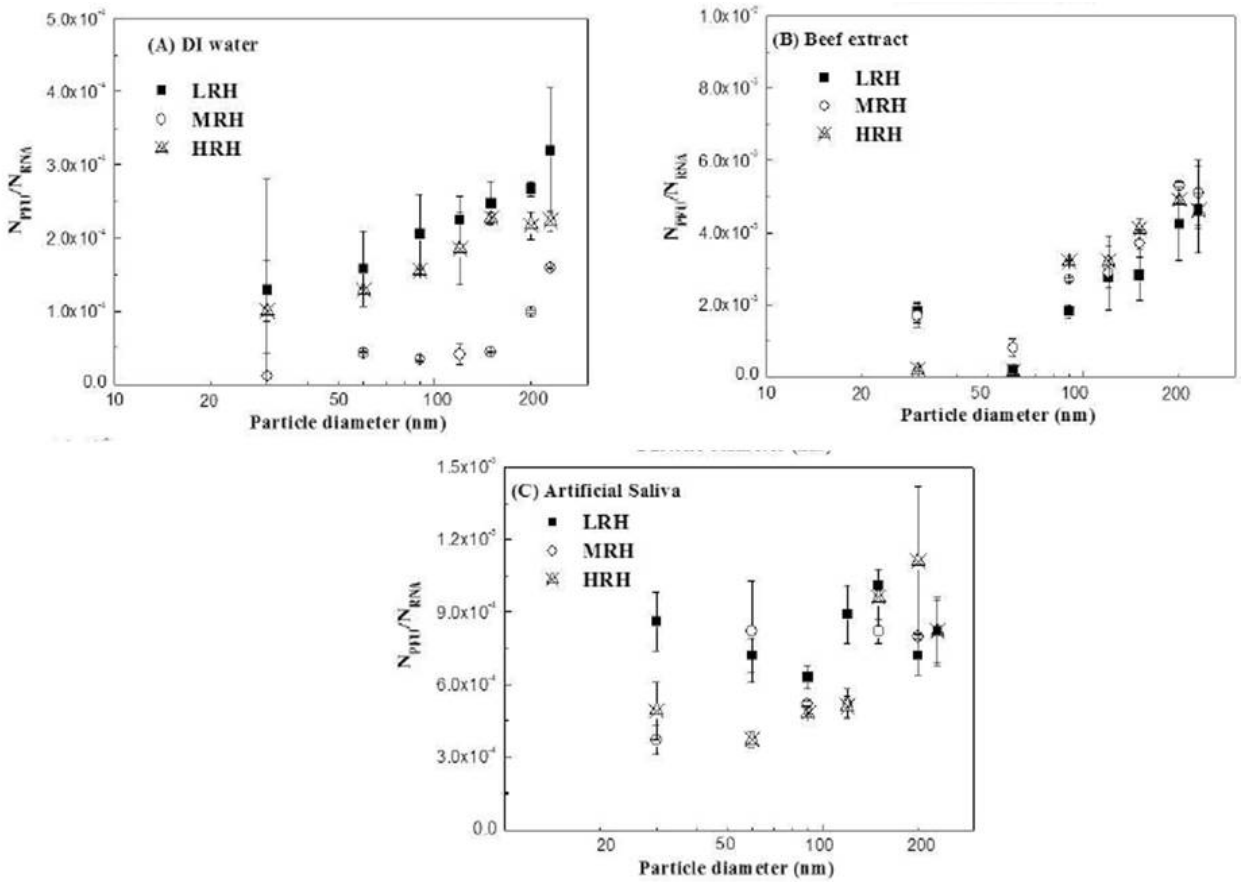

Figure 10. Stability Factors of MS2 as a Function of Diameter at Three Relative Humidities: A) DI Water, B) Beef Extract, and C) Artificial Saliva

Table 3. Slope of Least Squares Regression for N_{RNA} as a Function of Particle Size for Different Spray Media at Three Relative Humidities

Spray medium	Slope of N_{RNA} (R^2)		
	LRH	MRH	HRH
DI water	3.41 (0.99)	3.45 (0.99)	3.35 (0.99)
Beef extract	2.37 (0.99)	2.15 (0.98)	2.03 (0.99)
Artificial Saliva	1.82 (0.96)	1.83 (0.99)	1.83 (0.98)

might be explained by the larger volume fraction and surfactant properties of mucin. Mucin adsorbs to hydrophobic surfaces via protein–surface interactions and holds water molecules in hydrophilic oligosaccharide clusters. When MS2 was captured by mucin through hydrophobic interaction with MS2 protein, the hydrophilic part enabled viruses not to stick (Shi et al. 2000). Mantle and Husar (1993) reported that preincubation of plasmid-bearing *Yersinia enterocolitica* with intestinal mucin significantly reduced subsequent binding of the organism to polystyrene, suggesting that mucin may mask hydrophobic adhesions on the bacterial surface and make the microorganism more hydrophilic.

The stability of MS2 at specific sizes at different RHs was compared using the stability factor (N_{PFU}/N_{RNA}), as displayed in Figure 10. The stability of MS2 generated in DI water followed the order LRH > HRH > MRH ($p < 0.001$, Tukey's comparison < 0.05 for all). The stability factor of MS2 generally increased as a function of particle size, indicating the shielding effect of bigger particles. Indeed, the stability factor of MS2 at MRH was very small at smaller sizes; however, the value dramatically increased at larger size. It should be noted that stability factors for BE were higher than the values for DI water, indicating a protective effect of BE. Benbough (1971) reported that lower protein content in the medium led to a sharp decrease in viability and Schaffer et al. (1976) showed that the lowest concentration of protein affording virus stability was 0.1%. The slightly lower stability of MS2 in BE at LRH might be explained by crystallization of solute stressing MS2 (Trouwbor and de Jong 1973). In the same context, a protective effect of AS was confirmed, as its stability value was higher than that for solute-free medium, even though a lower stability factor was expected because of adverse effects of saliva components (Barlow and Donaldson 1973). Woo et al. (2012) reported the SEM image of super-aggregates when AS was applied to generate viruses, supporting the cross-linking effect of mucin. The viability of MS2 captured inside mucin linkages might be higher than of naked MS2.

The effect of RH on the stability factor was negligible. It might be explained by the holding of water molecules in hydrophilic oligosaccharide clusters (Shi et al. 2000). When water content is larger, there is less MS2 in a particle, resulting in a lower shielding effect. Although volume fractions in AS were shown to be higher than in BE, lower SFs were generally observed in AS. Because the volume contents of insoluble salts (0.3%) are the same, a possible reason might be soluble salt in AS, supported by Benbough's (1971) report that the soluble salt content of the suspending medium was the main reason for low viability at MRH. This result suggested that AS showed both a protective effect of insoluble mucin components and an adverse effect by soluble salt components.

4.2. Effects of Bioaerosol on the Release of Iodine from PSTI-treated Filter

The objective was to determine the effect of bioaerosol on the release of iodine from a PSTI-treated filter. It was hypothesized that the naturally occurring negative charge on the bioaerosol would induce release of iodine. Therefore, experiments were conducted to verify the hypothesis. Negatively charged MS2 was treated with or without charge neutralization, then passed through an iodine-treated filter medium. In addition, DI water was nebulized as the baseline condition.

The calibration curve of the DR/4000 V spectrophotometer was established, and the R^2 value was 0.9992 as shown in Figure 11. The iodine concentration of each test and its corresponding experimental condition are listed in Table 4. The pressure drop of the PSTI-treated filter was 2.4~2.5 in H_2O. There was no change in pressure drop across the filter medium through the entire course of experiments.

In the baseline experiment (DI water) without and with the test filter, measured concentrations were 0.014 mg/L and 0.024 mg/L, respectively. Introducing bioaerosol raised the concentrations to 0.017 mg/L (control), and 0.027–0.030 mg/L with the PSTI filter. Using a charge neutralizer had no observable effect on the result. However, the above data were very close to the detection limit (0.024 mg/L), so no conclusion can be drawn from the results to support a significant effect of MS2 bioaerosol on the release of iodine from the iodinated filter medium.

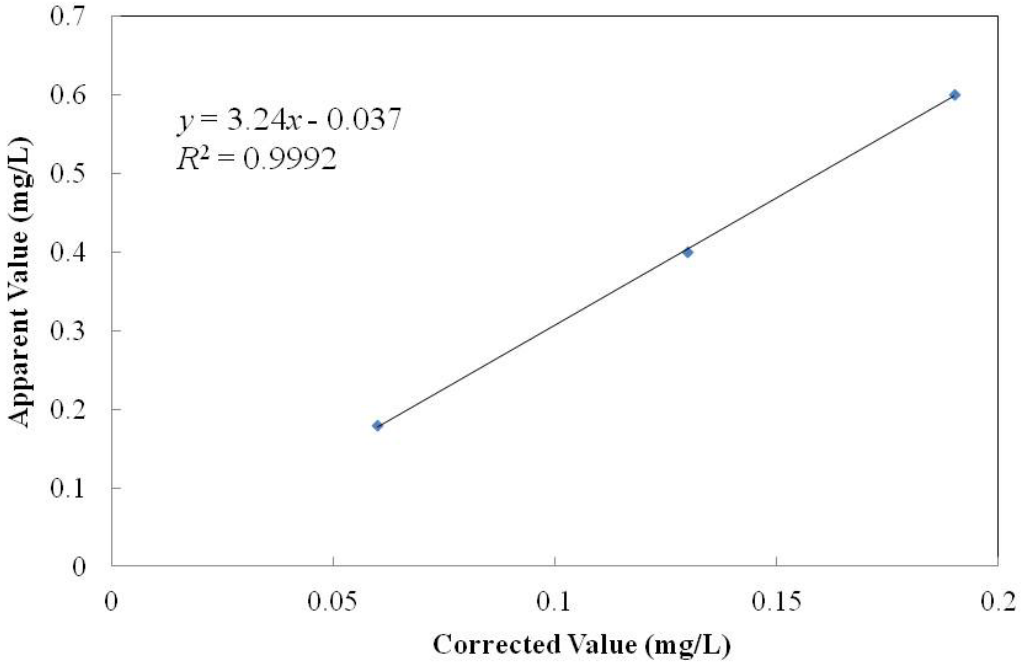

Figure 11. Calibration Curve for the DR/4000 V Spectrometer

Table 4. Iodine Concentration and Experimental Conditions for Each Test

No		T (°C)	RH (%)	Pressure gauge (in H_2O)	Iodine-treated filter	Neutralizer	Correct value
1	Blank (DI water)	-	-	-	-	-	0
2	1XPBS	-	-	-	-	-	0
3	Standard solution-1	-	-	-	-	-	0.0648
4	Standard solution-2	-	-	-	-	-	0.1296
5	Standard solution-3	-	-	-	-	-	0.1944
7	DI water (50 mL)	24	45	-	No	No	0.014
8	DI water (50 mL)	24	44	-	No	Yes	0.014
9	DI water (50 mL)	23	45	2.4	Yes	No	0.024
10	DI water (50 mL)	24	44	2.4	Yes	Yes	0.024
11	DI water (50 mL) + MS2 (10 mL)	23	45	-	No	No	0.017
12	DI water (50 mL) + MS2 (10 mL)	24	45	-	No	Yes	0.017
13	DI water (50 mL) + MS2 (10 mL)	24	46	2.5	Yes	No	0.027
14	DI water (50 mL) + MS2 (10 mL)	24	45	2.5	Yes	Yes	0.030

4.3. Method for Contamination of Filtering Facepiece Respirators by Deposition of MS2 Viral Aerosols

The focus of this study was to develop a method for reproducibly applying fixed amounts of representative viral particles generated as droplets/aerosols onto FFRs and other surfaces to support decontamination testing. A testing chamber was built and the optimal operating conditions were determined.

4.3.1. Determination of Operating Conditions

The impact of ultrasonic nebulization on viability of virus in the nebulizer reservoir was investigated by measuring viable counts over time. The results showed no significant difference in virus viability from 0 to 30 min ($p = 0.10$) (data not shown). Apparently, heat shock from ultrasonic vibration did not damage MS2 in the reservoir during droplet generation. To determine the effect of ultrasonication on virus during droplet generation, viability of viruses collected in the BioSampler after 5 and 10 min of generation was examined. The theoretical value after 5 min of nebulization is 3×10^5 PFU/mL when the virus titer in the reservoir is 1.0×10^7 PFU/mL. The 5-min time-weighted (0–5 and 5–10 min) average concentration of collected viruses in the BioSampler was around 3.2×10^5 PFU/mL, similar to the theoretical value. This demonstrated that the ultrasonic nebulizer can be used to produce droplets containing MS2 virus without adverse effects on its viability.

Figures 12A and 12B plot virus loading density as a function of loading time and of the viral titer in the nebulizer, respectively. As shown, the loading density had a linear relationship both with delivery time and with virus titer in the nebulization medium—as expected, based on the initial viability tests. This shows that these two parameters can be adjusted to select a desired loading density. It should be noted that this analysis assumed the extracted fraction to be 1; however, different types of FFRs will have different recovery values determined by their material properties and structure.

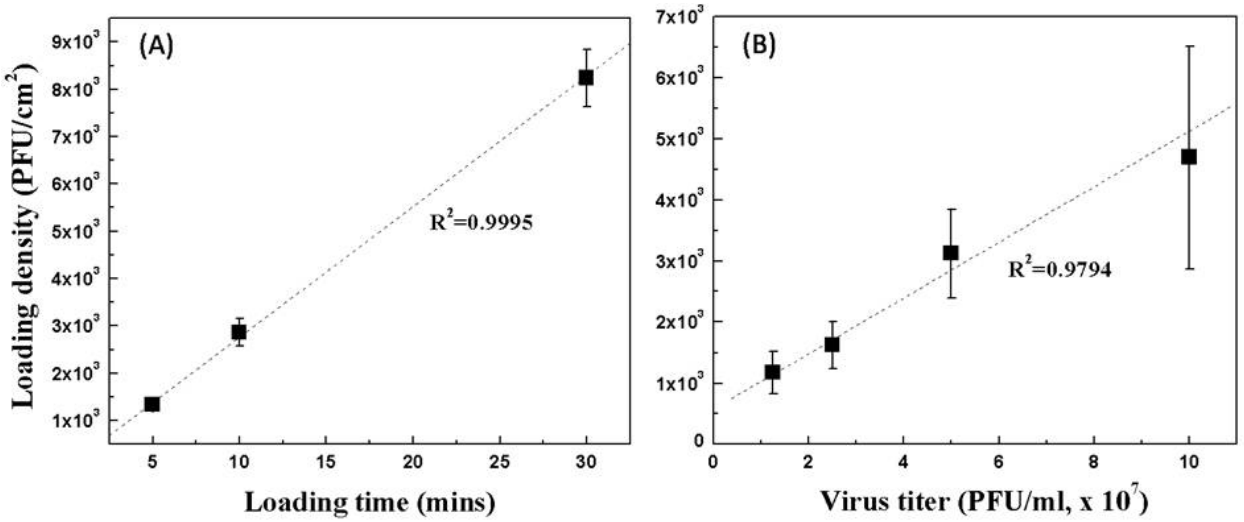

Figure 12. Loading Density as a Function of A) Loading Time and B) Virus Titer in the Nebulizer

Uniformity tests were conducted with the turntable at various speeds because Marple and Rubow (1983) observed improved uniformity of CV from 4.3% to 1.5% when they rotated their aerosol chamber at 0.56 rpm. Figure 13 shows the CVs from three runs as a function of turntable speed. The variation of the CVs was somewhat larger than what Marple and Rubow (1983) reported, due to variability working with a viable system (MS2) vs. a non-viable system (polystyrene latex (PSL) particles and dust).

The flow rate (2 Lpm) of this work is much lower than the rate (100 Lpm) used by Marple and Rubow (1983), and delivers a distribution of droplets that is sufficiently uniform (CV < 20%) even without the turntable. Differences among the six positions were not statistically significant (p = 0.73) for flat-sheet glass fiber filters. The reason for this uniformity is likely because settling is the dominant mechanism for large droplets in our system and the bioaerosols were spread through a symmetrical, six-port distributor. A straight fog stream was observed through the front window during the loading. Therefore, the turntable speed was not an important parameter to meet the uniformity criteria when the flatsheet filter was employed. Deposition of particles on FFRs after loading for 1 min was also shown by SEM (Figure 14) to be random across the fiber surface and without any specific pattern.

The criterion for minimum loading density—10^3 PFU/cm^2—was achieved for all conditions tested and could be easily increased if needed. Based on these results, the operating conditions to be discussed later were chosen to be 5-min loading time at a titer of 10^7 PFU/mL and 2 rpm turntable speed

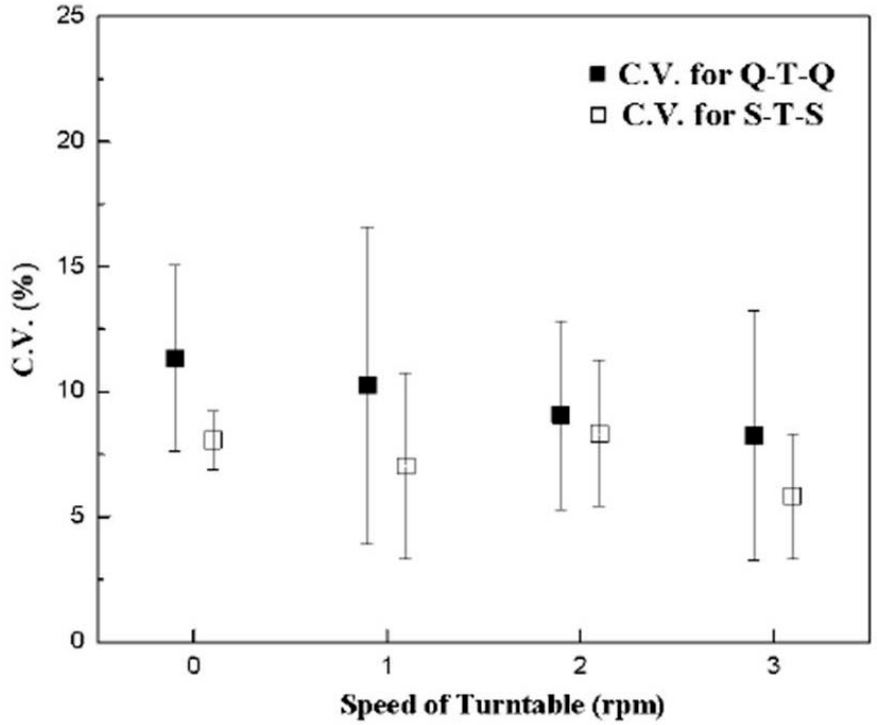

Figure 13. CVs for Q-T-Q and S-T-S as a Function of Turntable Speed

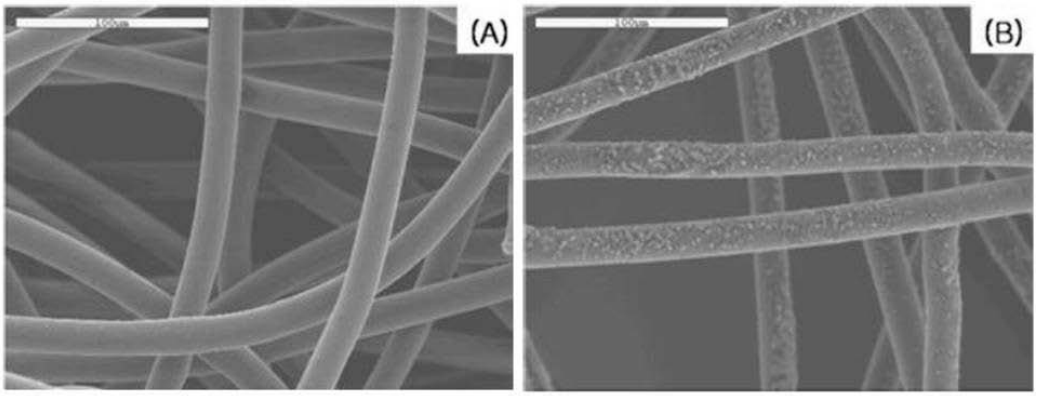

Figure 14. Scanning Electron Microscopic Images at 250×: A) Untreated FFR; B) Treated FFR

4.3.2. Droplet Size Distribution

Figure 15 shows the PSD of droplets generated by the ultrasonic nebulizer at different flow rates. PSDs of droplets generated at 1–3 Lpm were similar, with count median diameters (CMDs) and mass median diameters (MMDs) of 3.5 μm and 10 μm, respectively. The PSDs at 4 and 5 Lpm were slightly shifted to smaller diameters. Bimodal distribution was observed in the mass-based size distribution, with modes at 4~6 μm and larger than 20 μm. The theoretical CMD from the ultrasonic nebulizer can be determined from Equation 9 (Lang 1962):

$$d_{\mathrm{p}}(\mathrm{CMD}) = 0.73 \times \sqrt[3]{\frac{\sigma}{\rho f^2}} \qquad (9)$$

where d_{p} is the nebulized droplet size, σ is the surface tension of the liquid, ρ is the density of the liquid, and f is the frequency of the nebulizer. As shown, the droplet size is independent of the flow rate. The gentle airflow at 1–3 Lpm just carries the aerosol away from the liquid surface.

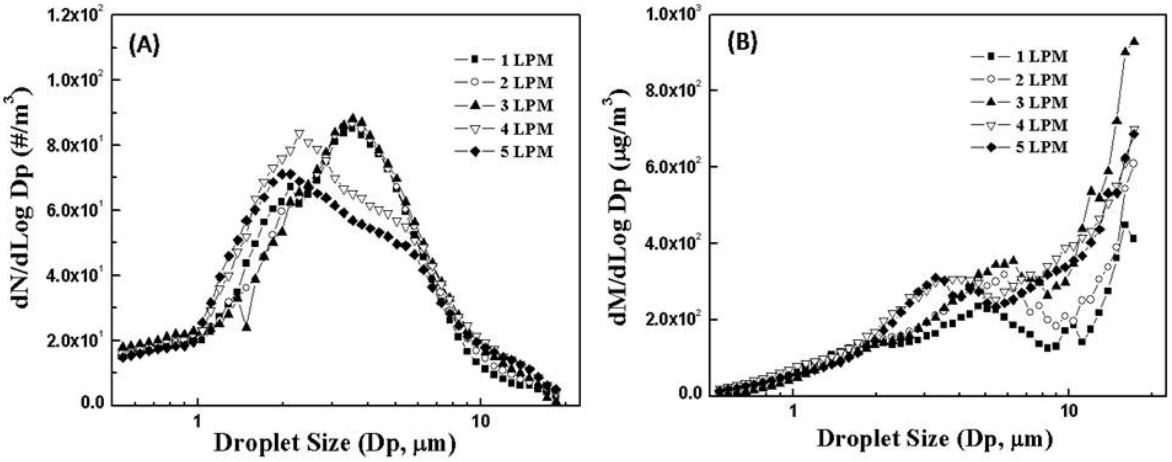

Figure 15. Size Distribution of Droplets Generated by the Ultrasonic Nebulizer at Five Flow Rates: A) Number- and B) Mass-based

However, at a higher flow rate, the larger volume of dry dilution air promotes evaporation and therefore results in a smaller droplet size. The frequency can be adjusted to generate droplets of other sizes. For example, droplets are expected to be 12.1 and 6.6 times larger, respectively, when lower frequencies of 60 kHz or 150 kHz are used instead of 2.4 MHz (Lang 1962).

The mucin concentration also plays an important role in determining the initial droplet size because it affects surface tension and density of the AS used. Mucin at 0.3% was chosen for the AS in this study to match the protein content in human saliva. Tripling the mucin concentration would reduce the median size to 40% of its original size because of the decrease in surface tension. In summary, the droplet size can be controlled by adjusting the composition of the spray medium, the frequency of the ultrasonic generator and the flow rate.

The droplet size decreases from the point of generation at the ultrasonic nebulizer all the way to the filter surface due to evaporation, and the size deposited depends on *T* and RH. Flow rates of the ultrasonic generator and the dilution air, and the temperature of the bubbler can be used to control RH, and heating tape (part (b) in Figure 3) can be used to adjust *T*. Figure 16 displays the droplet size distribution generated and loaded at 2 Lpm through the aerosol generator with 3 Lpm dry air to provide 35% RH. For this condition, cylinder air was used without a bubbler to achieve the LRH condition. MMDs for droplets generated and loaded were 9.2 and 3.2 μm, respectively, with corresponding CMDs of 3.4 and 1.8 μm , which are similar to human-generated droplet sizes reported in the literature (Morawska et al. 2009; Yang et al. 2007). If settling is considered the main mechanism acting in this chamber, the droplet's residence time is

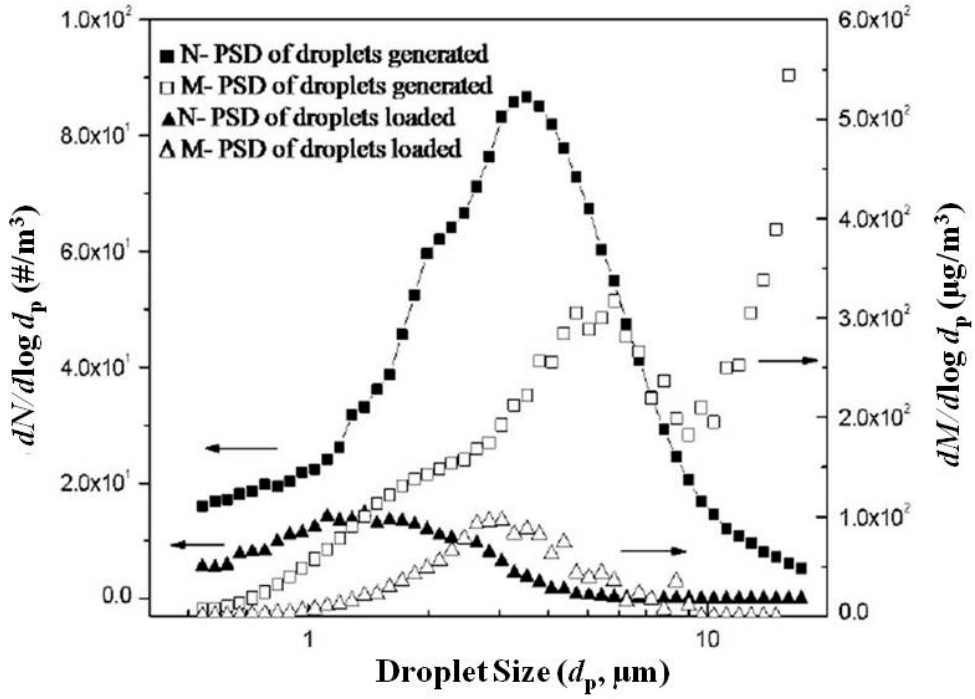

Figure 16. Number- and Mass-based Particle Size Distributions of Droplets Generated and Loaded through the Aerosol Generator at 2 Lpm with 3 Lpm Dry Air; 2-rpm Turntable Speed

0.13 s. The droplet's theoretical lifetime at 35% RH is around 0.15 s, which means that droplets reaching the FFR are almost completely evaporated. The size of a completely evaporated droplet, d_p, can be calculated according to Equation 10:

$$d_p = d_d \times \sqrt[3]{F_v} \quad (10)$$

where d_d is the droplet diameter, F_v is the volume fraction of solid material in the suspension in the nebulizer. For 0.3% mucin, the volume fraction is 0.06, whence d_p is calculated to be 1.9 μm when d_d is 9.2 μm. The reason the measured value is higher than the theoretical value is incomplete evaporation. After running the experiment, we noted that the filter surface was slightly damp, which is consistent with the above interpretation.

4.3.3. Loading onto NIOSH-certified FFRs

CVs for uniform deposition of droplets/aerosols onto substrates for six different FFRs were calculated by analyzing the infectivity of viruses extracted from the loaded filter (Table 5). The flexible nature of some FFRs makes it difficult to achieve deposition on the same spot with the same shape each time. For these, a holding medium is necessary to achieve low CV values. Fixed-form FFRs inherently cannot produce equal quarters because the shape is not symmetric. Operational variation while cutting the sample (e.g., uneven quarters) can also contribute to larger CV values. Consequently, the CV for Q-T-Q was higher than that for S-T-S over all FFRs. It is possible to use circular areas punched from a FFR so that the difference in shape will not influence the results. However, this was outside the scope of the study, which aimed to evaluate decontamination effectiveness using the entire FFR. Still, the average CVs for both Q-T-Q and S-T-S for all FFRs were lower than the respective criteria—20% and 40%—demonstrating the system's ability to consistently load the test agents. Table 5 also displays the results of the loading densities. As shown, all sets had sufficient quantity to meet the threshold criteria.

Table 5. Loading Density and Q-T-Q and S-T-S CVs for Six Different FFRs (*n*=3); Criteria for Q-T-Q and S-T-S CVs: 20% and 40%, Respectively

Shape	Type	No	Loading Density, PFU/cm^2	CV for Q-T-Q (%)	CV for S-T-S (%)
Fixed	P‡	1	$2.3\times10^3 \pm 0.3\times10^3$	12.07 ± 2.74	9.05 ± 2.22
	P	2	$2.9\times10^3 \pm 0.2\times10^3$	10.92 ± 2.09	5.89 ± 0.68
	S$^+$	3	$1.0\times10^3 \pm 0.1\times10^3$	15.41 ± 6.89*	10.12 ± 3.75
	P	4	$2.6\times10^3 \pm 0.2\times10^3$	18.04 ± 2.97	6.94 ± 3.26
Flexible	S	5	$1.2\times10^3 \pm 0.1\times10^3$	13.70 ± 1.59	9.17 ± 3.86
(duckbill)	S	6	$1.8\times10^3 \pm 0.2\times10^3$	13.19 ± 7.19	10.27 ± 1.71

*n=2, P‡: Particle respirator, S$^+$: Surgical respirator

Due to differences in surface properties, the loading densities of different respirator models can differ even when the same operating conditions are applied. Figure 17 shows the extraction efficiency of three types of FFRs at various extraction times. Different layer structures and properties of the FFRs are responsible for the differences, as discussed. The shape of the FFR is another reason for the differences in loading density. The loading densities reported in Table 5

were calculated based on each FFR's projected area. Loading density on the duck-bill-shaped FFR was lower owing to its different curvature. As shown, both factors can affect loading density. Nevertheless, a loading density can be easily achieved in a controlled fashion using the specified conditions and can be conveniently raised by increasing the loading time, virus titer, or both.

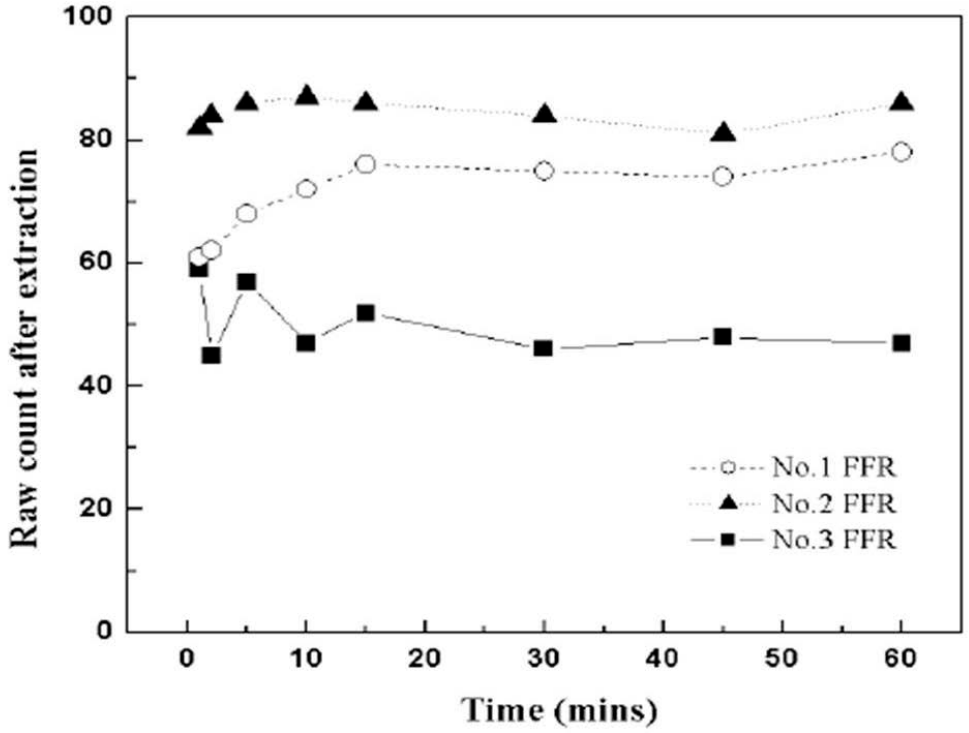

Figure 17. Recovery of Viable MS2 as a Function of Extraction Time for Three FFRs

4.4. Effects of Relative Humidity and Spray Medium on UV Decontamination of Filter Loaded with Viral Aerosols

This study investigated the IE of UV irradiation of viruses collected through different transmission modes and under various environmental conditions. For this, filters were contaminated by two pathways (droplet and aerosol) using three spraying media (DI water, BE in filtered, sterile DI water, and AS) at three RH conditions (LRH, MRH, and HRH). UV irradiation was applied at a constant intensity of 1.0 mW/cm^2 for different time intervals.

4.4.1. Effect of Transmission Mode with Different Media

Log IE is plotted in Figure 18 as a function of UV irradiation time for both droplet and aerosol modes in three different nebulizer media. HRH was applied for both loading and UV irradiation. For droplet transmission mode, the log IEs were 4.32, 2.32, and 1.98 after 60- min irradiation in DI water, AS and BE, respectively, whereas for aerosol transmission mode, the log IEs were 5.01, 2.68 and 2.32 in the same media. The IEs in this figure depend on three parameters:

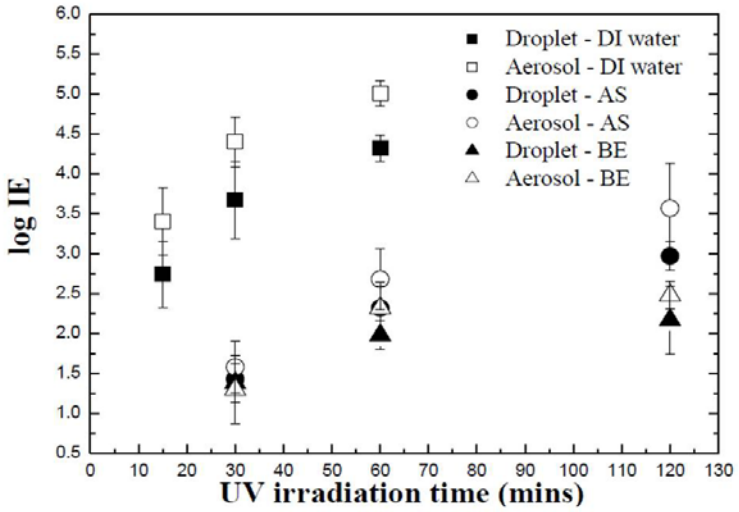

Figure 18. Log Inactivation Efficiency (IE) vs. UV Irradiation Time at HRH for Droplet and Aerosol Transmission Modes Loaded in Different Nebulizer Media at HRH

a) UV irradiation time: Extending the irradiation time increased the IE because the UV dose increased. When the application time increased from 30 to 60 min, the dose of UV irradiation doubled from 1.8 J/cm^2 to 3.6 J/cm^2, increasing the amount of damage to nucleic acids.

b) Transmission mode: IE for aerosols was higher than for droplets. Water in the droplets absorbs UV (Kowalski 2009; Prescott et al. 2006), and shielding of viruses near the center of the aggregate likely also contributes to this trend. The size of droplets generated from the ultrasonic nebulizer was 9~10 μm (Woo et al. 2010) whereas aerosols from the Collison nebulizer measured 1–2 μm (May 1973). Evaporation time for a 1-μm droplet at HRH is 0.0077 s at 20 °C. As the residence time of aerosol in the mixing chamber was 0.21 s, these particles reached equilibrium during transit. However, the evaporation time of 9–10 μm droplets at HRH and 20 °C was 0.63–0.7 s—much longer than the residence time—so the larger droplets retain much of their water at contact. The equation used to calculate the evaporation time is as follows (Hinds 1999):

$$t_{\text{evaporation time}} = \frac{R\rho_p d_d^2}{8D_v M\left(\frac{p_d}{T_d} - \frac{p_\infty}{T_\infty}\right)} \quad (11)$$

where R is the ideal gas law constant, ρ_p is the density of particle, d_d is the droplet size, D_v is the diffusion coefficient of water vapor molecule, M is the molecular weight of water, T_∞ and p_∞ are T and the pressure away from the droplet surface (i.e., the environmental conditions) and T_d and p_d are the same parameters at the droplet surface. Room temperature (20 °C) was applied for T_∞ and the equation below was used to determine T_d:

$$T_d = T_\infty + \frac{(6.65 + 0.345T_\infty + 0.0031T_\infty^{\,2})(S_R - 1)}{1 + (0.082 + 0.00782T_\infty)S_R} \quad (12)$$

where S_R is the saturation ratio. The partial pressure in kPa at a given T in K is calculated according to

$$p_d = \exp(16.7 - \frac{4060}{T_d - 37}) \quad (13)$$

c) Spraying medium: IEs in AS and in BE were much lower than in DI water for both aerosol and droplet transmission. The likely reason for this difference is a protective effect caused by solids in both AS and BE. From the composition of the media, the volume fractions of solids in DI water, BE and AS were 1×10^{-4}, 3.1×10^{-3} and 6.0×10^{-3}, respectively, after complete evaporation. DI water has a much lower solid content. SEM images, shown in Figure 19, of filters contaminated with MS2 viruses aerosolized in different media support this mode of protection. Images of MS2 generated in DI water and loaded on the filter (Figure 19 B) show aggregates in the range of 100 nm–1 μm on the substrate. Riemenschneider et al. (2010) and Jung et al. (2009) reported MS2 aggregates of around 200 nm for the MS2 suspension and 30–200 nm for captured aerosol particles.

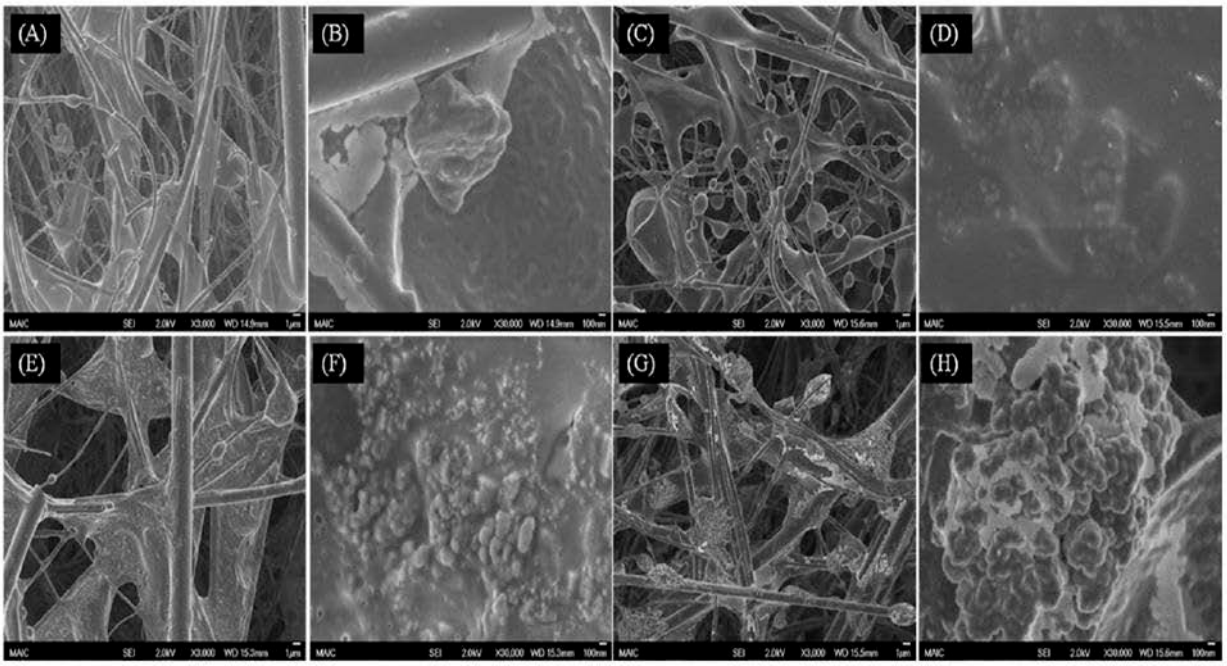

Figure 19. SEM images of a Filter Contaminated with Viruses Aerosolized in A) and B) DI Water, C) and D) 0.3% Beef Extract, E) and F) Artificial Saliva, and G) and H) Artificial Saliva without Mucus under HRH; Magnification of A), C), E) and G) 3,000× and of B), D), F) and H) 30,000×

MS2 aerosolized in BE instead of DI water was captured as oval-to-spherical features as shown in Figure 19 C. Precipitated BE solids formed a thick shell encapsulating the MS2 virions and/or aggregates, as displayed in Figure 19D. The solids in AS are water-insoluble mucin and various water-soluble salts. To test the hypothesis that the salts and mucin act separately to afford protection (Lee et al. 2011), MS2 was aerosolized from AS media prepared both with and without mucin. As aerosolized virions and aggregates load onto the filter, it is possible for them to form a wide size range of super-aggregates. Figure 19 H shows that grape-shaped super-

aggregates were observed in the absence of mucin. Multivalent cations of the soluble salts (Mg^{2+} and Ca^{2+}) can interact with negatively charged features on the MS2 surface to promote a high degree of virus aggregation (Sjogren and Sierka 1994). Encasement by a thin layer through the crosslinking network (Figure 19F) appears to result from gel formation caused by the presence of mucin. The similarity of the underlying structures in Figures 19 F and 19 H suggests that mucin contributes little or nothing to the aggregation process and simply encases the final configuration.

To isolate the UV-protective effect of water-insoluble mucin in AS, the IEs of MS2 nebulized in mucin-free AS medium and mucin-only medium were compared. To make a fair comparison, 0.3% and 0.6% volume fractions were considered. As shown in Figure 20, the log IEs in 0.3% mucin-free AS were 3.66, 4.33 and 4.94 after 30-, 60-, and 120-min irradiation, respectively, whereas the log IEs in 0.3% mucin medium were 3.12, 3.94, and 4.37, respectively. That log IEs in mucin-free AS were lower than those in DI water suggests a protective effect of water-soluble salts. The higher IE in 0.6% mucin-free AS compared to 0.3% mucin-free AS was expected because salts increase hydration and then more water can shield viruses. Contrary to that expectation, the difference between 0.3% and 0.6% mucin-free AS was not significant. The log IEs in 0.3% mucin-free AS were higher than those in 0.3% mucin medium (salt-free AS), indicating better protection by water-insoluble mucin than by various water-soluble salts.

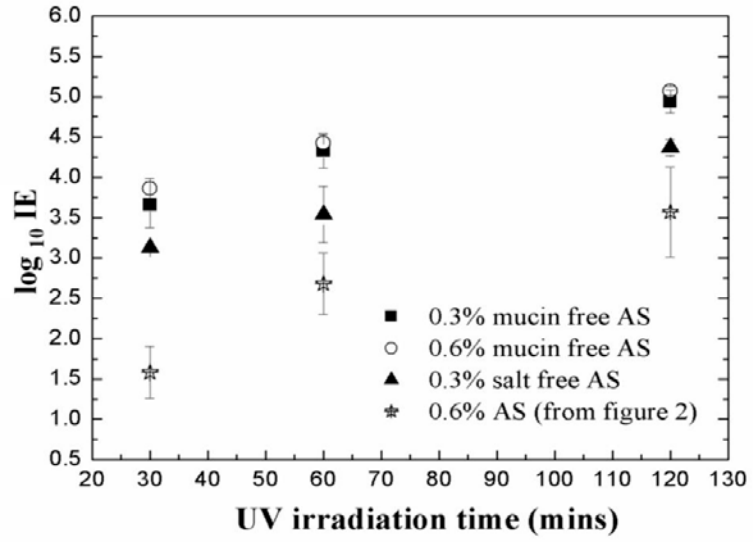

Figure 20. Log IE Virus Loading and UV Exposure at HRH for Aerosol Transmission Mode from 0.3% and 0.6% Mucin-free Artificial Saliva and 0.3% Salt-free Artificial Saliva as a Function of UV Irradiation Time

Relatively higher IEs in both mucin-free AS and salt-free AS than those in AS suggest that both encasement by water-insoluble mucin and aggregation by water-soluble salts contribute to the protection. In addition, that the encasement in BE provided better protection than in AS—even through the volume fraction of solid in BE is only half of that in AS—appears to indicate that the organic solids in BE are stronger absorbers at 254 nm and thus provide more-effective protection from UV radiation.

4.4.2. Effect of RH during both Loading and Inactivation

Log IEs measured after aerosol loading for 30 min followed by UV exposure for 60 min at different RHs are displayed in Figure 21. The corresponding general factor ANOVA results appear in Table 6. Because the strong effect of the spray medium (> 80% contribution, not shown) made it difficult to distinguish the RH effect, two-way ANOVA was also conducted for each spray medium. Referring to Figure 21, upon completion of the experiment, the highest IE, around log 5.8, was seen in filters subjected to UV irradiation after applying the MS2 in DI water at LRH. However, it should be noted that the actual IE at this condition might be somewhat higher because values measured under LRH during UV inactivation after aerosol loading in both LRH and MRH conditions were at the detection limit of our experimental system.

Table 6. Statistics in General Factor Analysis of Variances

	p value
Three-factor ANOVA for three media	
spray medium	< 0.0001*
RH during UV inactivation	0.0197*
RH during aerosol loading	< 0.0001*
Spray×RH during aerosol loading	< 0.0001*
Two-way ANOVA for DI water	
RH during aerosol loading	< 0.0001*
RH during UV inactiation	< 0.0001*
RH during UV inactivation × RH during aerosol loading	0.0118*
Two-way ANOVA for beef extract	
RH during aerosol loading	0.2202
RH during UV inactivation	0.4188
RH during UV inactivation × RH during aerosol loading	0.6278
Two-way ANOVA for artificial saliva	
RH during aerosol loading	0.4569
RH during UV inactivation	0.0204*
RH during UV inactivation × RH during aerosol loading	0.9983

SS: sum of squares, DF: degree of freedom, MS: mean square, *Significant parameter

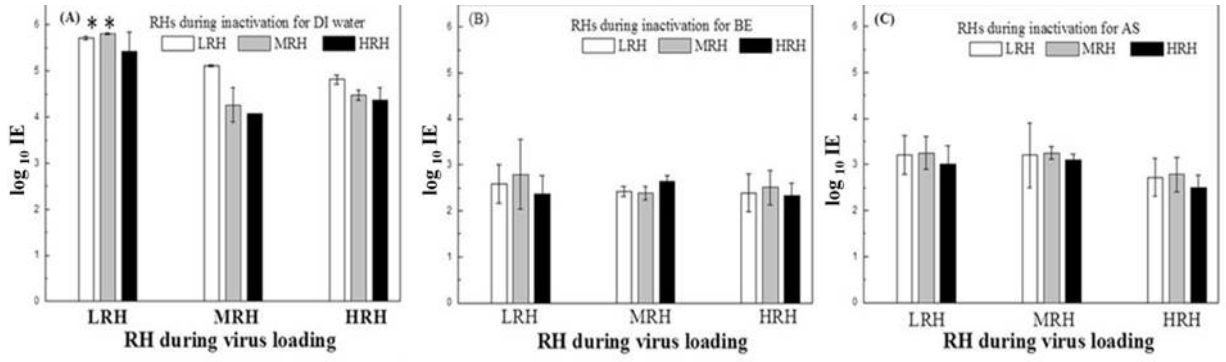

Figure 21. Log Natural Decay and Inactivation Efficiency as a Function of Relative Humidity during Both Loading and UV Inactivation: A) DI Water, B) 0.3% Beef Extract, and C) Artificial Saliva

For MS2 delivered in DI water, both RH during UV inactivation ($p < 0.0001$) and RH during aerosol loading ($p < 0.0001$) are significant, as is the interaction for both RHs ($p = 0.0118$). This may be attributed to a combination of intrinsic susceptibility of MS2 and susceptibility of MS2 to UV exposure, augmented by stress imposed on MS2 by aerosolization under different loading RHs. The second susceptibility was the more important parameter because the contribution of RH during inactivation (75%, not shown) was five times that of RH during aerosol loading (15%, not shown). In general, IEs at LRH were higher than those at both MRH and HRH, suggesting a protective contribution by a water layer. This is broadly consistent with a report that IE of UV against microbes dramatically dropped off above 70% RH.

Unlike in DI water, IEs in BE were not significantly influenced by RH during virus loading, during UV irradiation for 60 min, or by their interaction—IE was in the range of 2.4–2.8 logs under all nine sets of RH conditions. The contributions of both RH regimes are less than 6%, although the contribution of RH during inactivation is 1.9 times that of RH during virus loading, suggesting some effect of water on protection by the solid content. To investigate the protective effect of solid contents in BE directly, intensities of a 1.0-mW/cm^2 UV beam after penetrating BE solutions of different concentrations were compared. Values of 0.97, 0.78, 0.62 and 0.41 mW/cm^2 were found after penetration of solutions containing 0%, 0.1%, 0.3%, and 0.5% BE, respectively, supporting the conclusion above that UV absorbers in BE contribute significantly to its observed protective effect.

In AS, IEs fell in the range 2.7–3.2 logs under all conditions, showing that dissolved solids in these experiments eliminated sensitivity of the MS2 particles to RH during loading. However, RH during inactivation was a statistically significant factor ($p = 0.0204$). To distinguish the significance of the RH levels, a Tukey comparison was conducted and a difference was identified at HRH. Compared to BE, AS was less protective—even though the solid fraction of AS is larger—and the contribution of RH at both stages was larger (38%, not shown) in AS than in BE (6%, not shown). These are consistent with conclusions above from SEM images and UV absorption results that the two solid media act by different routes: solids in BE appear to encase the virions in a shell that provides environmental protection and some UV screening. In contrast, multivalent cations in AS appear to gather virions and promote formation of superclusters coated with a layer of mucin as a gel that affords less protection and is more sensitive to water than the BE shell.

4.4.3. Virus Susceptibility

When microbes are exposed to a biocidal factor, first-order decay of viability is commonly observed (Brickner et al. 2003), and the IE of UV irradiation as a function of time can be defined as

$$\mathrm{IE} = \frac{N_0}{N_s} = (A \times e^{-KCt})^{-1} \qquad (14)$$

where A is the fraction of the total initial population subject to fast decay, N_0 and N_s are the concentrations of airborne virus before and surviving after UV exposure, respectively; C is the UV intensity (W/m^2); t is time (s); and K is the susceptibility factor (m^2/J) for the virus. Although this equation gives a straight line semi-logarithmic plot, a shoulder at IE < 90% and tailing at the

low end were not incorporated (Brickner et al. 2003; Kowalski and Bahnfleth 2000). The shoulder represents the threshold dose; if the dose is insufficient, the virus shows negligible response or even recovers from the damage. Meanwhile, the slow decay curve at the tailing might be from a resistant minority of viruses and/or reaching the detection limit (Kowalski and Bahnfleth 2000).

Table 7 lists first-order decay *K*s derived from the experimental results. A higher *K* was seen for both loading and exposure in LRH. In addition—as expected—*K* at LRH in DI water was higher (by more than 10×) than in AS or BE. Table 8 lists UV susceptibilities reported for some other viruses. *K* for viruses is in the range 0.01–10. The value of MS2 in DI water is similar to that of a corona virus, which is of the same genomic type. Low *K* values for double-stranded and DNA-type viruses were expected both because their undamaged strands are able to repair UV-damaged segments and because RNA is a stronger UV absorber than DNA (Kowalski 2009). However, for double-stranded DNA-type viruses, values of *K* were found to vary widely, depending on the characteristics of individual viruses, rather than to follow a simple classification by genome type.

Table 7. Virus Susceptibility Factor *K* for Aerosol Transmission under Different Conditions

RH condition			*K* (m^2/J) in	
Loading	UV exposure	DI water	AS	BE
LRH	LRH	0.764	0.056	0.046
	MRH	0.267	0.043	0.040
	HRM	0.273	0.045	0.039
MRH	LRH	0.222	0.061	0.051
	MRH	0.189	0.058	0.044
	HRH	0.209	0.051	0.041
HRH	LRH	0.231	0.055	0.042
	MRH	0.222	0.056	0.044
	HRH	0.207	0.044	0.038

Table 8. Virus Susceptibility Factors (m^2/J) from Other Studies

Test Microbe	Type	<68%RH	>75%RH	Reference
Adenovirus	dsDNA*	0.039	0.068	Walker and Ko (2007)
Vaccinia	dsDNA	6.00	1.42	McDevitt et al. (2007)
Phage T7	dsDNA	0.33	0.22	Tseng and Li (2005)
Phage Phi 6	dsDNA	0.43	0.31	Tseng and Li (2005)
Phage phi X174	ssDNA	0.71	0.53	Tseng and Li (2005)
Corona virus	ssDNA	0.38	-	Walker and Ko (2007)

*dsDNA = double-stranded DNA, ssDNA = single-stranded DNA

4.5. Inactivation of Viral Aerosols by Microwave-Irradiation-Assisted HVAC Filtration

This study sought to evaluate the inactivation performance of microwave-irradiation assistance to HVAC filtration systems during on-the-fly filtration of MS2. Key parameters examined were

microwave power level, microwave application time, and RH. The thermal stability of the filter media was also investigated.

4.5.1. Temperature Measurement of Test Filters

TGA/differential thermal analysis (DTA) was used to determine the appropriate temperature range for microwave-assisted HVAC filtration because of concern that the polymer fiber of the filter might experience melting or other mutations during the thermal process. As displayed in Figure 22A, no residual moisture loss around 100 °C was observed in any of the three filters, showing the hydrophobicity of the filter material. For filters 1 and 2, two endothermic events were observed at 125–130 °C and at ~170 °C; for filter 3, no endothermic or exothermic event was observed over the range 25~300 °C, as shown in Figure 22B. Therefore, to avoid filter damage, 125 °C was set as the maximum *T* for microwave irradiation.

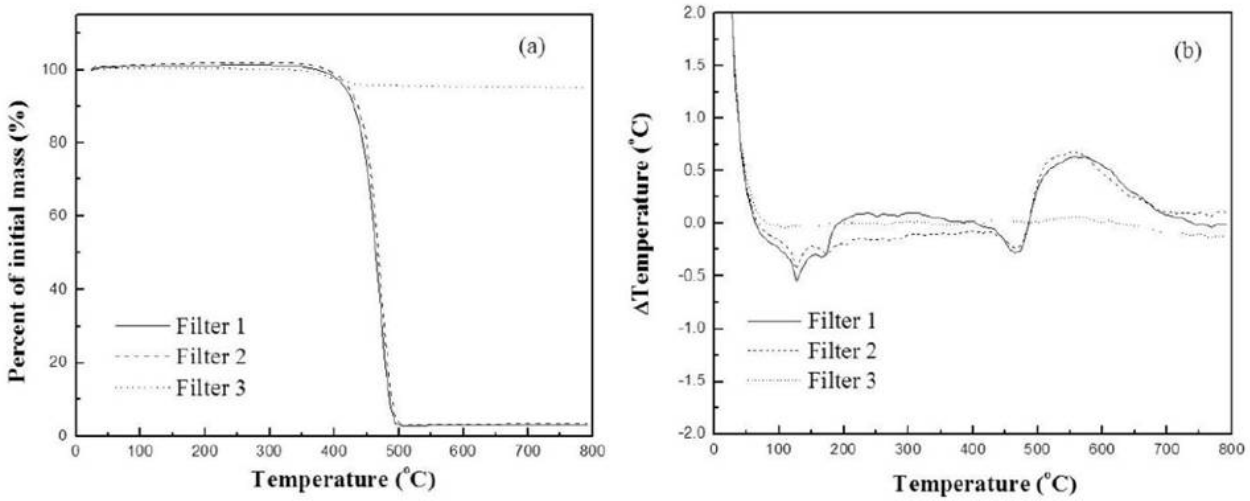

Figure 22. Thermal Stability Analysis for Three Filters: A) TGA, and B) DTA

Figure 23 displays *T* profiles of filters supported on a SiC disk running with a 4-Lpm flow rate at different microwave power levels and application times. Linear increase in *T* as application time increased was expected. However, the results showed a different trend. At 250 W, *T* did not increase much after 2.5 min, likely due to the balance between heating by microwave irradiation and cooling by the air stream. At 375 W for 10 min/cycle, the max *T* was around 120 °C, whereas it reached 165 °C without airflow, illustrating the cooling effect by the air stream. Based on the *T* measurement, a maximum power level of 375 W was selected to investigate the IE and SF in this study. Higher power levels of 500 W and 750 W were selected for only filter 3 because of its high thermal stability.

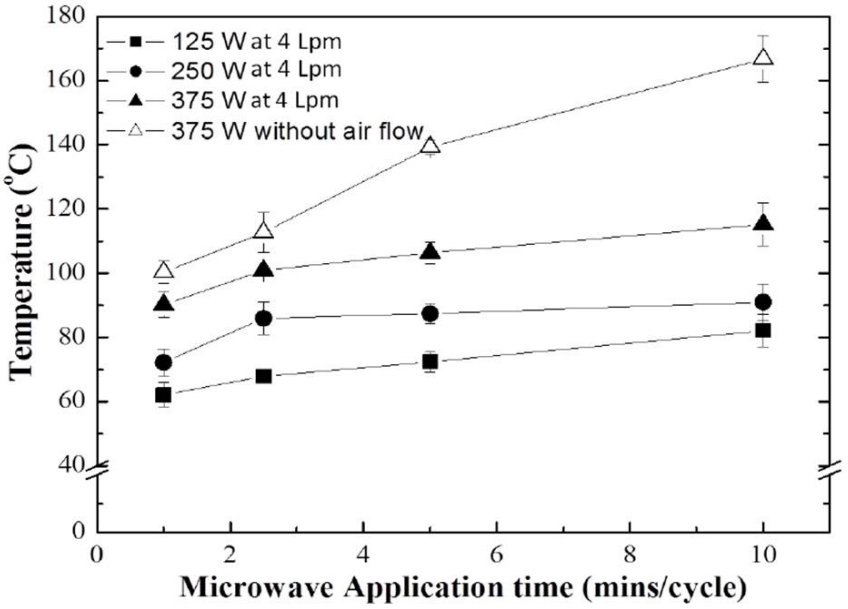

Figure 23. Temperature of Three Filters as a Function of Microwave Application Time at Three Microwave Power Levels

4.5.2. Inactivation Efficiency and Survival Fraction

For filter 1, the IE of the microwave-irradiation-assisted filtration system and the SF on the filter surface as a function of microwave power at four different microwave application times are displayed in Figures 24A and B, respectively. As shown, IE increased and SF decreased as microwave power increased and as application time was extended. For the IE, changes to both microwave power level ($p < 0.01$) and application time ($p < 0.01$) were significant. The IE is attributed to two factors: 1) physical capture by the filtration mechanism and 2) inactivation of viruses during flight. At the lowest setting—125 W for 1 min/cycle—no additional disinfection was observed beyond the mechanical log removal efficiency of 0.53 (i.e., 71%) wherein the physical FE ($1-C_D/C_E$) of filter 1 was ~73%. At a power level of 375 W, 3.0 and 3.5 logs of the viable MS2 were disinfected when microwave irradiation was applied for 5 and 10 min/cycle, respectively. This suggests that an application time of 5 min/cycle is sufficient to disinfect MS2. Significant influences of both microwave irradiation time ($p = 0.02$) and power level ($p = 0.03$) upon SF were seen. The trends of SF were similar to those of IE, although a much lower SF was expected at higher microwave power levels because of the longer exposure time of 30 min for the SF as compared to the shorter flight time of less than 5 s for the IE. However, at 375 W applied for 5 and 10 min/cycle, a higher value of log IE was observed than the absolute value of log SF.

Physical capture is one possible reason for the higher log IE. However, log IEs after deducting the inherent removal efficiency were still higher than the absolute values of the log SF (2.5 and 2.9 vs. 1.8 and 2.5). This may be caused by the high *T* of the SiC disk. Damit et al. (2011) reported that exposure of MS2 to the high *T* of 250 °C for 1 s resulted in 4-log SF. *T*s of the SiC disk at 375 W immediately after irradiation at 5 and 10 min/cycle were 172 °C and 203 °C, respectively, whereas *T*s of the filters on the SiC disk were 107 °C and 117 °C. Thickness of the

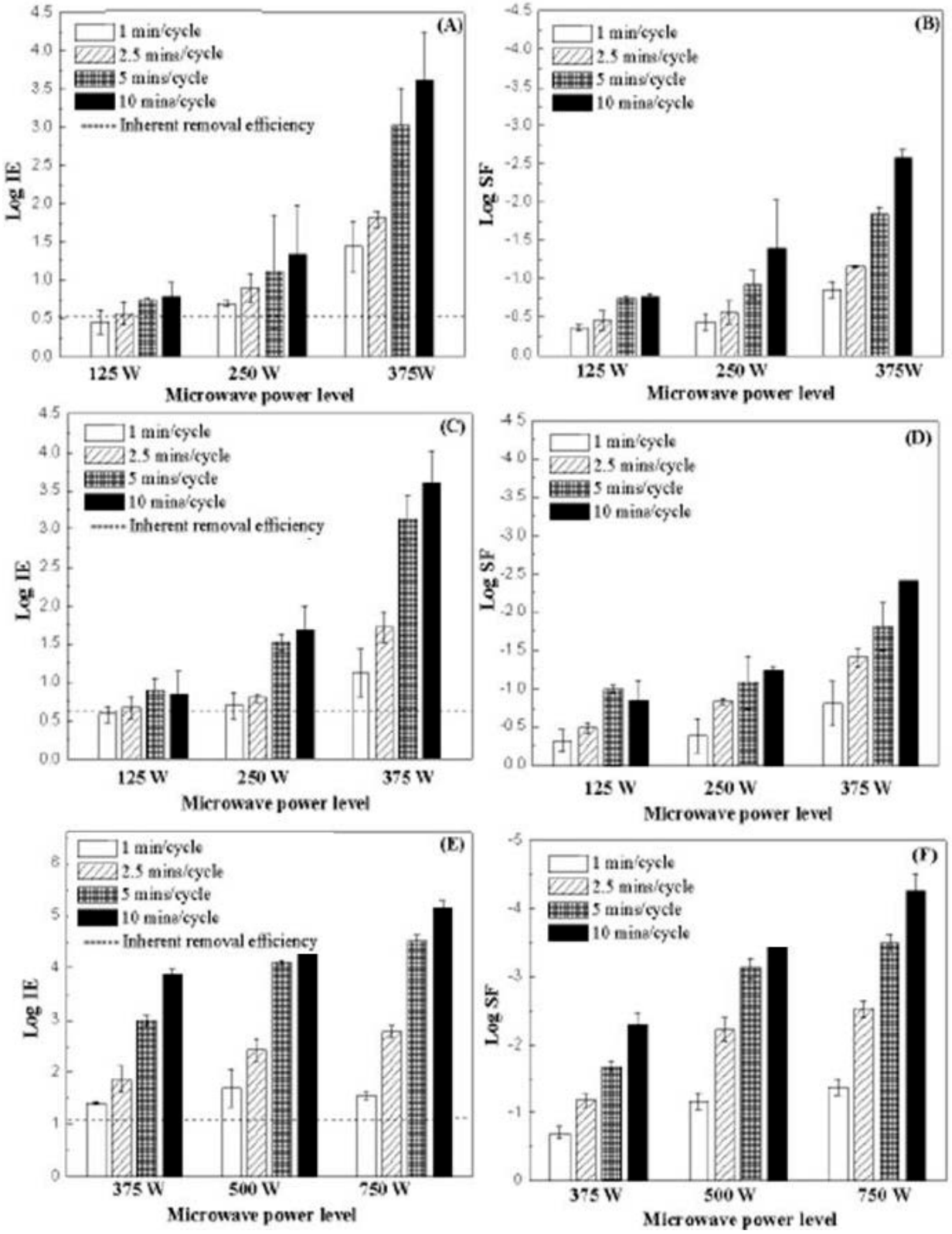

Figure 24. Log Inactivation Efficiency and Log Survival Fraction: A) and B) Filter 1, C) and D) Filter 2, and E) and F) Filter 3

SiC disk was 2.54 cm, and viruses passing through the disk were exposed to these high temperatures for 0.5 s. This exposure during flight could contribute to the higher IE. For filter 2, similar results were seen (Figures 24C and D), although the inherent FE was slightly higher than that of filter 1. For filter 3, IE and SF at 375, 500 and 750 W are displayed in Figures 24E and F. As shown, IE and SF at 375 W are similar to those for filters 1 and 2, although the higher inherent FE was around 95%. At 500 W and 750 W, log SFs of -3.47 and -4.23 were seen, respectively. *T*s of filter 3 on the SiC disk at 500 W and 750 W for 10 min/cycle were 143 °C and 171 °C, respectively. This result suggests that the thermal stability of filter material is an important factor for microwave disinfection applications.

4.5.3. Effective Temperature

Comparing the microwave irradiation power level and application time data revealed that filter disinfection can be characterized by a *threshold temperature*, i.e., *T* at which inactivation starts to increase sharply. Similarly, an *effective temperature*, defined as the minimum *T* that must be reached for effective disinfection (2-log or greater), can also be identified. The threshold and effective temperatures can be estimated in Figure 25, which displays log IE and log SF as a function of *T* reached after microwave irradiation. The data pattern greatly resembles a two-stage process—an initial accumulation of energy, and then a catastrophic release, simply indicating a threshold temperature has been reached. The IE remained unsatisfactory until the threshold *T* near 90 °C, and it reached 2 logs at 109 °C. SF also started to rise around 90 °C and reached 2 logs at 116 °C. Once *T* of the filter reaches this threshold value, effective disinfection of the virus can be assumed.

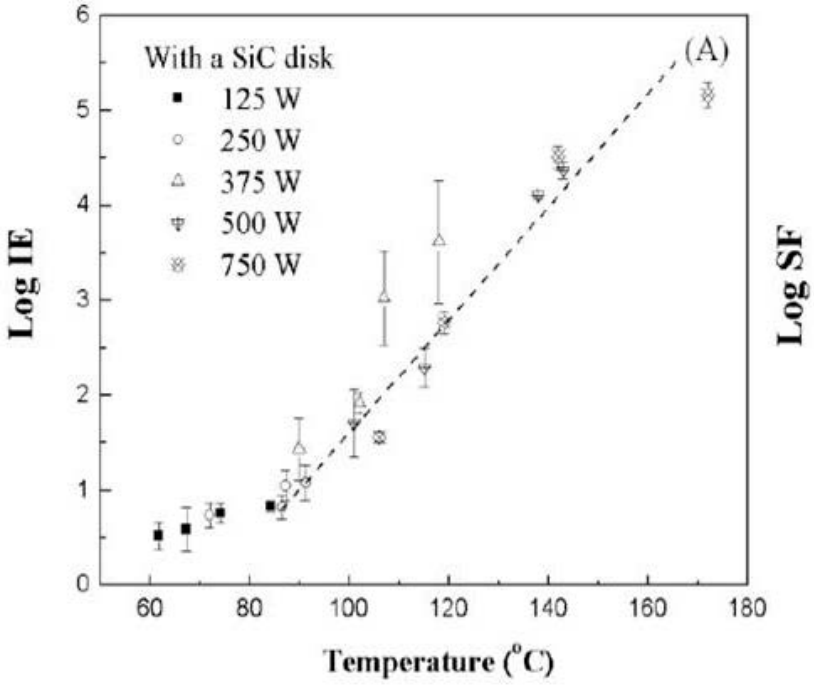

Figure 25. Microwave Inactivation Performance: A) Log Inactivation Efficiency and B) Log Survival Fraction As a Function of the Temperature Reached during Microwave Irradiation of Filter 1 for 125, 250 and 375 W and Filter 3 for 500 and 750 W

IE and SF of each filter against MS2 can also be expressed as a function of T via a log-linear relationship above the threshold temperature, as displayed in Table 9. Although different intercepts and slopes were expected because of different inherent physical removal efficiency and thermal properties of filter, the difference was not significant ($p < 0.05$).

Table 9. Linear Relationship of IE and SF of MS2 with Temperature (T)

Filter 1	Log IE = -7.14 (-7.65)[a] + 0.087T (p = 0.04)	Log SF = 4.67 - 0.057T ($p < 0.01$)
Filter 2	Log IE = -6.69 (-7.46) + 0.077T (p = 0.02)	Log SF = 4.81 - 0.060T ($p < 0.01$)
Filter 3	Log IE = -6.57 (-7.60) + 0.078T ($p < 0.01$)	Log SF = 5.05 - 0.061T ($p < 0.01$)
All filters[b]	Log IE = -6.83 (-7.57) + 0.080T (p = 0.02)	Log SF = 5.01 - 0.060T ($p < 0.01$)

[a]The values in parentheses in log IEs are the intercepts calculated with inherent filtration efficiency deducted.

[b]The relationships were obtained from all IEs and SFs above threshold temperature of three filters.

Furthermore, when the intercepts of log IE were corrected by deducting the inherent FE, the results showed no difference among all three filters (p = 0.02). Therefore, in and near the temperature region studied, the IE and SF of MS2 for a microwave-irradiation-assisted filtration system can generally be expressed as

$$\text{Log IE} - \log \text{IE}_{\text{inherent filtration}} = \log \text{IE}_{\text{microwave}} = -7.57 + 0.08\,T$$

$$\text{Log SF} = 5.01 - 0.06\,T \qquad (15)$$

Thus, the threshold temperature for an HVAC filter having 99.9% FE to reach 6-log IE for MS2 is ~132 °C.

Although thermal effect is recognized as a major factor for microwave inactivation, Khalil and Villota (1989) compared the distortion of RNA subunits in *S. aureus* after microwave and conventional heat treatments, and found destruction of the 23S RNA only by microwave treatment, indicating the possibility of a nonthermal effect. In addition, Betti et al. (2004) reported a nonthermal effect of microwaves against plants and viruses at a sublethal temperature, and Wu and Yao (2010) confirmed visible changes of bacteria and fungi after microwave heat treatment by environmental scanning EM. Hence, in this study nonthermal effects were investigated by studying morphological changes and SFs with and without microwaves at the same temperature. Figure 26 displays temperature profiles of a conventional and a microwave oven. Temperatures of the conventional oven were selected to match the temperature profiles of the microwave oven at 250 W and 375 W. The conventional oven's temperature was stable for 30 min of test time. For the microwave oven operated at 250 W, a steady-state temperature profile was observed after 10 min. However, temperatures around 90 °C at 250 W might be insufficient to inactivate MS2. Therefore, 375 W was selected for observations of morphological changes through SEM.

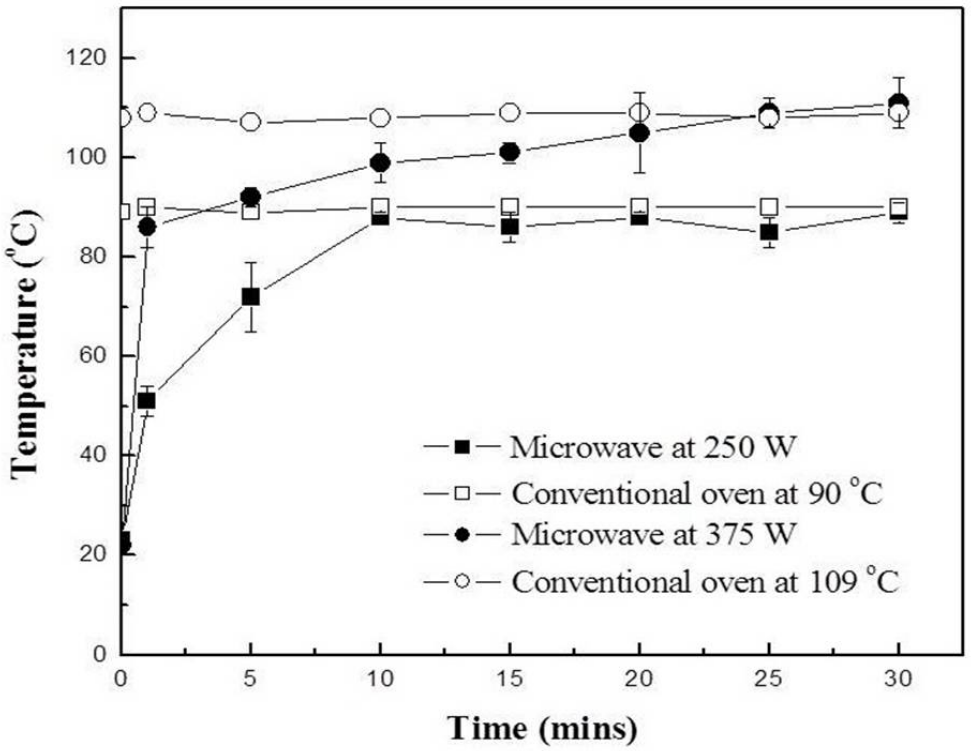

Figure 26. Temperature of Microwave and Conventional Ovens as a Function of Application Time. The Error Bar Represents One Standard Deviation.

Figure 27 displays SEM images of untreated, conventional-oven-treated, and microwave-treated virus-contaminated filters. As shown in Figure 27B and C, the heat of both the conventional oven and the microwave oven made the water evaporate (or removed it in some other way), and then aggregation was observed. However, no significant difference in morphology was seen, even though the concentration of microwave-treated viruses was lower than that of conventional-oven-treated viruses. SFs of viruses on the substrates after heat treatment by microwave oven and conventional oven were also compared but no significant difference was shown, indicating that no non-thermal effect of microwaves can be elucidated in this study.

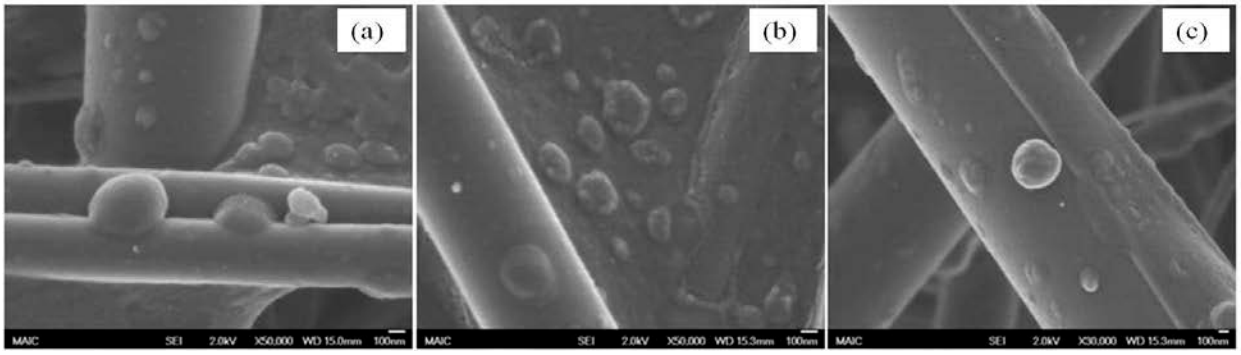

Figure 27. SEM Images of Virus-contaminated Filters at 50,000× Magnification: A) Untreated, B) Conventional-heat-treated, and C) Microwave-treated

4.5.4. Effect of relative humidity on inactivation performance

RH is a key parameter for the inactivation of viruses. However, when a SiC disk is used, it is difficult to discern the effect of RH because of the overwhelming thermal effect of the SiC disk. Therefore, to isolate the effects of RH, a quartz frit was used as a support instead of a SiC disk. Figures 28A and B, respectively, display IE through the system and SF on the filter surface as a function of microwave power level applied to filter 1 for 5 min/cycle under three RHs.

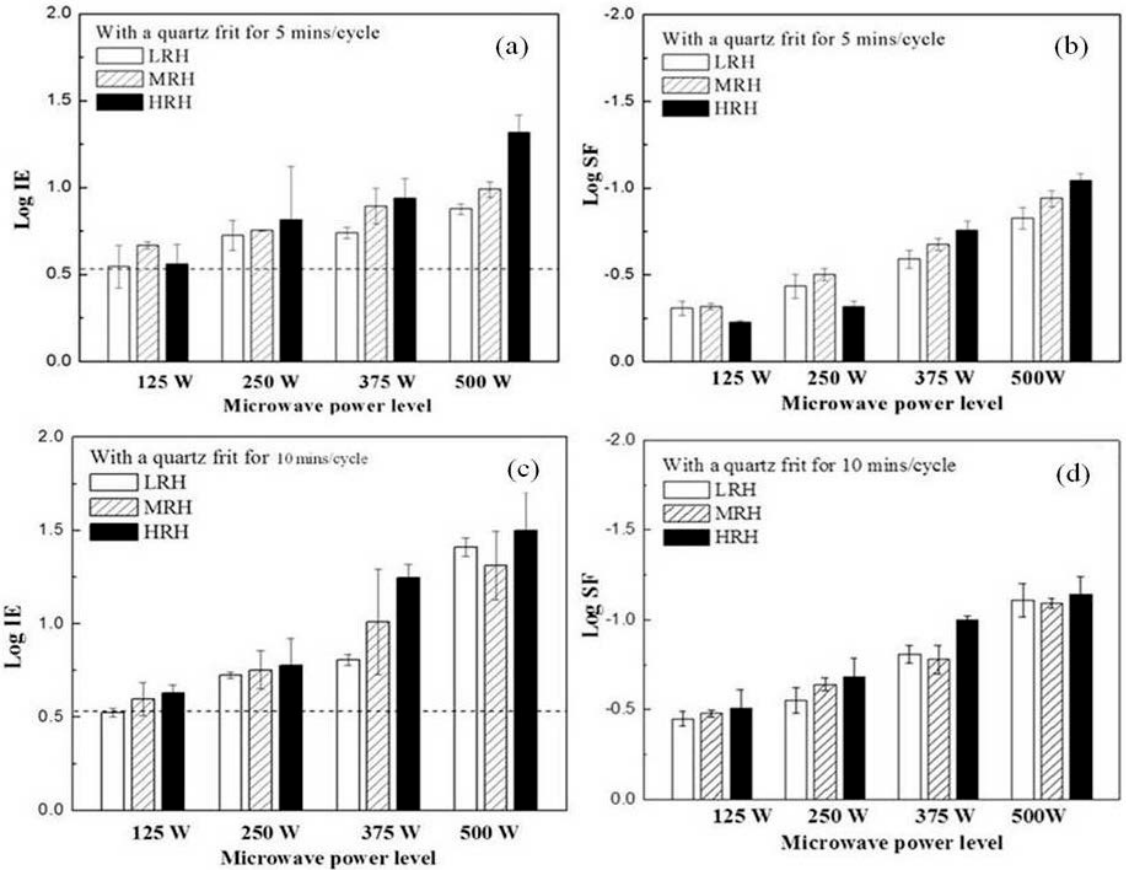

Figure 28. Log Inactivation Efficiency by Microwave-irradiation-assisted Filtration System and Log Survival Fraction on Filter Surface as a Function of Microwave Power Level: A) and B) for 5 min/cycle and C) and D) for 10 min/cycle

IE ($p = 0.01$) significantly increased and SF ($p < 0.01$) significantly decreased as the application time increased. By design the quartz frit did not absorb microwave irradiation, which resulted in a lower filter *T* and less-pronounced viral inactivation capacity compared to treatment with the SiC disk. Log IEs of 0.8, 0.9 and 1.3 were obtained at 30%, 60% and 90% RH, respectively, at 500 W ($p < 0.01$). Unlike the results with a SiC disk, log IE corrected for FE of the filter itself was lower than the absolute value of log SF, indicating that the lower *T* of the support is insufficient to inactivate MS2. At the higher power level, a high IE and lower SF were seen under HRH, which may be explained by the mechanism of microwave irradiation. The higher water content can contribute to more-efficient heating induced by the molecular vibrations of water (Fisher et al. 2011). However, the RH effect was not observed at 500 W for 10 min/cycle

in Figure 28C and D. The different phenomenon can be explained by the increased concentration of water vapor at higher *T* and the higher temperature itself. At HRH, final *T*s were 27, 43, 66 and 81 °C after 5 min/cycle, and 49, 62, 78 and 89 °C after 10 min/cycle at 125, 250, 375 and 500 W, respectively. These results suggest that RH is a significant parameter from 50~80 °C and that it ceases to be significant above 90 °C.

4.5.5. Degradation of Filters after Microwave Irradiation

Pressure drops of the test filters were measured before and after microwave treatment to inspect for degradation of the filters due to the microwave treatment (Table 10). The initial pressure drops (at 5.3 cm/s) of 0.45, 0.62, and 1.20 in H_2O for filters 1, 2 and 3, respectively, were maintained throughout several microwave irradiation tests at 375 W for 10 min/cycle. There was no significant difference in pressure drop between the control and the treated filters, indicating no melting or degradation. SEM images also showed no visible morphological changes.

Table 10. Pressure drop of the filter at face velocity of 5.3 cm/s before and after microwave treatment at 375 W for 10 mins/cycle

	Pressure drop (in H_2O)		
No. treatment	Filter 1	Filter 2	Filter 3
0 (Control)	0.45	0.62	1.2
1	0.45	0.62	1.2
2	0.45	0.60	1.2
5	0.46	0.60	1.2

4.5.6. Comparison to other Disinfection Technologies

Numerous disinfection technologies, including energetic techniques and chemical treatments, with or without filtration systems, have been studied. A study investigating bleach disinfection with 0.1% sodium hypochlorite aerosol and UV germicidal irradiation (UVGI) at a wavelength of 254 nm achieved 2-log SF of MS2; however, bleach and UVGI have limitations of chemical release and low penetration, respectively (Vo et al. 2009). Rengasamy et al. (2010) and Woo et al. (2011) confirmed inactivation by biocidal filters incorporating antimicrobial agents, e.g., silver, copper, oxygen species, titanium dioxide and dialdehyde polysaccharides, but these filters did not reach 2-log SF within 30 min. Compared to other filter disinfection technologies, the microwave-assisted filtration system was at least as effective as all of these—and caused no filter damage or chemical formation.

As a direct disinfection technology without filters, an electrostatic precipitator (ESP) at ±6 kV was reported by Kettleson et al. (2009)) to exhibit 2-log IE of MS2 and at -10 kV it could reach above 6-log IE. Comparing these results with the present study is difficult because of different inactivation mechanisms (thermal effect vs. radical reaction). However, using negative corona in ESP disinfection requires cautioned because of the formation of ozone. Grinshpun et al. (2010) demonstrated 2-log IE of MS2 by dry heat treatment at 125 °C for 0.24 s. This value is similar to that obtained in this study after deducting the inherent FE, and it confirms the thermal effect of microwaves.

5. CONCLUSIONS AND RECOMMENDATIONS

5.1. Conclusions

PSDs of both infectious and total viruses in pure media without solute followed volumetric size distribution, whereas those in spray media containing solutes followed a lower dimension of size, such as surface or number size distribution. Aggregation by MS2 itself and encasement by inert salts afforded a higher stability factor because of a shielding effect and reduction of the air–water interface. In addition, for MS2 aerosols generated in a gel-forming medium, e.g., AS, the protective effect was observed but no effect of RH could be distinguished.

The use of a charge neutralizer caused no observable effect on the release of iodine from the filter. However, the data obtained were very close to the detection limit (0.024 mg/L), so the experiment should be repeated at higher concentration before a firm conclusion can be drawn about the effect of MS2 bioaerosols on the release of iodine from iodine-treated filters.

To properly evaluate and compare various decontamination/inactivation technologies, the ability to produce representative human respiratory secretions in a consistent and controlled manner for delivering aerosolized droplets containing viral agents is critically important. A simple system for producing, delivering, and loading of consistent challenges of droplets/aerosols containing virus onto FFRs was developed and assessed in this study. The respective CVs for S-T-S and Q-T-Q for the six NIOSH-certified FFRs tested were lower than 20% and 40%. The droplet size could be altered by tuning the frequency of the ultrasonic nebulizer, by changing the composition of the dispersion aerosolized, and by adjusting *T* and RH inside the chamber. Droplets emulating bioaerosols released during coughing and sneezing could be produced using specific conditions and the loading density could be achieved by controlling the loading time and the virus titer in the nebulization medium. This system allows for development and validation of a standard method for loading bioaerosol challenges to compare different decontamination techniques. It also has utility for loading surfaces to study fomite transmission and reaerosolization of particles from surfaces. It can be further applied to generate and load droplets and aerosols of different sizes and to load onto materials other than FFRs.

Microwave-assisted filtration was demonstrated to be an efficient approach for inactivating viral aerosols. Microwave power and application time were key operating parameters for controlling the disinfection effectiveness of viral agents. Both factors combined to yield a threshold inactivation *T* of around 90 °C. SF and IE changed sharply above 90 °C and reached 2 logs at 109 °C and 116 °C, respectively. RH was another pivotal parameter for viability of viruses at medium *T*s (50~80 °C), but it became insignificant at *T*s above 90 °C. Thermal effect was identified to be the major mechanism in the conditions studied.

The threshold *T* required to reach target IE and SF could be calculated using two simple equations below:

$$\log \mathrm{IE} - \log \mathrm{IE}_{\text{inherent filtration}} = \log \mathrm{IE}_{\text{microwave}} = -7.57 + 0.08T$$

$$\log \mathrm{SF} = -5.01 - 0.06\,T$$

By applying microwave power to a thermally stable filter material supported on a SiC disc, a high IE—around 5 logs through the system—can be reached at temperatures lower than for other dry heat treatments.

From the study examining the effects of transmission mode and environmental conditions on the sensitivity of MS2 coli phage to UV disinfection, we conclude that, unlike in microwave treatment, RH is an important parameter for UV disinfection of filters; the solid component in the spraying medium is also important. High water content that absorbs UV and shielding of viruses near the center of the aggregate might be responsible for lower inactivation. IE was lower following droplet transmission than aerosol transmission, largely owing to the higher water content of the larger droplets, which shields viruses from UV exposure. Lower *K*s were observed for viruses in BE and AS than in DI water, which is attributed to protective effects exerted by solids present in the respective media. In these experiments, BE was slightly more protective than AS and acted by different mechanisms. The protective effect of solids followed the order water-insoluble solid (BE) > water-insoluble viscous solid (mucin) > water-soluble solid (salts). When these solids were present, RH was not a significant parameter in decontamination by UV exposure. If the susceptibility factor is obtained for the target microbial species, the appropriate UV dose for surface decontamination can be determined.

5.2. Recommendations

Further studies are needed to apply the novel decontamination method against viral aerosols: 1) development of an analytical model for disposition of viruses in aerosol in different spray media—this model will be a very useful tool in designing an effective strategy to improve filtration and IE and for assessing probability of infection by respiratory deposition of a given viral aerosol; 2) an HVAC system incorporating microwave disinfection should be tested in a full-scale application—energy consumption is an important factor in evaluating the functional value of this technology for real applications; 3) after staining of the lipid with a dye (uranyl acetate), TEM studies will be helpful to elucidate aggregation and encasement of viruses. A high concentration of dye allows easy observation of the morphology of MS2, but it can also alter the isoelectric point, artifactually changing the aggregation modes. Hence, the morphology by TEM should be observed only after determining the optimal dye concentration for MS2.

6. REFERENCES

APHA (1995). "Standard Methods for the Examination of Water and Wastewater 4500-CI G." American Public Health Association, Washington, DC.

Aps, J. K. M., and Martens, L. C. (2005). "Review: The Physiology of Saliva and Transfer of Drugs into Saliva." *Forensic Sci.Int.*, 150(2–3), 119–131.

Aranha–Creado, H., and Brandwein, H. (1999). "Application of Bacteriophages as Surrogates for Mammalian Viruses: A Case for Use in Filter Validation Based on Precedents and Current Practices in Medical and Environmental Virology." *PDA J Pharm Sci Technol*, 53, 75–82.

ASME (2009). *Code on Nuclear Air and Gas Treatment, AG-1*, American Society of Mechanical Engineers, New York, NY.

Awuah, G. B., Ramaswamy, H. S., Economides, A., and Mallikarjunan, K. (2005). "Inactivation of *Escherichia coli* K-12 and *Listeria Innocua* in Milk Using Radio Frequency (RF) Heating." *Innov. Food Sci. Emerg. Technol.*, 6(4), 396–402.

Bansil, R., Stanley, H. E., and Lamont, J. T. (1995). "Mucin Biophysics." *Annu. Rev. Physiol.*, 57, 635–657.

Barlow, D. F., and Donaldson, A. I. (1973). "Comparison of Aerosol Stabilities of Foot-and-Mouth Disease Virus Suspended in Cell-Culture Fluid or Natural Fluids." *J. Gen. Virol.*, 20(3), 311–318.

Baron, P. A., Estill, C. F., Deye, G. J., Hein, M. J., Beard, J. K., Larsen, L. D., and Dahlstrom, G. E. (2008). "Development of an Aerosol System for Uniformly Depositing *Bacillus anthracis* Spore Particles on Surfaces." *Aerosol Sci. Technol.*, 42(3), 159–172.

Barrett, L. W., and Rousseau, A. D. (1998). "Aerosol Loading Performance of Electret Filter Media." *Am. Ind. Hyg. Assoc. J.*, 59(8), 532–539.

Beggs, C. B., Noakes, C. J., Sleigh, P. A., Fletcher, L. A., and Kerr, K. G. (2006). "Methodology for Determining the Susceptibility of Airborne Microorganisms to Irradiation by an Upper-Room UVGI System." *J. Aerosol Sci.*, 37(7), 885–902.

Benbough, J. E. (1971). "Some Factors Affecting Survival of Airborne Viruses." *J. Gen. Virol.*, 10(3), 209–220.

Berg, G., Chang, S. L., and Harris, E. K. (1964). "Devitalization of Microorganisms by Iodine." *J Virology*, 22, 469–481.

Betti, L., Trebbi, G., Lazzarato, L., Brizzi, M., Calzoni, G. L., Marinelli, F., Nani, D., and Borghini, F. (2004). "Nonthermal Microwave Radiations Affect the Hypersensitive Response of Tobacco to Tobacco Mosaic Virus." *J. Altern. Complem. Med.*, 10(6), 947–957.

Borkow, G., and Gabbay, J. (2004). "Putting Copper into Action: Copper-Impregnated Products with Potent Biocidal Activities." *FASEB J.*, 18(12), 1728–1730.

Brady–Estevez, A. S., Schnoor, M. H., Kang, S., and Elimelech, M. (2010). "SWNT–MWNT Hybrid Filter Attains High Viral Removal and Bacterial Inactivation." *Langmuir*, 26(24), 19153–19158.

Brickner, P. W., Vincent, R. L., First, M., Nardell, E., Murray, M., and Kaufman, W. (2003). "The Application of Ultraviolet Germicidal Irradiation to Control Transmission of Airborne Disease: Bioterrorism Countermeasure." *Public Health Rep.*, 118(2), 99–114.

Brion, G. M., and Silverstein, J. (1999). "Iodine Disinfection of a Model Bacteriophage, MS2, Demonstrating Apparent Rebound." *J. Water Res.*, 23, 169–179.

Campanha, N. H., Pavarina, A. C., Brunetti, I. L., Vergani, C. E., Machado, A. L., and Spolidorio, D. M. P. (2007). "*Candida albicans* Inactivation and Cell Membrane Integrity Damage by Microwave Irradiation." *Mycoses*, 50(2), 140–147.

CDC (2009). "Fact Sheet: Novel H1N1 Flu Situation Update." <http://www.cdc.gov/h1n1flu.update.htm>. (September 15, 2009).

CDC (2012). "The National Personal Protective Technology Laboratory (NPPTL)." <http://www.cdc.gov/niosh/npptl/topics/respirators/disp_part/RespSource3.html>. (March 1, 2012).

Cecchini, C., Verdenelli, M. C., Orpianesi, C., Dadea, G. M., and Cresci, A. (2004). "Effects of Antimicrobial Treatment on Fiberglass–Acrylic Filters." *J. Appl. Microb.*, 97(2), 371–377.

Chang, J. C. H., Ossoff, S. F., Lobe, D. C., Dorfman, M. H., Dumais, C. M., Qualls, R. G., and Johnson, J. D. (1985). "UV Inactivation of Pathogenic and Indicator Microorganisms." *Appl. Environ. Microb.*, 49(6), 1361–1365.

Chuaybamroong, P., Thunyasirinon, C., Supothina, S., Sribenjalux, P., and Wu, C. Y. (2011). "Performance of Photocatalytic Lamps on Reduction of Culturable Airborne Microorganism Concentration." *Chemosphere*, 83(5), 730–735.

Cote, R. J. (1999). "Media Composition, Microbial, Laboratory Scale." *Encyclopedia of Bioprocess Technology: Fermentation, Biocatalysis, and Bioseparation*, M. C. Flickinger, and S. W. Drew, eds., John Wiley & Sons, New York, NY, 104–122.

Damit, B., Lee, C., and Wu, C. Y. (2011). "Flash Infrared Radiation Disinfection of Fibrous Filters Contaminated with Bioaerosols." *J. Appl. Microb.*, 110(4), 1074–1084.

Di Ionno, L., and Messier, P. J. (2004). "Iodinated Thermal-Fused Polymer as a Biocidal Additive to Commercial and Chemical-Resistant Coatings." *Surf. Coat. Int. Pt. B, Coat. Trans.*, 87(4), 265–272.

Diaz–Arnold, A. M., and Marek, C. A. (2002). "The Impact of Saliva on Patient Care: A Literature Review." *J. Prosthet. Dent.*, 88(3), 337–343.

Dodds, M. W. J., Johnson, D. A., and Yeh, C. K. (2005). "Health Benefits of Saliva: A Review." *J. Dent.*, 33(3), 223–233.

Duleba–Majek, M. (2009). "Transmission of UV Radiation through Woven Fabrics in Dependence on the Inter-Thread Spaces." *Fibres Text. East. Eur.*, 17(2), 34–38.

ECDC (2009). "Daily Update—Pandemic (H1N1)." <http://ecdc.europa.eu/en/healthtopics/Documents/091020_Influenza_AH1N1_Situation_Report_0900hrs.pdf>. (October 29, 2009).

Edwards, D. A., Man, J. C., Brand, P., Katstra, J. P., Sommerer, K., Stone, H. A., Nardell, E., and Scheuch, G. (2004). "Inhaling to Mitigate Exhaled Bioaerosols." *PNAS*, 101(50), 17383–17388.

Elhafi, G., Naylor, C. J., Savage, C. E., and Jones, R. C. (2004). "Microwave or Autoclave Treatments Destroy the Infectivity of Infectious Bronchitis Virus and Avian Pneumovirus but Allow Detection by Reverse Transcriptase–Polymerase Chain Reaction." *Avian Pathol.*, 33(3), 303–306.

Eninger, R. M., Adhikari, A., Reponen, T., and Grinshpun, S. A. (2008). "Differentiating between Physical and Viable Penetrations when Challenging Respirator Filters with Bioaerosols." *Clean—Air, Soil, Water*, 36(7), 615–621.

FDA (2007). "Emergency Use Authorization of Medical Products." <http://www.fda.gov/RegulatoryInformation/Guidances/ucm125127.htm>. (May 25, 2012).

Feather, G. A., and Chen, B. T. (2003). "Design and Use of a Settling Chamber for Sampler Evaluation Under Calm-Air Conditions." *Aerosol Sci. Technol.*, 37(3), 261–270.

Fina, L. R., Hassouna, N., Horacek, G. L., Lambert, J. P., and Lambert, J. L. (1982). "Viricidal Capability of Resin–Triiodide Demand-Type Disinfectant." *Appl. Environ. Microb.*, 44(6), 1370–1373.

Fisher, E., Rengasamy, S., Viscusi, D., Vo, E., and Shaffer, R. (2009). "Development of a Test System To Apply Virus-Containing Particles to Filtering Facepiece Respirators for the Evaluation of Decontamination Procedures." *Appl. Environ. Microb.*, 75(6), 1500–1507.

Fisher, E. M., Williams, J. L., and Shaffer, R. E. (2011). "Evaluation of Microwave Steam Bags for the Decontamination of Filtering Facepiece Respirators." *Plos One*, 6(4), 7.

Floyd, R., and Sharp, D. G. (1977). "Aggregation of Poliovirus and Reovirus by Dilution in Water." *Appl. Environ. Microb.*, 33(1), 159–167.

Foarde, K. K., Hanley, J. T., and Veeck, A. C. (2000). "Efficacy of Antimicrobial Filter Treatments." *ASHRAE J.*, 42(12), 52–58.

Grinshpun, S. A., Adhikari, A., Li, C. L., Yermakov, M., Reponen, L., Johansson, E., and Trunov, M. (2010). "Inactivation of Aerosolized Viruses in Continuous Air Flow with Axial Heating." *Aerosol Sci. Technol.*, 44(11), 1042–1048.

Hach (2012). "Iodine Method 8031." Hach Company, Loveland, CO.

Hamid, M., Thomas, T., El–Saba, A., Stapleton, W., Sakla, A., and Rahman, A. (2001). "The Effects of Microwaves on Airborne Microorganisms." *J. Microwave Power EE*, 36(1), 37–45.

Hatch, G. L., Lambert, J. L., and Fina, L. R. (1980). "Some Properties of the Quaternary Ammonium Anion-Exchange Resin–Triiodide Disinfectant for Water." *Ind. Eng. Chem. Prod. Res. Develop.*, 19(2), 259–263.

Heimbuch, B., Laventure, G., McDonald, R., Burr, E., Proudfoot, E., and Wander, J. (2004). *Antimicrobial Efficiency of Iodinated Individual Protection Filters*. AFRL-ML-TY-TP-2004-4561, Air Force Research Laboratory, Tyndall AFB, FL.

Heimbuch, B. K., Wallace, W. H., Kinney, K., Lumley, A. E., Wu, C. Y., Woo, M. H., and Wander, J. D. (2011). "A Pandemic Influenza Preparedness Study: Use of Energetic Methods to Decontaminate Filtering Facepiece Respirators Contaminated with H1N1 Aerosols and Droplets." *Am. J. Infect. Control*, 39(1), E1–E9.

Heimbuch, B. K., and Wander, J. D. (2006). *Bioaerosol Challenges to Antimicrobial Surface Treatments: Enhanced Efficacy Against MS2 Coli Phage of Air Filter Media Coated with Polystyrene-4-methyltrimethylammonium Triiodide*. AFRL-ML-TY-TP-2006-4527, Air Force Research Laboratory, Tyndall AFB, FL.

Hinds, W. C. (1999). "Bioaerosols." *Aerosol Technology: Properties, Behavior, and Measurement of Airborne Particles*, John Wiley & Sons, New York, NY, pp. 394–401.

Hinds, W. C. (1999). "Filtration." *Aerosol Technology: Properties, Behavior, and Measurement of Airborne Particles*, John Wiley & Sons, Inc., New York, pp. 183–205.

Hinds, W. C. (1999). "Production of Test Aerosols." *Aerosol Technology: Properties, Behavior, and Measurement of Airborne Particles*, John Wiley & Sons, Inc., New York, p. 431.

Hogan, C. J. J., Kettleson, E. M., Lee, M. H., Ramaswami, B., Angenent, L. T., and Biswas, P. (2005). "Sampling Methodologies and Dosage Assessment Techniques for Submicrometer and Ultrafine Virus Aerosol Particles." *J. Appl. Microb.*, 99, 1422–1434.

Humphrey, S. P., and Williamson, R. T. (2001). "A Review of Saliva: Normal Composition, Flow, and Function." *J. Prosthet. Dent.*, 85(2), 162–169.

Hwang, G. B., Jung, J. H., Jeong, T. G., and Lee, B. U. (2010). "Effect of Hybrid UV–Thermal Energy Stimuli on Inactivation of *S. epidermidis* and *B. subtilis* Bacterial Bioaerosols." *Sci. Total Environ.*, 408(23), 5903–5909.

IOM (2006). *Reusability of Facemasks during an Influenza Pandemic Facing the Flu*, National Academies Press, Washington, D.C.

Jones, D. A., Lelyveld, T. P., Mavrofidis, S. D., Kingman, S. W., and Miles, N. J. (2002). "Microwave Heating Applications in Environmental Engineering—A Review." *Resour. Conserv. Recycl.*, 34(2), 75–90.

Jung, J. H., Hwang, G. B., Lee, J. E., and Bae, G. N. (2011). "Preparation of Airborne Ag/CNT Hybrid Nanoparticles Using an Aerosol Process and Their Application to Antimicrobial Air Filtration." *Langmuir*, 27(16), 10256–10264.

Jung, J. H., Lee, J. E., and Kim, S. S. (2009). "Generation of Nonagglomerated Airborne Bacteriophage Particles Using an Electrospray Technique." *Anal. Chem.*, 81(8), 2985–2990.

Jung, J. H., Lee, J. E., Lee, C. H., Kim, S. S., and Lee, B. U. (2009). "Treatment of Fungal Bioaerosols by a High-Temperature, Short-Time Process in a Continuous-Flow System." *Appl. Environ. Microb.*, 75(9), 2742–2749.

Kang, S., Mauter, M. S., and Elimelech, M. (2009). "Microbial Cytotoxicity of Carbon-Based Nanomaterials: Implications for River Water and Wastewater Effluent." *Environ. Sci. Technol.*, 43(7), 2648–2653.

Kettleson, E. M., Ramaswami, B., Hogan, C. J., Lee, M. H., Statyukha, G. A., Biswas, P., and Angenent, L. T. (2009). "Airborne Virus Capture and Inactivation by an Electrostatic Particle Collector." *Environmental Science & Technology*, 43(15), 5940–5946.

Khalil, H., and Villota, R. (1989). "The Effect of Microwave Sublethal Heating on the Ribonucleic Acids of *Staphylococcus aureus*." *J. Food Protect.*, 52(8), 544–548.

Kiel, J. L., Sutter, R. E., Mason, P. A., Parker, J. E., Morales, P. J., Stribling, L. J. V., Alls, J. L., Holwitt, E. A., Seaman, R. L., and Mathur, S. P. (2002). "Directed Killing of Anthrax Spores by Microwave-Induced Cavitation." *IEEE Trans. Plasma Sci.*, 30(4), 1482–1488.

Kim, S. W., Raynor, P. C., Kuehn, T. H., Goyal, S. M., Ramakrishnan, M. A., Anantharaman, S., and Farnsworth, J. E. (2008). "Optimizing the Recovery of Surrogates for Bacterial Bioterrorism Agents from Ventilation Filters." *Clean—Soil Air Water*, 36(7), 601–608.

Kowalski, W. (2008). "Air-Treatment Systems for Controlling Hospital-Acquired Infections." *HPAC Engineering*, http://hpac.com/iaq-amp-ventilation/air-treatment-systems-controlling-hospital-acquired-infections

Kowalski, W., and Bahnfleth, W. (2000). "UVGI Design Basics for Air and Surface Disinfection." *HPAC Eng.*, January, 100–111.

Kowalski, W. J. (2009). *Ultraviolet Germicidal Irradiation Handbook UVGI for Air and Surface Disinfection*, Springer–Verlag, New York, NY.

Kujundzic, E., Hernandez, M., and Miller, S. L. (2007). "Ultraviolet Germicidal Irradiation Inactivation of Airborne Fungal Spores and Bacteria in Upper-Room Air and HVAC In-Duct Configurations." *J. Environ. Eng. Sci.*, 6(1), 1–9.

Kujundzic, E., Matalkah, F., Howard, C. J., Hernandez, M., and Miller, S. L. (2006). "UV Air Cleaners and Upper-Room Air Ultraviolet Germicidal Irradiation for Controlling Airborne Bacteria and Fungal Spores." *J. Occup. Environ. Hyg.*, 3(10), 536–546.

Kujundzic, E., Zander, D. A., Hernandez, M., Angenent, L. T., Henderson, D. E., and Miller, S. L. (2005). "Effects of Ceiling-Mounted HEPA–UV Air Filters on Airborne Bacteria Concentrations in an Indoor Therapy Pool Building." *J. Air Waste Manage. Assoc.*, 55(2), 210–218.

Lambert, J. L., Fina, G. T., and Fina, L. R. (1980). "Preparation and Properties of Triiodide–Quaternary, Pentaiodide–Quaternary, and Heptaiodide–Quaternary-Ammonium Strong Base Anion-Exchange Resin Disinfectants." *Ind. Eng. Chem. Prod. Res. Develop.*, 19(2), 256–258.

Lang, R. J. (1962). "Ultrasonic Atomization of Liquids." *J. Acous. Soc. Am.*, 34(1), 6–8.

Lee, B. U. (2011). "Life Comes from the Air: A Short Review on Bioaerosol Control." *Aerosol Air Qual. Res.*, 11(7), 921–927.

Lee, I. S., Kim, H. J., Lee, D. H., Hwang, G. B., Jung, J. H., Lee, M., Lim, J., and Lee, B. U. (2011). "Aerosol Particle Size Distribution and Genetic Characteristics of Aerosolized Influenza A H1N1 Virus Vaccine Particles." *Aerosol Air Qual. Res.*, 11(3), 230–237.

Lee, J. H., Wu, C. Y., Lee, C. N., Anwar, D., Wysocki, K. M., Lundgren, D. A., Farrah, S., Wander, J., and Heimbuch, B. K. (2009). "Assessment of Iodine-Treated Filter Media for

Removal and Inactivation of MS2 Bacteriophage Aerosols." *J. Appl. Microb.*, 107(6), 1912–1923.

Lee, Y. H., and Lee, B. U. (2006). "Inactivation of Airborne *E. coli* and *B. subtilis* Bioaerosols Utilizing Thermal Energy." *J. Microbiol. Biotechnol*, 16, 1684–1689.

Lehtimaki, M., and Heinonen, K. (1994). "Reliability of Electret Filters." *Build. Environ.*, 29(3), 353–355.

Li, H. W., Wu, C. Y., Tepper, F., Lee, J. H., and Lee, C. N. (2009). "Removal and Retention of Viral Aerosols by a Novel Alumina Nanofiber Filter." *J. Aerosol Sci.*, 40(1), 65–71.

Lin, C. Y., and Li, C. S. (2002). "Control Effectiveness of Ultraviolet Germicidal Irradiation on Bioaerosols." *Aerosol Sci. Technol.*, 36(4), 474–478.

Lin, X., Reponen, T., Willeke, K., Wang, Z., Grinshpun, S. A., and Trunov, M. (2000). "Survival of Airborne Microorganisms during Swirling Aerosol Collection." *Aerosol Sci. Technol.*, 32, 184–196.

Lore, M. B., Sebastian, J. M., Brown, T. L., Viner, A. S., McCullough, N. V., and Hinrichs, S. H. (2012). "Performance of Conventional and Antimicrobial-Treated Filtering Facepiece Respirators Challenged with Biological Aerosols." *J. Occup. Environ. Hyg.*, 9(2), 69–80.

Madigan, M. T., and Martinko, J. M. (2006). *Brock Biology of Microorganisms*, Prentice Hall, Upper Saddle River, NJ.

Mantle, M., and Husar, S. D. (1993). "Adhesion of *Yersina enterocolitica* to Purified Rabbit and Human Intestinal Mucin." *Infect. Immun.*, 61(6), 2340–2346.

Marchin, G. L., Fina, L. R., Lambert, J. L., and Fina, G. T. (1983). "Effect of Resin Disinfectant-I_3 and Disinfectant-I_5 on *Giardia muris* and *Giardia lamblia*." *Appl. Environ. Microb.*, 46(5), 965–969.

Marple, V. A., and Rubow, K. L. (1983). "An Aerosol Chamber for Instrument Evaluation and Calibration." *Am. Ind. Hyg. Assoc. J.*, 44(5), 361–367.

May, K. R. (1973). "The Collison Nebulizer: Description, Performance and Application." *J. Aerosol Sci.*, 4(3), 235–243.

McDevitt, J. J., Lai, K. M., Rudnick, S. N., Houseman, E. A., First, M. W., and Milton, D. K. (2007). "Characterization of UVC Light Sensitivity of Vaccinia Virus." *Appl. Environ. Microb.*, 73(18), 5760–5766.

Memarzadeh, F., Olmsted, R. N., and Bartley, J. M. (2010). "Applications of Ultraviolet Germicidal Irradiation Disinfection in Health Care Facilities: Effective Adjunct, but not Stand-Alone Technology." *Am. J. Infect. Control*, 38(5), S13–S24.

Menzies, D., Popa, J., Hanley, J. A., Rand, T., and Milton, D. K. (2003). "Effect of Ultraviolet Germicidal Lights Installed in Office Ventilation Systems on Workers' Health and Wellbeing: Double-Blind Multiple Crossover Trial." *Lancet*, 362(9398), 1785–1791.

Messier, P. J. (1999). "Disinfection of Air Using an Iodine/Resin Disinfectant."US Patent No. 5980827.

Messier, P. J. (2000). "Iodine/Resin Disinfection and Procedure for the Preparation Thereof."US Patent No. 6045820.

Morawska, L., Johnson, G. R., Ristovski, Z. D., Hargreaves, M., Mengersen, K., Corbett, S., Chao, C. Y. H., Li, Y., and Katoshevski, D. (2009). "Size Distribution and Sites of Origin of Droplets Expelled from the Human Respiratory Tract during Expiratory Activities." *J. Aerosol Sci.*, 40(3), 256–269.

Nardell, E. A. (2008). "Safety of Upper-Room Ultraviolet Germicidal Air Disinfection for Room Occupants: Results from the Tuberculosis Ultraviolet Shelter Study." *Public Health Reports*, 123(1), 52–60.

Nowack, B., Krug, H. F., and Height, M. (2011). "120 Years of Nanosilver History: Implications for Policy Makers." *Environ. Sci. Technol.*, 45(4), 1177–1183.

O'Connell, K. P., Bucher, J. R., Anderson, P. E., Cao, C. J., Khan, A. S., Gostomski, M. V., and Valdes, J. J. (2006). "Real-Time Fluorogenic Reverse Transcription–PCR Assays for Detection of Bacteriophage MS2." *J. Appl. Environ. Microb.*, 72(1), 478–483.

Peccia, J., and Hernandez, M. (2001). "Photoreactivation in Airborne *Mycobacterium parafortuitum*." *Appl. Environ. Microb.*, 67(9), 4225–4232.

Peccia, J., and Hernandez, M. (2004). "UV-Induced Inactivation Rates for Airborne *Mycobacterium bovis* BCG." *J. Occup. Environ. Hyg.*, 1(7), 430–435.

Peccia, J., Werth, H. M., Miller, S., and Hernandez, M. (2001). "Effects of Relative Humidity on the Ultraviolet Induced Inactivation of Airborne Bacteria." *Aerosol Sci. Technol.*, 35(3), 728–740.

Pellerin, C. (1994). "Alternatives to Incineration—There is More Than One Way to Remediate." *Environ. Health Perspect.*, 102(10), 840–845.

Perier, C., Bove, J., and Vila, M. (2012). "Mitochondria and Programmed Cell Death in Parkinson's Disease: Apoptosis and Beyond." *Antioxid. Redox Sign.*, 16(9), 883–895.

Pollini, M., Russo, M., Licciulli, A., Sannino, A., and Maffezzoli, A. (2009). "Characterization of Antibacterial Silver Coated Yarns." *J. Mater. Sci.—Mater. Med.*, 20(11), 2361–2366.

Prescott, L. M., Harley, J. P., and Klein, D. A. (2006). *Microbiology*, McGraw–Hill Companies, Inc., New York, NY.

Rastogi, V. K., Wallace, L., and Smith, L. S. (2007). "Disinfection of *Acinetobacter baumannii*-Contaminated Surfaces Relevant to Medical Treatment Facilities with Ultraviolet C Light." *Milit. Med.*, 172(11), 1166–1169.

Ratnesar–Shumate, S., and Wu, C. Y. (2004). *Capture of Aerosols by Iodinated Fiber Media*, AFRL-ML-TY-TR-2004-4556. Air Force Research Laboratory.

Ratnesar–Shumate, S., Wu, C. Y., Wander, J., Lundgren, D., Farrah, S., Wanakule, P., Blackburn, M., and Lan, M. F. (2008). "Evaluation of Physical Capture Efficiency and Disinfection Capability of a Novel Iodinated Filter Medium." *Aerosol Air Qual. Res.*, 8(1), 1–18.

Rengasamy, A., Zhuang, Z. P., and BerryAnn, M. S. (2004). "Respiratory Protection against Bioaerosols: Literature Review and Research Needs." *Am. J. Infect. Control*, 32(6), 345–354.

Rengasamy, S., Fisher, E., and Shaffer, R. E. (2010). "Evaluation of the Survivability of MS2 Viral Aerosols Deposited on Filtering Face Piece Respirator Samples Incorporating Antimicrobial Technologies." *Am. J. Infect. Control*, 38(1), 9–17.

Riemenschneider, L., Woo, M. H., Wu, C. Y., Lundgren, D., Wander, J., Lee, J. H., Li, H. W., and Heimbuch, B. (2010). "Characterization of Reaerosolization from Impingers in an Effort to Improve Airborne Virus Sampling." *J. Appl. Microb.*, 108(1), 315–324.

Ryan, K., McCabe, K., Clements, N., Hernandez, M., and Miller, S. L. (2010). "Inactivation of Airborne Microorganisms Using Novel Ultraviolet Radiation Sources in Reflective Flow-Through Control Devices." *Aerosol Sci. Technol.*, 44(7), 541–550.

Schaffer, F. L., Soergel, M. E., and Straube, D. C. (1976). "Survival of Airborne Influenza-Virus —Effects of Propagating Host, Relative Humidity, and Composition of Spray Fluids." *Arch. Virol.*, 51(4), 263–273.

Sharma, V. K., Yngard, R. A., and Lin, Y. (2009). "Silver Nanoparticles: Green Synthesis and Their Antimicrobial Activities." *Adv. Colloid Interface Sci.*, 145(1–2), 83–96.

Shi, L., Ardehali, R., Caldwell, K. D., and Valint, P. (2000). "Mucin Coating on Polymeric Material Surfaces to Suppress Bacterial Adhesion." *Colloid. Surface. B*, 17(4), 229–239.

Sjogren, J. C., and Sierka, R. A. (1994). "Inactivation of Phage MS2 by Iron-Aided Titanium-Dioxide Photocatalysis." *Appl. Environ. Microb.*, 60(1), 344–347.

Taylor, S. L., Fina, L. R., and Lambert, J. L. (1970). "New Water Disinfectant—An Insoluble Quaternary Ammonium Resin–Triiodide Combination that Releases Bactericide on Demand." *Appl. Microb.*, 20(5), 720–722.

Trouwbor, T., and de Jong, J. C. (1973). "Interaction of Some Factors in Mechanism of Inactivation of Bacteriophage-MS2 in Aerosols." *Appl. Microb.*, 26(3), 252–257.

Tseng, C. C., and Li, C. S. (2005). "Inactivation of Virus-Containing Aerosols by Ultraviolet Germicidal Irradiation." *Aerosol Sci. Technol.*, 39(12), 1136–1142.

USEPA (1984). *US EPA Manual of Methods for Virology*, EPA/600/4-84-013, USEPA Environmental Monitoring and Support Laboratory, Cincinnati, OH.

Valegard, K., Liljas, L., Fridborg, K., and Unge, T. (1990). "The 3-Dimensional Structure of the Bacterial-Virus MS2." *Nature*, 345(6270), 36–41.

Veerman, E. C. I., van den Keybus, P. A. M., Vissink, A., and Nieuw Amerongen, A. V. (1996). "Human Glandular Salivas: Their Separate Collection and Analysis." *Euro. J. Oral Sci.*, 104(4), 346–352.

Vingerhoeds, M. H., Blijdenstein, T. B. J., Zoet, F. D., and van Aken, G. A. (2005). "Emulsion Flocculation Induced by Saliva and Mucin." *Food Hydrocolloids*, 19(5), 915–922.

Viscusi, D. J., Bergman, M. S., Eimer, B. C., and Shaffer, R. E. (2009). "Evaluation of Five Decontamination Methods for Filtering Facepiece Respirators." *Ann. Occup. Hyg.*, 53(8), 815–827.

Vo, E., Rengasamy, S., and Shaffer, R. (2009). "Development of a Test System To Evaluate Procedures for Decontamination of Respirators Containing Viral Droplets." *Appl. Environ. Microb.*, 75(23), 7303–7309.

Walker, C. M., and Ko, G. (2007). "Effect of Ultraviolet Germicidal Irradiation on Viral Aerosols." *Environ. Sci. Technol.*, 41(15), 5460–5465.

Wang, C. S. (2001). "Electrostatic Forces in Fibrous Filters—A Review." *Powder Technol.*, 118(1–2), 166–170.

Wang, J., Kim, S. C., and Pui, D. Y. (2008). "Investigation of the Figure of Merit for Filters with a Single Nanofiber Layer on a Substrate." *J. Aerosol Sci.*, 39(4), 323–334.

Wong, L., and Sissions, C. H. (2001). "A Comparison of Human Dental Plaque Microcosm Biofilms Grown in an Undefined Medium and a Chemically Defined Artificial Saliva." *Arch. Oral Biol.*, 46(6), 477–486.

Woo, M. H., Grippin, A., Anwar, D., Smith, T., Wu, C. Y., and Wander, J. D. (2012). "Effects of Relative Humidity and Spraying Medium on UV Decontamination of Filters Loaded with Viral Aerosols." *Appl. Environ. Microb.*, 78(16), 5781–5787.

Woo, M. H., Hsu, Y. M., Wu, C. Y., Heimbuch, B., and Wander, J. (2010). "Method for Contamination of Filtering Facepiece Respirators by Deposition of MS2 Viral Aerosols." *J. Aerosol Sci.*, 41(10), 944–952.

Woo, M. H., Lee, J. H., Rho, S. G., Ulmer, K., Welch, J. C., Wu, C. Y., Song, L., and Baney, R. H. (2011). "Evaluation of the Performance of Dialdehyde Cellulose Filters against Airborne and Waterborne Bacteria and Viruses." *Ind. Eng. Chem. Res.*, 50(20), 11636–11643.

Wu, Y., and Yao, M. S. (2010). "Inactivation of Bacteria and Fungus Aerosols Using Microwave Irradiation." *J. Aerosol Sci.*, 41(7), 682–693.

Wu, Y., and Yao, M. S. (2011). "Effects of Microwave Irradiation on Concentration, Diversity and Gene Mutation of Culturable Airborne Microorganisms of Inhalable Sizes in Different Environments." *J. Aerosol Sci.*, 42(11), 800–810.

Xu, P., Kujundzic, E., Peccia, J., Schafer, M. P., Moss, G., Hernandez, M., and Miller, S. L. (2005). "Impact of Environmental Factors on Efficacy of Upper-Room Air Ultraviolet Germicidal Irradiation for Inactivating Airborne Mycobacteria." *Environ. Sci. Technol.*, 39(24), 9656–9664.

Xu, P., Peccia, J., Fabian, P., Martyny, J. W., Fennelly, K. P., Hernandez, M., and Miller, S. L. (2003). "Efficacy of Ultraviolet Germicidal Irradiation of Upper-Room Air in Inactivating Airborne Bacterial Spores and Mycobacteria in Full-Scale Studies." *Atmos. Environ.*, 37(3), 405–419.

Xu, Z. Q., Wu, Y., Shen, F. X., Chen, Q., Tan, M. M., and Yao, M. S. (2011). "Bioaerosol Science, Technology, and Engineering: Past, Present, and Future." *Aerosol Sci. Technol.*, 45(11), 1337–1349.

Xu, Z. Q., and Yao, M. S. (2011). "Effects of Single-Walled Carbon Nanotube Filter on Culturability and Diversity of Environmental Bioaerosols." *J. Aerosol Sci.*, 42(6), 387–396.

Yang, S., Lee, W. M. G., Huang, H. L., Huang, Y. C., Luo, C. H., Wu, C. C., and Yu, K. P. (2007). "Aerosol Penetration Properties of an Electret Filter with Submicron Aerosols with Various Operating Factors." *J. Environ. Sci. Heal. A*, 42, 51–57.

Yang, S. H., and Lee, G. W. M. (2005). "Filtration Characteristics of a Fibrous Filter Pretreated with Anionic Surfactants for Monodisperse Solid Aerosols." *J. Aerosol Sci.*, 36(4), 419–437.

Yang, S. H., Lee, G. W. M., Chen, C. M., Wu, C. C., and Yu, K. P. (2007). "The Size and Concentration of Droplets Generated by Coughing in Human Subjects." *J. Aerosol Med.*, 20(4), 484–494.

Yen, Y.–L., Lin, H.–L., Lin, H.–J., Chen, P.–C., Chen, C.–R., Chang, G.–H., and Guo, H.–R. (2004). "Photokeratoconjunctivitis Caused by Different Light Sources." *Am. J. Emerg. Med.*, 22(7), 511–515.

Yoon, K. Y., Byeon, J. H., Park, C. W., and Hwang, J. (2008). "Antimicrobial Effect of Silver Particles on Bacterial Contamination of Activated Carbon Fibers." *Environ. Sci. Technol.*, 42(4), 1251–1255.

Yun, K. M., Hogan, C. J. J., Matsubayashi, Y., Kawabe, M., Iskandar, F., and Okuyama, K. (2007). "Nanoparticle Filtration by Electrospun Polymer Fibers." *Chem. Eng. Sci.*, 62, 4751–4759.

Zhang, Q., Damit, B., Welch, J., Park, H., Wu, C. Y., and Sigmund, W. (2010). "Microwave Assisted Nanofibrous Air Filtration for Disinfection of Bioaerosols." *J. Aerosol Sci.*, 41(9), 880–888.

Appendix A: Preliminary Test for Droplet Loading Chamber

A.1. Methods

Before construction of the droplet loading chamber, an experiment was conducted to verify uniform deposition of aerosols using a small chamber, shown in Figure A-1. A 600-mg/L solution of fluorescein was applied to evaluate the areal distribution of the deposition. The fluorescein aerosols were generated by an ultrasonic nebulizer with a flowrate of 0.5 Lpm for 5 min. Four square Lydall filters 1 in long, placed in the small chamber as shown in Figure A-2, were used as the collection media. After loading, the fluorescein was extracted into 50 mL of 0.1 N NH_4OH solution for 30 min using a wrist-action shaker. The concentration of fluorescein was then analyzed by a fluorometer (Turner Fluorometer, Model 112).

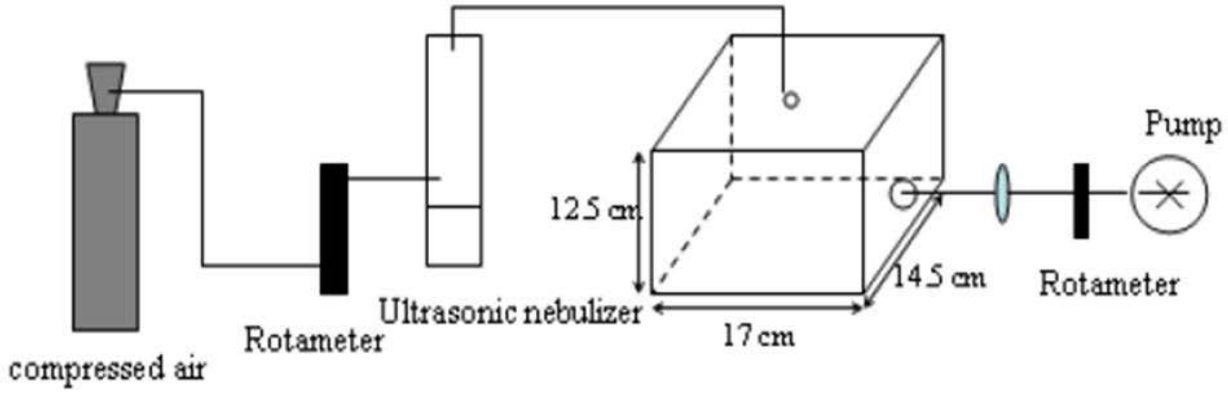

Figure A-1. Experimental Setup for Aerosol Loading Experiment inside a Small Chamber

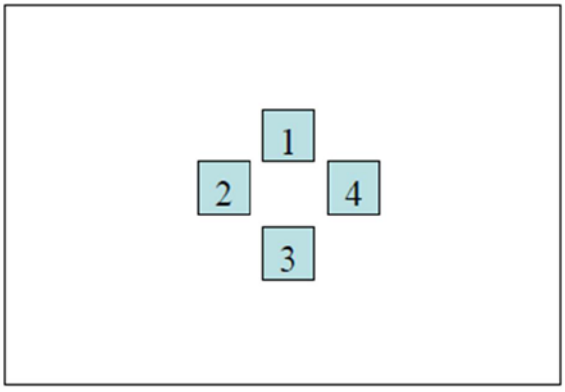

Figure A-2. Filter Location in the Small Chamber for Uniform Distribution Experiment

A.2. Determination of Operating Conditions

Before and after each experiment, the chamber was decontaminated by isopropyl alcohol for 30 min. Six samples were placed onto the support on the turntable using sterile forceps. A titer of around 10^7 PFU/mL in the ultrasonic nebulizer with 5 min loading time was calculated to

provide sufficient loading density (>10^3 PFU/cm^2). The titer was prepared by adding 0.3 mL virus stock suspension into 30 mL artificial saliva. Droplets from the ultrasonic nebulizer passed through the distributor and entered the chamber through six inlets. The size of the generated and loaded droplets can be controlled by the frequency of the ultrasonic generator, RH and *T*. For this study, the frequency of the generator was 2.4 MHz and the environmental conditions were 20 ± 2 °C and 35 ± 5% RH. Low RH was chosen because the survivability of MS2 is high under this condition. After loading, the residual droplets were allowed to incubate for 5 min, and the FFR samples were taken out for extraction and assay.

Optimal conditions to extract the virus from the FFRs were investigated by comparing virus counts recovered using different agitation methods, extraction media, and extraction times. The experimental procedures were as follows: (1) a glass fiber filter (GelmanScience, No. 61630) of 25 mm diameter was loaded with a known virus titer, and (2) after 10 min, viruses were extracted from each contaminated filter for a selected period of time by a selected agitation method as listed in Table A-1.

Table A-1 Agitation methods to extract the MS2 bacteriophage on filter

Agitation Method	Applied time (min)	Final time* (min)	Specific conditions
Shaking	1, 2, 5,10, 15, 30, 45, 60	15	10° angle
Vortexing	1, 2, 5, 10, 30, 60	1	3200 rpm
Rotating	1, 3, 5, 10, 30, 60	10	8 rpm
Sonication	1, 5, 10, and 15	10	40 KHz

Final time*: Used for comparison as shown in Figure A-4

To evaluate the influence of the ultrasonic process on viability of the virus, bioaerosols produced at different times were collected in a BioSampler and their viabilities were compared. The MS2 survival efficiency might be affected by the nebulization fluid, and the storage and extraction time. To examine MS2's survivability in the spray medium, DI water and AS were tested. The ultrasonic nebulizer was run with a flow rate of 1 Lpm and a loading time of 5 min. After the loading, 0.25 M glycine solution was applied to extract MS2 on the filter using a wrist-action shaker (Model 75, Burrell Scientific, Pittsburgh, PA) for later analysis of the virus concentration. Sample extraction times were 1, 2 and 5 min. Samples were then kept in the refrigerator for 2 days for the second analysis. SF was defined as the ratio of the virus concentration after 2 days to the virus concentration in the extraction solution at the initial time.

A.3. Results

A.3.1. Fluorescein Test

Calibration results of the fluorometer under four modes (Figure A-3) indicate that the instrument performs linearly in the concentration range of interest in this study. The results of the deposition experiment are shown in Table A-2, which displays the reading from the fluorometer under a select mode that was then converted according to the calibration curve to acquire the concentration. The final concentration was averaged from three modes (1×, 3×, and 10×). The corresponding CV was 4.69%, which satisfies the criterion of 20% and demonstrates the uniformity of this method.

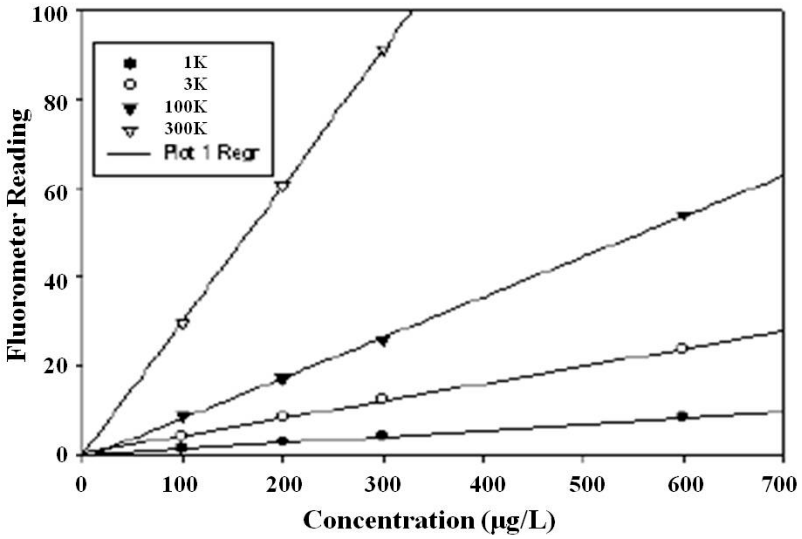

Figure A-3. Calibration Curves for the Fluorometer in Four Gain Modes

Table A-2. Fluorescein Concentrations from Four Filters at Three Instrument Gains

No.	1×		3×		10×		
	Reading	Con. (µg/L)	Reading	Con. (µg/L)	Reading	Con. (µg/L)	Avg. Con. (µg/L)
1	8.09	585.50	23.70	589.97	51.96	586.02	587.16
2	7.23	522.73	21.35	527.63	46.43	524.58	524.98
3	7.82	565.80	22.98	571.65	49.90	563.13	566.86
4	7.84	567.26	23.00	572.16	50.40	568.69	569.37

A.3.2. Determination of Extraction Conditions

Results from tests of agitation methods are displayed in Figure A-4. Extraction efficiency for the wrist-action shaker was 1.25, 1.54 and 1.89 times higher than vortexing, rotating and sonication, respectively. This is different from previous research on best extraction methods. Edwards et al (2004) showed similar extraction efficiencies of MS2 from FFR coupons by vortexing and by shaking. Kim et al. (2008) showed that shaking gave twice higher efficiency than vortexing BG spores into ATCC medium (organic matter). The suggestion from these limited examples is that the efficiency may be both species and medium dependent.

Of the extraction media tested in Figure A-5, glycine gave the highest recovery. Hence, in this study, 0.25 M glycine was selected as the extraction buffer instead of DI water or 1X PBS. Two reasons are proposed for its higher extraction efficiency. First, glycine is a zwitterion, which can combine with both cations and anions and provide more interaction sites. Second, glycine solutions have high ionic strength, which can degrade the double layer at particle surfaces. The effect of extraction time is shown in Figure A-6. Fifteen min of extraction gave the best recovery. Less than 10 min may not be sufficient to extract the virus efficiently and more than 15 min may cause damage to the virus due to excessive mechanical stress and air contact. From these results, the condition chosen to extract MS2 from samples is 15 min in 25 mL of 0.25 M glycine solution on a wrist action shaker at a 10° angle.

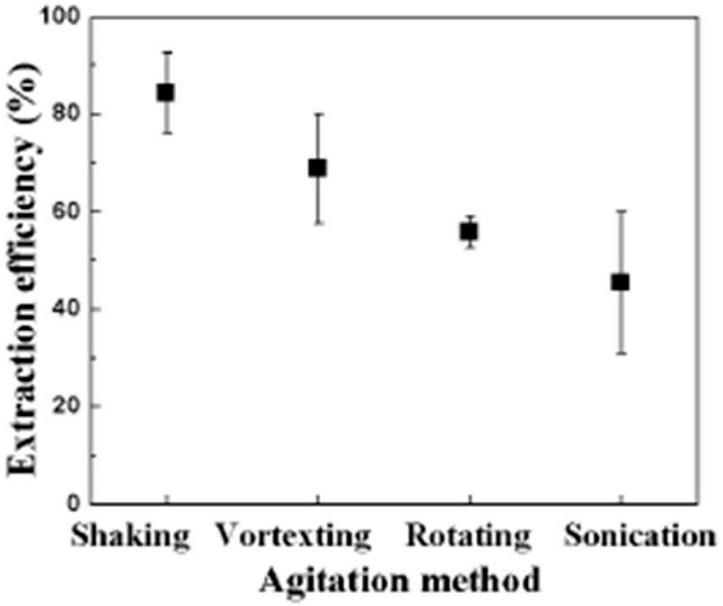

Figure A-4. MS2 Extraction Efficiency based on Agitation Method; Error Bars Represent One Standard Deviation.

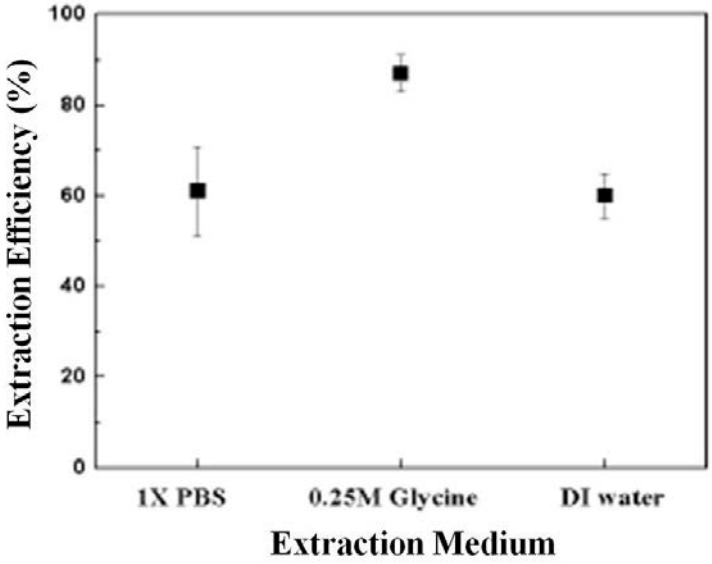

Figure A-5. MS2 Extraction Efficiency Based on Extraction Time. Error Bars Represent One Standard Deviation

A.3.3. Viability during Ultrasonic Nebulization

The impact of ultrasonic nebulization on viability of virus in the nebulizer reservoir was investigated by comparing the viable counts over time. The results showed no significant difference in virus viability from 0 to 30 min (p = 0.10). Apparently, the heat shock from

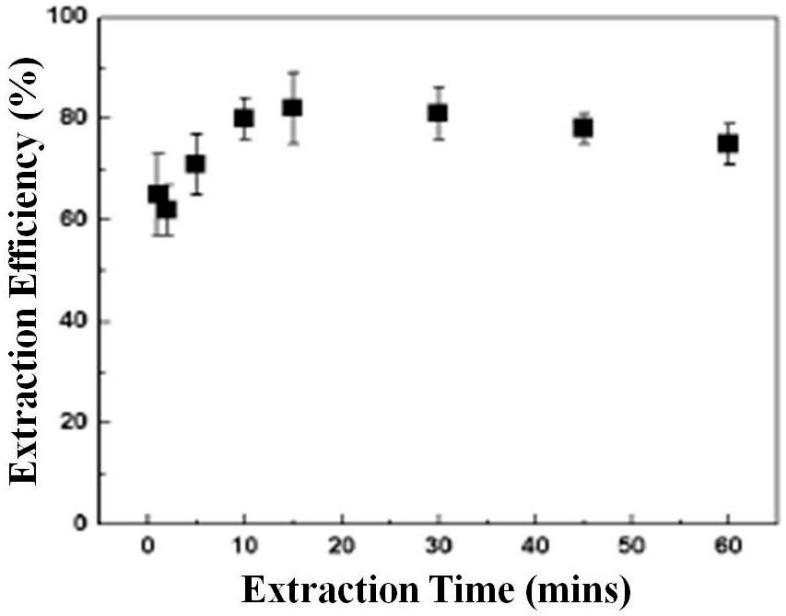

Figure A-6. MS2 Extraction Efficiency Based on Extraction Time; Error Bars Represent One Standard Deviation

ultrasonic vibration caused no damage to MS2 in the reservoir during droplet generation. To determine the effect of the ultrasonics on virus aerosol during droplet generation, viability of viruses collected in the BioSampler after 5 and 10 min of generation was examined. The theoretical concentration in the BioSampler after 5 min of collection is 3×10^5 PFU/mL when the virus titer in the reservoir is 1.0×10^7 PFU/mL. The 5-min time-weighted (0–5 and 5–10 min) average concentration of collected viruses in the BioSampler was around 3.2×10^5 PFU/mL, similar to the theoretical value. As demonstrated, the ultrasonic generator can be used to produce droplets containing viruses without adversely affecting viability.

A.3.4. Effect of Saliva on Viability

As shown in Table A-3, extraction time does not affect the SF significantly. However, SFs were higher after application in AS than in DI water. The around 1 SFs from AS also imply that MS2 concentration can still be accurately analyzed after 2 days if AS is used as the medium and the sample is kept in the refrigerator.

Table A-3. Survival Fraction in Two Media after Storage for 48 Hours (in Duplicate)

Time (mins)	DI water			Artificial saliva		
	Concentration (PFU/mL)		Survival fraction	Concentration (PFU/mL)		Survival fraction
	0 days	2 days		0 days	2 days	
1	284	223.5	0.78	260	240.5	0.93
2	283	275	0.97	290	306	1.06
5	257	225.5	0.88	295	301	1.02

Appendix B: Microwave-Assisted PAN Nanofiber Filtration System for Viral Aerosol

Static inactivation tests for MS2 on PAN NF filters were carried out by delivering 500 W of microwave power. As shown in Table B-1, SF dropped by 2 logs in less than 90 s. This result suggests that microwave irradiation can effectively decontaminate NF filters loaded with MS2.

Table B-1. Survival Fraction of MS2 under Microwave Irradiation: Static On-filter Inactivation at 500 W

	Microwave irradiation time (s)		
	30	60	90
Mean SF (%)	33.25	4.14	0.81
SD (%)	6.34	0.81	0.34

To evaluate the inactivation performance of the microwave-irradiation-assisted NF filtration system during in-flight filtration against MS2, experiments were conducted using the system displayed in Figure 5 with PAN NF filters. Operating conditions similar to those described in Section 3.6 with duplicate tests were applied. The IE (C_E/C_c, Eq. 8) for MS2 under different microwave powers and time intervals are shown in Figure B-1. As shown, the inactivation effect of microwave against MS2 was dependent on both microwave power and time.

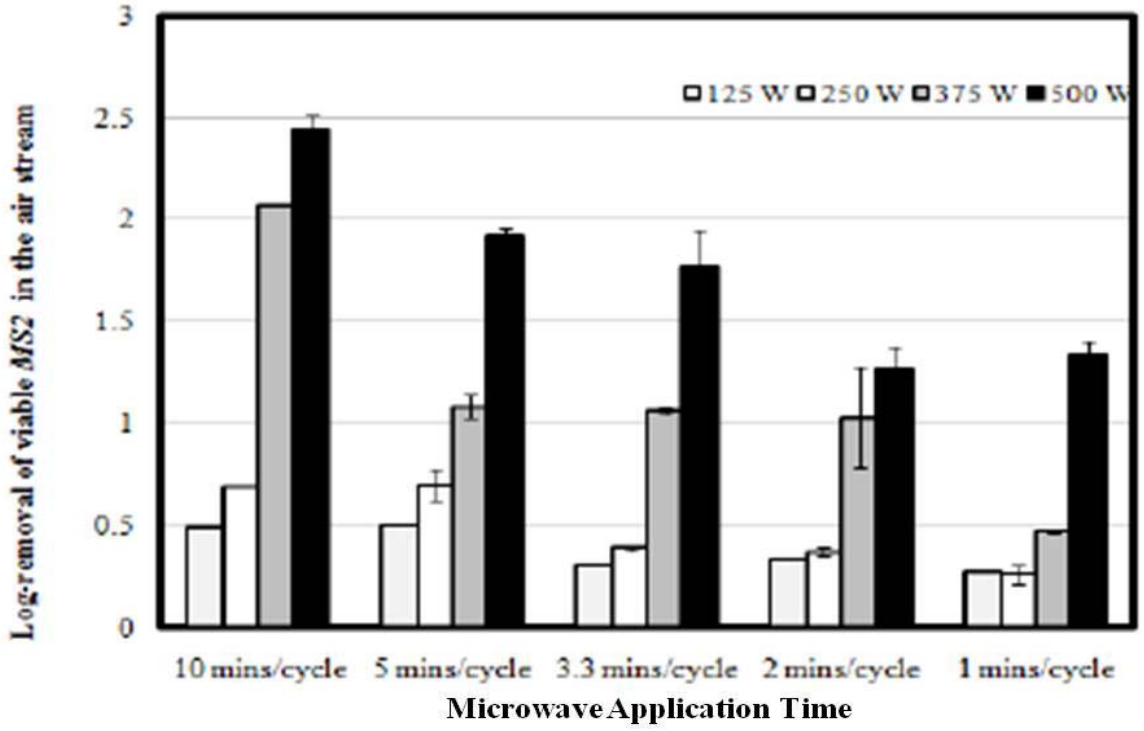

Figure B-1. Log Inactivation Efficiency as a Function of Microwave Application Time for Microwave-irradiation-assisted Filtration System Using a PAN Nanofiber Filter

A 2.4-log IE was shown with continuous microwave treatment at maximum power (500 W). However, the mechanical properties of the PAN filter were altered after continuous testing by the high temperature. To avoid this phenomenon, partially crosslinked PAN having high thermal stability was employed instead of the original PAN filter. Similar IE as that for the PAN filter was observed (Figure B-2), but without observable damage to the filter. Inactivation of MS2 phage here is less pronounced than that of *E. coli* as reported in Zhang et al. (2010). This may be explained as MS2 having greater heat resistance than *E. coli*.

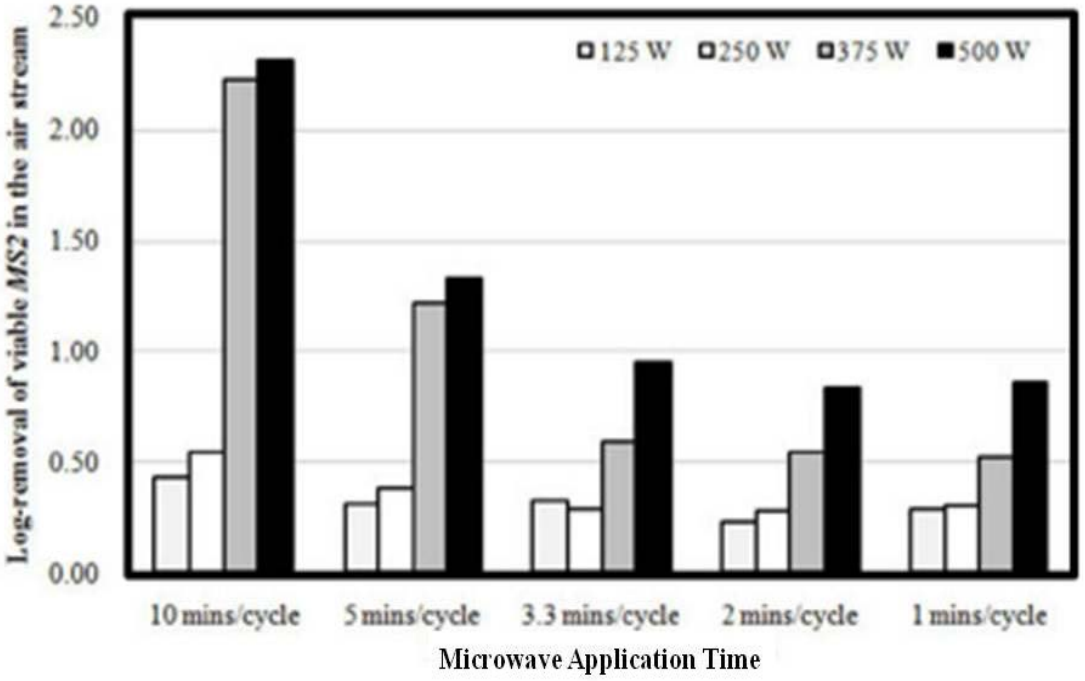

Figure B-2. Log Inactivation Efficiency as a Function of Microwave Application Time for Microwave-irradiation-assisted Filtration System Using a Croslinked PAN Nanofiber Filter

LIST OF ABBREVIATIONS, SYMBOLS AND ACRONYMS

ACF	activated carbon fiber (filter)
ANOVA	analysis of variance
AS	Artificial saliva
BE	beef extract
CMD	count median diameter
CNT	carbon nanotube
CT	threshold cycle (to detect DNA by PCR)
CV	coefficient of variation
DI	deionized (water)
DNA	deoxyribonucleic acid
DPD	*N*, *N*-diethyl-*p*-phenylenediamine
FDA	Food and Drug Administration
eV	electron-volt
FE	filtration efficiency
FFR	filtering facepiece respirator
GHz	gigahertz
HEPA	high-efficiency particulate air (filter)
HRH	high relative humidity (90 ± 5%)
HVAC	heating, ventilation and air conditioning
ID	infective dose
IE	inactivation efficiency
IR	infrared
J/cm^2	joules per square centimeter
K	virus susceptibility factor (in m^2/J)
Lpm	liter(s) per minute
LRH	low relative humidity (30 ± 5%)
mg/L	milligrams per liter
min	minute(s)
MMD	mass median diameter
MPPS	most-penetrating particle size
MRH	medium relative humidity (60 ± 5%)
MS2	MS2 bacteriophage (in this study, ATCC®, 15597-B1™)
mW/cm^2	milliwatts per square centimeter
NF	nanofiber
$N_{\text{Theo PFU}}$	theoretical value of N_{PFU} (number of MS2 PFUs per particle (equation 3))
NIOSH	National Institute for Occupational Safety and Health
NP	nanoparticle
PAN	polyacrylonitrile
PBS	phosphate-buffered saline (medium)
PCR	polymerase chain reaction
PFU	plaque-forming unit(s)
PFU/mL	plaque-forming units per milliliter (of suspension)
PSD	particle size distribution
PSL	polystyrene latex (particles)

PSTI	polystyrene-4-(trimethylammonium)methyl triiodide
Q-T-Q	quarter-to-quarter (variation)
RH	relative humidity
RNA	ribonucleic acid
rpm	rotations per minute
s	second(s)
SARS	Severe Acute Respiratory Syndrome
SEM	scanning electron microscopic (image)
SF	survival fraction
SiC	silicon carbide
SMPS	scanning mobility particle sizer
S-T-S	sample-to-sample variation
T	temperature
TGA	thermogravimetric analysis
TGA–SDTA	thermogravimetric analysis with simultaneous differential thermal analysis
TSB	tryptone soy broth (medium)
UV	ultraviolet (light)
vol %	concentration (of the component) by volume = $100 \times \text{volume}_{\text{component}}/\text{volume}_{\text{total}}$
W	watt